

**Leveraging Generative Design and Point Cloud Data  
to Improve Conformance to Passing Lane Layout**

by

Faeze Momeni Rad

A thesis submitted in partial fulfilment of the requirements for the degree of

Master of Science

in

Transportation Engineering

Department of Civil and Environmental Engineering  
University of Alberta

© Faeze Momeni Rad, 2023

# Abstract

The inadequate design of highway elements is a major contributing factor to traffic collisions. Guidelines and regulations for highway design serve as a structured framework for engineers, providing essential direction to create compliant models. These rules are established to ensure the safety and well-being of road users, addressing aspects such as road geometry, signage, lane markings, and more. Developing the best and most efficient solution within specific design requirements involves evaluating various choices. Generative design is a process that employs algorithms and computational methods to generate and assess design solutions, aiming to find the most optimal outcome meeting criteria like safety, capacity, efficiency, and sustainability.

Building Information Modeling (BIM) involves creating a digital model of a structure, incorporating physical and operational attributes. This thesis employs a user-friendly, logic-based language to describe rules for designing highway passing lanes. The integration of BIMKit enhances the highway design process, streamlining and improving efficiency. Leveraging the faster evaluation process of generative design facilitates the creation of highway passing lanes. The objective is to analyze 16 real-world existing passing lanes in Alberta, demonstrating the method's applicability in the transportation field.

Focusing on passing lanes within the transportation system offers a manageable starting point to grasp the challenges of adopting the proposed approach without overwhelming complexity. It allows for a gradual build-up of generative design expertise, enhancing our understanding before tackling broader aspects. Improving conformance to passing lane designs directly impacts road safety and traffic flow, demonstrating the practical benefits of generative design.

Traffic sign placement, governed by clear safety and regulatory guidelines, offers a well-defined basis for generative algorithms. The availability of relevant data facilitates accurate model training. This approach serves as a proof of concept for generative design in highway transportation, initially concentrating on traffic signs as a controlled testing ground before expanding to more complex design rules including other passing lane characteristics.

The analysis aims to determine the compatibility of the current passing lanes with the design guidelines recommended by the MUTCD and the Highway Geometric Design Guide of the Alberta government. Subsequently, generative designs conforming to code requirements are proposed, ensuring they meet necessary standards and specifications. The examination reveals significant improvements in overall score and guideline adherence through the implementation of generative design and required adjustments. The compatibility of the considered passing lanes increases from an initial average of 61.82% to an impressive 91.31% after leveraging generative design techniques.

The results highlight the importance of incorporating generative design in the transportation domain. By utilizing advanced algorithms and computational methods, generative design greatly enhances infrastructure planning and design efficiency, providing a powerful tool for engineers to create innovative and compliant solutions for highway projects.

*To my dear parents, **Mahnosh** and **Omid**,  
and my beloved sister, **Bahareh**,  
whose unwavering support and inspiration have been truly remarkable*

# Acknowledgements

I am deeply grateful to all those who have supported me throughout this academic journey and contributed to the successful completion of this thesis.

First and foremost, I would like to express profound gratitude to Professor Karim El-Basyouny, my MSc study supervisor at the University of Alberta. His unwavering encouragement, limitless patience, and generous support have been instrumental in my academic journey. This work would not have come to fruition without his guidance, extensive knowledge, and patience. His dedication to scientific research and outlook on life has profoundly impacted my future career path. The two years spent working under his mentorship have been the most fruitful and exhilarating of my professional life. Through his mentorship, I have significantly honed my reading, writing, and critical thinking skills. The experience of working with him has been nothing short of extraordinary. His kindness, thoughtfulness, and boundless enthusiasm have been a constant source of inspiration.

I extend my heartfelt appreciation to Dr. Eleni Stroulia and Dr. Stephen Wong, esteemed dissertation committee members, for their valuable participation in my defence committee.

I want to give special acknowledgement to Christoph Peter Sydora, whose introduction to the world of generative design and BIMKit opened up new horizons for my research. His continuous assistance, support, and constructive feedback were pivotal in completing this endeavour. Without his guidance, I would not have been able to navigate the complexities of my thesis.

I would also like to thank Maged Kamal Gouda for teaching me to work with LiDAR data.

I extend my heartfelt appreciation to my family and friends for their unwavering support, encouragement, and love. Their presence has been a constant source of strength and motivation. Their insightful guidance illuminated my path and gave me the confidence to pursue my graduate studies. I am deeply indebted to them for being my support pillars throughout this journey.

Once again, thank you all from the bottom of my heart.

# Contents

|   |             |
|---|-------------|
| <b>ABSTRACT .....</b>   | <b>II</b>   |
| <b>CONTENTS.....</b>  | <b>VI</b>   |
| <b>LIST OF TABLES .....</b>   | <b>VIII</b> |
| <b>LIST OF FIGURES .....</b>  | <b>IX</b>   |
| <b>INTRODUCTION.....</b>  | <b>1</b>    |
| 1.1    BACKGROUND .....   | 1           |
| 1.2    RESEARCH MOTIVATION .....  | 3           |
| 1.3    RESEARCH OBJECTIVE.....  | 3           |
| 1.4    THESIS STRUCTURE.....  | 4           |
| <b>LITERATURE REVIEW .....</b>  | <b>5</b>    |
| 2.1    APPLICATION OF LIDAR IN TRANSPORTATION AND HIGHWAY ENGINEERING .....                   | 5           |
| 2.2    SUMMARY OF APPLICATION OF LIDAR IN TRANSPORTATION AND HIGHWAY ENGINEERING STUDIES..... | 8           |
| 2.3    HIGHWAY DESIGN ASSESSMENTS .....   | 10          |
| 2.4    SUMMARY OF HIGHWAY DESIGN ASSESSMENTS .....  | 12          |
| 2.5    HIGHWAY DESIGN METHODS.....  | 12          |
| 2.6    SUMMARY OF HIGHWAY DESIGN METHODS .....  | 14          |
| <b>DATA DESCRIPTION.....</b>  | <b>15</b>   |
| 3.1    HIGHWAY 3 .....  | 20          |
| 3.2    HIGHWAY 9 .....  | 20          |
| <b>RESEARCH METHODOLOGY .....</b>   | <b>21</b>   |
| 4.1    VEHICLE TRAJECTORY CALCULATION .....   | 21          |
| 4.2    POINT FILTRATION .....   | 22          |
| 4.3    POINT EXTRACTION .....   | 24          |
| 4.4    TRANSFORMING POINT DATA INTO 3D (OR 2D) MESH STRUCTURES .....                          | 25          |
| 4.5    RULE LANGUAGE.....   | 27          |
| 4.6    MODEL CHECKING .....   | 30          |
| 4.7    GENERATIVE DESIGN .....  | 37          |
| <b>RESULTS &amp; DISCUSSION .....</b>   | <b>39</b>   |
| 5.1    PASSING LANE 1 .....   | 40          |
| 5.2    PASSING LANE 2 .....   | 44          |
| 5.3    PASSING LANE 3 .....   | 48          |
| 5.4    PASSING LANE 4 .....   | 52          |
| 5.5    PASSING LANE 5 .....   | 56          |
| 5.6    PASSING LANE 6 .....   | 60          |
| 5.7    PASSING LANE 7 .....   | 64          |
| 5.8    PASSING LANE 8 .....   | 68          |
| 5.9    PASSING LANE 9 .....   | 72          |
| 5.10   PASSING LANE 10.....   | 76          |
| 5.11   PASSING LANE 11.....   | 80          |
| 5.12   PASSING LANE 12.....   | 84          |

|   |   |            |
|---|---|------------|
| 5.13  | PASSING LANE 13 .....                               | 88         |
| 5.14  | PASSING LANE 14 .....                               | 92         |
| 5.15  | PASSING LANE 15 .....                               | 96         |
| 5.16  | PASSING LANE 16 .....                               | 100        |
| 5.17  | SUMMARY .....                                       | 104        |
| <b>CONCLUSION &amp; RECOMMENDATIONS .....</b> |   | <b>108</b> |
| 6.1   | RESEARCH CONTRIBUTIONS.....                         | 109        |
| 6.2   | RESEARCH LIMITATIONS & FUTURE RECOMMENDATIONS ..... | 109        |
| <b>REFERENCES.....</b>                        |   | <b>113</b> |

# List of Tables

|  |     |
|--|-----|
| TABLE 1: SUMMARY OF STUDIES ON THE APPLICATION OF LiDAR IN HIGHWAY GEOMETRIC ..... | 8   |
| TABLE 2: TRAFFIC SIGNS.....  | 19  |
| TABLE 3: GEOMETRICAL RELATIONS FOR RULE EXPRESSIVENESS .....                       | 28  |
| TABLE 4: OBJECT DESCRIPTION.....   | 29  |
| TABLE 5: RULES.....  | 31  |
| TABLE 6: MODELLING RESULTS .....   | 105 |



# List of Figures

|  |     |
|--|-----|
| FIGURE 1: VIRTUAL IMAGE OF THE LIDAR POINT CLOUD SAMPLE FOR A PASSING LANE ..... | 17  |
| FIGURE 2: SIGNING FOR PASSING AND CLIMBING LANES.....                            | 18  |
| FIGURE 3: RESULTS FOR PASSING LANE 1 ON HIGHWAY 3 .....                          | 43  |
| FIGURE 4: RESULTS FOR PASSING LANE 2 ON HIGHWAY 3 .....                          | 47  |
| FIGURE 5: RESULTS FOR PASSING LANE 3 ON HIGHWAY 3 .....                          | 51  |
| FIGURE 6: RESULTS FOR PASSING LANE 4 ON HIGHWAY 3 .....                          | 55  |
| FIGURE 7: RESULTS FOR PASSING LANE 5 ON HIGHWAY 3 .....                          | 59  |
| FIGURE 8: RESULTS FOR PASSING LANE 6 ON HIGHWAY 3 .....                          | 63  |
| FIGURE 9: RESULTS FOR PASSING LANE 7 ON HIGHWAY 3 .....                          | 67  |
| FIGURE 10: RESULTS FOR PASSING LANE 8 ON HIGHWAY 3 .....                         | 71  |
| FIGURE 11: RESULTS FOR PASSING LANE 9 ON HIGHWAY 9 .....                         | 75  |
| FIGURE 12: RESULTS FOR PASSING LANE 10 ON HIGHWAY 9 .....                        | 79  |
| FIGURE 13: RESULTS FOR PASSING LANE 11 ON HIGHWAY 3 .....                        | 83  |
| FIGURE 14: RESULTS FOR PASSING LANE 12 ON HIGHWAY 3 .....                        | 87  |
| FIGURE 15: RESULTS FOR PASSING LANE 13 ON HIGHWAY 3 .....                        | 91  |
| FIGURE 16: RESULTS FOR PASSING LANE 14 ON HIGHWAY 3 .....                        | 95  |
| FIGURE 17: RESULTS FOR PASSING LANE 15 ON HIGHWAY 3 .....                        | 99  |
| FIGURE 18: RESULTS FOR PASSING LANE 16 ON HIGHWAY 3 .....                        | 103 |

# Chapter 1

## Introduction

### 1.1 Background

The Safe System Approach is a complete framework that aims to achieve zero fatalities and fatal injuries on transportation networks. It acknowledges that humans are prone to making mistakes, so the transportation system should be designed to minimize the impact of those errors. To put this into practice, the Safe System Approach utilizes the five E's of traffic safety (engineering, education, enforcement, evaluation, and engagement) as guidance [1]. Engineering involves designing and operating the road transport system, covering infrastructure, vehicles, and technology. Education aims to educate road users about safe attitudes and behaviours. Enforcement ensures compliance with road rules and laws through policing and sanctions. Evaluation assesses the effectiveness of the Safe System Approach and identifies areas that need improvement. Finally, engagement involves collaborating with stakeholders such as road users, communities, and industry to create support for the Safe System Approach and encourage active participation [2]. Therefore, road infrastructure design and its engineering and evaluation are critical elements of the Safe System Approach since they play a crucial role in reducing the number and severity of road collisions.

The improper design of highway elements significantly contributes to traffic collisions. Guidelines and regulations for highway design serve as a framework for engineers, providing them with the necessary guidance to create compliant models. These rules are established to ensure the safety and well-being of road users by addressing various aspects of the design process, including the design of road geometry, signage, lane markings, and more. Traffic signs and lane markings are essential components of highway design that ensure road safety. Any inaccuracies or deficiencies in these design elements can result in misunderstandings, confusion, and, ultimately, collisions. Therefore, designing, maintaining and evaluating these elements accurately is crucial to minimize the risk of road collisions. They facilitate communication between traffic engineers responsible for designing and regulating traffic flow on roadways and the road users who rely on these signs to navigate the roads safely and efficiently [3]. They offer significant and relevant

details regarding the circumstances and restrictions of the roadway. Researchers have shown considerable interest in extracting these features due to their crucial role in developing vehicle guidance applications for Autonomous Vehicles [4]. Due to the vast scale of contemporary transportation networks, conventional manual methods for designing signs are inefficient, time-consuming, labour-intensive, and prone to low accuracy. Additionally, such methods can cause traffic disruptions and are economically unfeasible. Hence, transportation departments worldwide are actively concentrating on automating this sign-designing process.

Finding the best and optimal solution for a specific set of design requirements and constraints involves examining various design choices. Generative design is a process that consists in using algorithms and computational methods to generate and evaluate design solutions. This process encompasses a broad spectrum of techniques and methods utilized in the CAD domain [5]. Generative highway design is a specific application of generative design that focuses on optimizing highway designs. The aim is to find the most optimal solution that meets specific criteria, such as safety, capacity, efficiency, and sustainability. The process typically involves defining the problem, creating a generative design framework, generating design options, evaluating and refining them, and implementing the selected design.

BIM, short for Building Information Modeling, refers to a process that entails developing a structure's digital model comprising physical and operational attributes [6]. Using off-site construction and BIM technology offers numerous advantages to the construction sector, including decreased material waste and the development of sustainable construction solutions [7]. BIM can improve safety in highway design and construction projects in several ways. It can assist with the analysis and simulation of the highway design, enabling engineers to assess multiple scenarios and determine the most efficient and cost-effective solutions. It also allows for creating a comprehensive and precise model that includes various elements, enhancing communication and collaboration between professionals working on the project, such as civil engineers, surveyors, and architects. It enables the creation of 3D models of the highway, which can spark engineers' creativity and facilitate design visualisation [5]. This capability allows stakeholders to gain a deeper understanding of the proposed project, which can help them identify potential conflicts or issues before construction starts, ultimately reducing the need for design changes during the construction phase. This process can lead to cost and time savings for the project.

The primary reference for implementing generative design techniques in our research is the Manual on Uniform Traffic Control Devices (MUTCD) [8] and the Highway Geometric Design Guide, specifically Chapter B, which is published by the government of Alberta [9]. MUTCD is a set of guidelines and standards developed by the Federal Highway Administration (FHWA) to ensure uniformity and consistency in the design, application, and placement of traffic control devices such as signs, signals, and pavement markings on public roads.

## **1.2 Research Motivation**

This thesis uses a user-friendly, logic-based language that allows for the description of rules in designing passing lanes on highways. With the assistance of BIMKit, the highway design process is enhanced, providing a more efficient and streamlined approach. This language was used to build a model-checking system, which has the potential to automate the entire highway design process. Notably, this language supports the creation of complex rules as logical expressions that consider geometrical properties and relationships. Therefore, the thesis leverages the efficient evaluation process, which is much faster than manual checking, to facilitate the generative design of passing lanes on highways. Using the rules outlined in the thesis, the generative design process can produce optimal design that meet the applicable code requirements.

## **1.3 Research Objective**

The primary objective of this thesis is to analyze the design of existing passing lanes on the highways located in the province of Alberta. This analysis aims to determine the compatibility of the current passing lanes with the design guidelines recommended by the MUTCD and the Highway Geometric Design Guide of the government of Alberta. Once the compliance checking step has been completed, the next stage involves proposing generative designs that conform to the relevant code requirements. The designs will be presented optimally, meeting the required standards and specifications. In summary, the objectives of the project can be outlined as follows:

1. Extract relevant highway features and characteristics from point cloud data.
2. Assess the efficacy of current passing lane designs using BIMKit technology and its model-checking process.
3. Apply generative design to determine compliance to current guidelines and enhance the infrastructure's design within the existing framework.

4. Augment our understanding of the existing highway conditions and identification of prominent deficiencies in signage placement and accuracy for passing lanes.

## **1.4 Thesis Structure**

The remainder of this thesis is structured as follows: Chapter two reviews prior research on LiDAR data applications in the transportation field, highway design assessment, and highway design methods. Chapter three provides comprehensive details regarding the study areas and data descriptions. Chapter four introduces the methodology utilized for data analysis. Chapter five presents the analysis results and examines the study's discoveries. Chapter six concludes with a summary of the primary conclusions and research contributions and a discussion of the study's limitations and recommendations for future research.

# Chapter 2

## Literature Review

### 2.1 Application of LiDAR in Transportation and Highway Engineering

Light Detection and Ranging (LiDAR) is an optical remote sensing technology that collects data about the surrounding environment using near-infrared light rays. The laser scanners emit beams toward the objects in their vicinity, and by analyzing the characteristics of the reflected beams, they compute the distance to the point at which each beam was reflected [4].

Applying LiDAR data in transportation engineering has garnered considerable interest among researchers and practitioners, leading to a substantial body of literature. Many studies have leveraged LiDAR data to tackle a broad range of challenges in the transportation engineering field. These challenges include assessing road conditions [10], [11], [12], [13], [14], monitoring traffic [15], [16], [17], aiding autonomous vehicle navigation [18], [19], [20], detecting pedestrians [21], [22], [23], [24], facilitating transportation planning by mapping transportation network infrastructures [25], [26], [3], [27], [28], [29], [30], [31], and other related applications.

The accuracy and precision of LiDAR data in evaluating road conditions make it an invaluable asset for pavement management and maintenance, owing to its exceptional reliability and effectiveness. In the initial application of LiDAR data for detecting pavement distress, Chang et al., in their study, noted that precise 3D point-cloud data with elevation information was captured through scanning. Then specific distress features were extracted using a grid-based processing approach. The experimental findings demonstrated that the severity and extent of pavement distress could be accurately and automatically quantified, allowing for precise estimation of the required materials for repair and maintenance [10]. Guo's paper presents a comprehensive and automated approach for reconstructing road surface features utilizing terrestrial mobile LiDAR technology [11]. Automatic detection of potholes is critical in determining effective strategies for maintaining asphalt-surfaced pavements. Kang's paper presents the development of a pothole detection system and method that utilizes 2D LiDAR and cameras for accurate and automated detection of potholes [12]. Ravi et al. introduced a novel approach for mapping potholes on road surfaces as part of their ongoing research. They utilized state-of-the-art 3D LiDAR technology

with ultra-high accuracy, which was integrated into a mobile wheel-mounted mapping system [13]. In a different undertaking, he proposed an innovative algorithm for inspecting pavement surfaces using mobile mapping systems that operate at highway speeds. This approach presents a distinct method for efficiently and effectively evaluating the condition of road surfaces while in motion [14].

LiDAR data has the potential to offer exact and accurate data on vehicle speed, direction, and volume, which can be utilized to analyze traffic flow patterns, pinpoint bottlenecks, and optimize traffic signal timings to improve traffic management strategies. Yao's paper outlines a holistic strategy for urban traffic analysis utilizing airborne LiDAR data, including an adaptive 3D segmentation method for vehicle extraction. The findings suggest that airborne LiDAR data can enhance traffic monitoring products such as vehicle counts, location, and velocity, in addition to traditional products like building models, DEMs, and vegetation models [15]. Another Yao paper presents a comprehensive scheme that utilizes airborne LiDAR data to analyze urban traffic in real-life scenarios. The approach combined successive vehicle detection with a motion classification method and employed knowledge about the shape of the vehicles to derive their velocity [16]. In a separate research endeavour, researchers introduced a tracking framework that utilizes roadside LiDAR data to detect and track vehicles, to accurately estimate vehicle speeds [17].

LiDAR data plays a crucial role in the development and operation of autonomous vehicles (AVs), serving as a vital component that provides essential information for perception, mapping, localization, and safety. In their paper, Gouda et al. introduced a novel simulation-based approach for evaluating the "readiness" of highways for autonomous vehicles (AVs) by utilizing 3D point cloud data. The proposed approach was subsequently compared to a state-of-the-art raycasting approach, providing a unique and innovative method for assessing highways in the context of AVs [18]. The correct identification and understanding of lane markings are crucial for the successful operation of AVs, as they heavily rely on this information for navigation and decision-making on the road. In a research study, the authors presented a technique for evaluating obstructions of lane markings on a roadway, utilizing a point cloud representation obtained through LiDAR scanners. The primary objective of this research was to establish a new approach to examine and enhance the visibility of lane markings in anticipation of the widespread use of AVs [20].

LiDAR data has the potential to enhance safety in diverse environments, including urban regions, parking lots, and school zones, by facilitating pedestrian detection. A study offered a valuable analysis of how LiDAR-based features can be used for pedestrian detection in urban scenarios. The study's main aim was to investigate the potential of LiDAR sensors to provide useful information for detecting pedestrians. To achieve this goal, the study utilized a method that exclusively used LiDAR-based features to extract relevant information to improve pedestrian detection [21]. Due to the poor clarity of visual images at night, other studies suggested alternative approaches for detecting pedestrians. Those approaches involve utilizing a high-definition LiDAR system, which does not rely on visual images to recognize pedestrians [23], [24].

By utilizing LiDAR data to map transportation network infrastructures, transportation planners can gain significant insights and information that can aid in making informed decisions and developing transportation plans that are both effective and efficient while also being sustainable. LiDAR technology can extract several types of information from paved roadways. These include features like traffic sign information [26], [3], [31], road markings [25], and other design elements such as guardrails [29], vertical profiles [27], and light poles [30]. Additionally, LiDAR data can be utilized to obtain roadside clearance parameters critical for ensuring roadway safety [28].

A literature review was conducted by Gargoum and El Basyouny that explored the various applications of LiDAR data in transportation engineering [4]. Their evaluation has revealed that most of the past studies in this domain have focused on utilizing LiDAR datasets for inventorying and mapping on-road and roadside features. However, there hasn't been enough emphasis given to exploring the potential of LiDAR technology to enhance the efficiency of extracting and assessing the geometric design elements of roads. Utilizing innovative techniques and methods to exploit LiDAR data effectively can significantly improve the accuracy and efficiency of road design and maintenance processes. Such advancements could have profound implications for transportation infrastructure, leading to safer and more reliable road networks and ultimately improving mobility and quality of life for individuals and communities.



## 2.2 Summary of Application of LiDAR in Transportation and Highway Engineering Studies

Table 1 summarises various studies exploring the application of LiDAR technology in transportation engineering. The table includes information about the authors of the studies, the title of the study, and the specific applications of LiDAR data used in each study. Some of the LiDAR data applications in transportation engineering included in the table are road condition assessment, traffic monitoring, pedestrian detection, and transportation network infrastructure mapping. The table can serve as a valuable resource for researchers and practitioners interested in exploring LiDAR technology's potential in transportation engineering.

In summary, the application of LiDAR technology in transportation engineering has tremendous potential to transform the field, and the use of LiDAR technology in transportation engineering has gained significant attention. It has been applied in various studies, such as assessing road conditions, monitoring traffic, and detecting pedestrians. However, there is a lack of exploration of LiDAR's potential to improve the efficiency of extracting and evaluating geometric design elements of roads. Using innovative techniques and methods to exploit LiDAR data effectively, we can significantly enhance the accuracy and efficiency of road design and maintenance processes. These improvements can dramatically impact transportation infrastructure, resulting in safer and more dependable road networks and ultimately benefiting individuals' and communities' mobility and quality of life.

Table 1: Summary of studies on the application of LiDAR in highway geometric

| <b>Authors</b>         | <b>Title</b>   | <b>Application of LiDAR</b>          |
|------------------------|--|--------------------------------------|
| Chang et al. 2005 [10] | Detection of pavement distresses using 3D laser scanning technology  | Pavement Distress Detection          |
| Ravi et al. 2021 [14]  | Pavement distress and debris detection using a mobile mapping system with 2d profiler LiDAR                    | Pavement Distress Detection          |
| Guo et al. 2015 [11]   | Automatic reconstruction of road surface features by using terrestrial mobile LiDAR                            | Road Surface Features Reconstruction |
| Kang et al. 2017 [12]  | Pothole detection system using 2D LiDAR and camera   | Pothole Detection                    |
| Ravi et al. 2020 [13]  | Pothole mapping and patching quantity estimates using LiDAR-based mobile mapping systems                       | Pothole Detection                    |
| Yao et al. 2011 [15]   | Extraction and motion estimation of vehicles in single-pass airborne LiDAR data towards urban traffic analysis | Urban Traffic Analysis               |

|                            |   |   |
|----------------------------|---|---|
| Yao et al. 2012 [16]       | Airborne traffic monitoring in large areas using LiDAR data--theory and experiments   | Traffic Monitoring                        |
| Zhang et al. 2020 [17]     | Vehicle tracking and speed estimation from roadside LiDAR   | Traffic Monitoring                        |
| Gouda et al. 2021 [18]     | Octree-based point cloud simulation to assess the readiness of highway infrastructure for autonomous vehicles                                     | Highway Assessment for AVs                |
| Gouda et al. 2021 [19]     | Automated assessment of infrastructure preparedness for autonomous vehicles   | Highway Assessment for AVs                |
| Gouda et al. 2022 [20]     | Safety Assessment of Lane Marking for Autonomous Vehicles Using Light Detection and Ranging (LiDAR) Data  | Lane Marking Occlusion Assessment for AVs |
| Premebida et al. 2009 [21] | Exploiting LiDAR-based features on pedestrian detection in urban scenarios  | Pedestrian Detection                      |
| Kidono et al. 2011 [22]    | Pedestrian recognition using high-definition LiDAR  | Pedestrian Detection                      |
| Tang et al. 2017 [23]      | Multi-cue pedestrian detection from 3D point cloud data   | Pedestrian Detection                      |
| Lin et al. 2018 [24]       | Pedestrian detection from LiDAR data via cooperative deep and hand-crafted features   | Pedestrian Detection                      |
| Guan et al. 2014 [25]      | Using mobile laser scanning data for automated extraction of road markings  | Road Marking Detection                    |
| Ai et al. 2015 [26]        | Critical assessment of an enhanced traffic sign detection method using mobile LiDAR and INS technologies  | Traffic Sign Detection                    |
| Gargoum et al. 2017 [3]    | Automated highway sign extraction using LiDAR data  | Traffic Sign Detection                    |
| Gargoum et al. 2018 [27]   | Feasibility of extracting highway vertical profiles from LiDAR data   | Highway Vertical Profile Extraction       |
| Gouda et al. 2021 [28]     | Automated object detection, mapping, and assessment of roadside clear zones using LiDAR data  | Roadside Clear Zones Detection            |
| Yue et al. 2021 [29]       | Automatic detection and mapping of highway guardrails from mobile LiDAR point clouds  | Highway Guardrails Detection              |
| Gouda et al. 2022 [30]     | Fully automated algorithm for light pole detection and mapping in rural highway environment using mobile light detection and ranging point clouds | Light Pole Detection                      |
| Gouda et al. 2022 [31]     | Traffic sign extraction using deep hierarchical feature learning and mobile light detection and ranging (LiDAR) data on rural highways            | Traffic Sign Detection                    |

## 2.3 Highway Design Assessments

Assessing the suitability of current roads for autonomous vehicles is a necessary step in ensuring that our transportation infrastructure is adequately prepared for the future of transportation [32]. The requirements of autonomous vehicles are distinct from those of conventional vehicles, and the existing road infrastructure may not be adequately equipped to address them. For instance, autonomous vehicles mandate precise and distinct road markings, excellent visibility, and reliable communication infrastructure. The process of reassessing current roads for autonomous driving compatibility includes thoroughly evaluating the road infrastructure and implementing necessary improvements to meet the demands of autonomous vehicles. To improve the reliability and preparedness of Connected and Autonomous Vehicles (CAV) systems, professionals have recommended conducting an evaluation of the current road geometry to identify areas with unfavourable conditions for CAVs and deploying Vehicle to Infrastructure (V2I) communication, which is essential in providing CAVs with necessary information related to the road at critical locations [33].

There are numerous ways to evaluate the design of highways, each with its unique advantages and limitations. Current road maintenance and assessment methods rely heavily on manual surveying techniques and field observations, requiring significant labour and specialized training from transportation agencies. This approach can be time-consuming and costly and may not always provide the most precise results [28]. In their work, the predominant method for evaluating highway geometric design is comparing it to established design standards. These standards, usually created and set by national or state transportation agencies based on research, analysis, and best practices, help engineers and designers ensure that the roadway design meets the minimum safety and operational requirements. The characteristics and geometry of the physical features of a road are determined by a variety of factors, including the placement of traffic signs, the presence or absence of shoulders on the sides of the road, the lane width, the sight distance, the location of bus stops, bike lanes, and pedestrian crossing facilities, and the physical separation of the two directions of the road segment by a median barrier [34]. In addition, the horizontal alignment and its associated geometric attributes, such as curvature, slope, and superelevation, are also critical factors that contribute to the overall safety and efficiency of the

roadway [35]. By comparing the roadway design to design standards, adjustments can be made to improve the design as needed.

Safety performance functions and simulation modelling are alternative methods utilized for assessing highway geometric design, in addition to comparing the design to established design standards. Safety performance functions use statistical models that correlate the frequency and severity of collisions to different roadway characteristics, such as geometric design features [36], [37], [38]. These functions help predict the safety performance of various design alternatives and detect hazardous areas needing further safety enhancements. Simulation modelling, on the other hand, is the process of creating a digital representation of a roadway and analyzing the movement of traffic in different situations. This is done using specialized computer software like VISSIM, a highly useful tool for traffic engineers and transport planners. VISSIM is a behaviour-based, microscopic traffic simulation software that can be used for various purposes. It helps evaluate highway design and predict traffic flow under different conditions [39]. It should be noted that safety performance functions and simulation modelling are primarily designed to assess the safety of highway geometric design, such as pavement characteristics, roadway alignment, and cross-section design. They do not specifically address traffic sign placement or other elements of highway design.

Consequently, there is a growing demand for exploring alternative approaches utilizing emerging technologies, including machine learning, artificial intelligence, and remote sensing technologies such as LiDAR [40], [28] to improve road maintenance and assessment efficiency and accuracy. In a recent study, Gouda et al. introduced an innovative methodology for assessing the sight distance of highways in diverse autonomous vehicle driving scenarios. The approach was based on the utilization of typical commercial vehicle sensor set designs and specifications, providing a novel perspective on the subject matter [19]. The importance of considering all relevant geometric design features in highway assessment cannot be overemphasized. The aforementioned paper appears to have focused exclusively on two critical aspects of highway design: stopping sight distance and speed limit. However, it is crucial to consider other design features as well, given that they also play a vital role in determining the overall safety and efficiency of highways. Consequently, to provide a more comprehensive evaluation of the design features of highways, a framework will be developed within the scope of this paper. Taking a more comprehensive approach to assessing highway design features makes it possible to identify

potential issues early on and implement appropriate mitigation strategies to ensure that highways remain safe and effective for all users.

## **2.4 Summary of Highway Design Assessments**

To prepare the transportation infrastructure for the future, assessing the current roads' suitability for autonomous vehicles is essential. There are various ways to evaluate the highways' design, such as comparing them to established standards, safety performance functions, and simulation modelling. However, the current highway assessment methods rely heavily on manual surveying and field observations, which can be time-consuming, costly, and imprecise. Furthermore, it is essential to highlight that while safety performance functions and simulation modelling methods help evaluate the safety performance of highway geometric design features such as roadway alignment, cross-section design, and pavement characteristics, they do not comprehensively address all design elements of highways, including the placement of traffic signs on the roadway. Therefore, exploring alternative approaches that use emerging technologies, including machine learning, artificial intelligence, and remote sensing technologies, is becoming more popular to improve road maintenance and assessment efficiency and accuracy. A framework will be developed to provide a comprehensive evaluation of the highways' design features, identifying potential issues early on and implementing appropriate mitigation strategies for safety and effectiveness.

## **2.5 Highway Design Methods**

Highway design methods are a set of techniques and approaches that transportation planners and engineers employ to create efficient and safe roadways. Designing complex items necessitates thoroughly exploring multiple options and possibilities by designers and engineers, who must evaluate various alternatives before ultimately arriving at a final decision [41]. Given the complex nature of highway design and the numerous potential solutions, manual design may not be sufficient to achieve the optimal solution due to the complexity of the task and the multiple variables that need to be considered [42].

Genetic algorithms (GAs) have emerged as a popular tool in engineering design, finding application in diverse fields such as mechanical engineering, electrical engineering, aerospace engineering, architecture, civil engineering, and beyond [43]. The flexibility and versatility of GAs make them a valuable resource for designers seeking to optimize complex design problems across a range of domains. Rodriguez proposed an optimization model that addressed the joint selection and design of highway safety and travel time improvement projects. The model incorporated a GA that utilized surrogate models to accelerate the discovery of optimal solutions. By leveraging this approach, designers were able to efficiently identify high-quality solutions for the optimization model, resulting in improved highway safety and travel time [44].

Also, combining GIS (Geographic Information System) and GAs has proven to be a powerful and effective method for tackling complex engineering challenges, especially in transportation. Several research studies have explored the utilization of the integrated approach of GIS and GA for optimizing highway alignments [45], [42], [46]. Jong aimed to construct a model employing a GIS database and GAs to optimize smooth horizontal alignments that adhere to AASHTO's minimum-radius constraints. His findings indicated that the proposed model could generate alignments that met highway design standards while also optimising complex cost functions, including user costs, which had previously been overlooked in many existing models [42].

As implemented in modern CAD platforms, generative design allows architects and engineers to comprehensively investigate many potential design options [41]. It has become a valuable tool in different fields as it allows for exploring a vast array of design options. Shea's assertion that generative design systems aim to create new design processes that generate novel and efficient designs that are feasible to construct using current computing and manufacturing technologies accurately represents the current purpose of generative design [47]. To the author's knowledge, previous attempts to design highways have not given enough attention to generative design as a possible option. This method uses algorithms and computer software to generate multiple design options and select the optimal one based on predefined criteria. Therefore, to bridge this gap, the present study seeks to employ this design approach in highway design.

## **2.6 Summary of Highway Design Methods**

Transportation planners and engineers use various techniques and methods to create safe and efficient roadways. Due to the complexity of highway design and the many potential solutions, manual design may not be sufficient to achieve the optimal outcome. GAs offer a flexible and versatile tool for highway designers to optimize complex design problems. Additionally, combining GAs with GIS (Geographic Information System) has proven to be an effective approach to address complex engineering challenges in transportation, including highway element design optimization. Despite its benefits, generative design has not been considered sufficiently in previous highway design efforts. The current study seeks to incorporate this approach into highway design to improve the overall process to address this issue.

## Chapter 3

### Data Description

This paper describes a study that utilized mobile LiDAR technology to collect data from several highways in Alberta, Canada. The Alberta Transportation Agency collected the data using a laser scanner mounted on a moving vehicle that captured information as it travelled along the designated routes. The laser scanner utilized for this study was the RIEGL VMX 450, known for its ability to generate highly detailed and accurate 360° LiDAR point clouds.

The precision of LiDAR systems, such as the RIEGL VMX 450, is subject to variability influenced by several factors, including the specific model and the manner in which it undergoes calibration and operational usage. Generally recognized for their exceptional precision in measuring distances, RIEGL LiDAR systems are noted for their capacity to provide highly accurate range measurements. The degree of inaccuracy in these measurements is typically quantified in units of distance error, often expressed in millimeters or centimeters. In the case of the RIEGL VMX 450 LiDAR system utilized in this study, it exhibits a documented inaccuracy of 8 millimeters. Consequently, this implies that measurements of distance furnished by the LiDAR system may deviate by as much as 8 millimeters when compared to actual distances in the physical environment. It is imperative to recognize and account for this potential margin of error when interpreting distance measurements acquired through the LiDAR system.

The study involved gathering data while traffic was moving, usually at speeds that reached a maximum of 100 km/h without causing any disruptions to the traffic flow. Provincial surveys were conducted at 90 km/h, resulting in LiDAR point densities ranging from 150 to 1000 points/m<sup>2</sup> on the pavement surface. The information collected for a specific highway was stored in separate LAS files, each representing a 3D model of a 4 km ( $\approx$  2.49 mi) section of the road. These files are large, approximately 500 MB, which suggests that the LiDAR model is highly detailed, with vast information on millions of individual data points.

Mobile LiDAR systems can capture data from numerous angles, and this is an advantage that distinguishes them from other LiDAR systems. The various viewpoints allow the system to collect a large number of points, resulting in a higher point density that accurately captures the physical features of the environment. A notable advantage of having a higher point density due to



the varied angles from which Mobile LiDAR systems collect data is the improved visibility of vertical elements, including buildings, signs, and trees [48]. These features' detailed and accurate portrayal provides valuable information about their dimensions and distances, enabling better comprehension and interpretation. In addition to its enhanced visibility of vertical features, the Mobile LiDAR system's ability to generate a high point density is also beneficial for other industries. For instance, the detailed depiction of the road surface enables a more accurate assessment of the road condition, identification of assets, and planning maintenance strategies. This precise information allows for cost-effective and efficient road maintenance operations. Incorporating LiDAR data in evaluating and maintaining highways can usher in a new era of asset management, design analysis, and road safety assessments [48].

Two distinct collections of LiDAR data are available: Mobile LiDAR and Airborne LiDAR. The ability of Mobile LiDAR to generate a high point density is highly advantageous to several industries, including but not limited to urban planning, transportation infrastructure management, and disaster response. On the other hand, data obtained from Airborne LiDAR has a lower density of measurement points than Mobile LiDAR, but it provides superior visibility for pavements and building surfaces [49]. However, it offers a subpar perspective when capturing information on vertical surfaces. In other words, while Airborne LiDAR may not be the most efficient method for collecting detailed data on vertical features, it is highly effective at accurately measuring flat surfaces such as roads and building roofs [50]. Therefore, each data type has strengths and weaknesses, making them more suitable for some applications than others.

The Mobile LiDAR data gathered on each point comprises various parameters such as x, y, and z coordinates, intensity measurements and scanning angle information. The LiDAR point cloud for one of the passing lane segments is presented as a virtual image in Figure 1. The modelling results and discussion section visually present the LiDAR data for each passing lane.

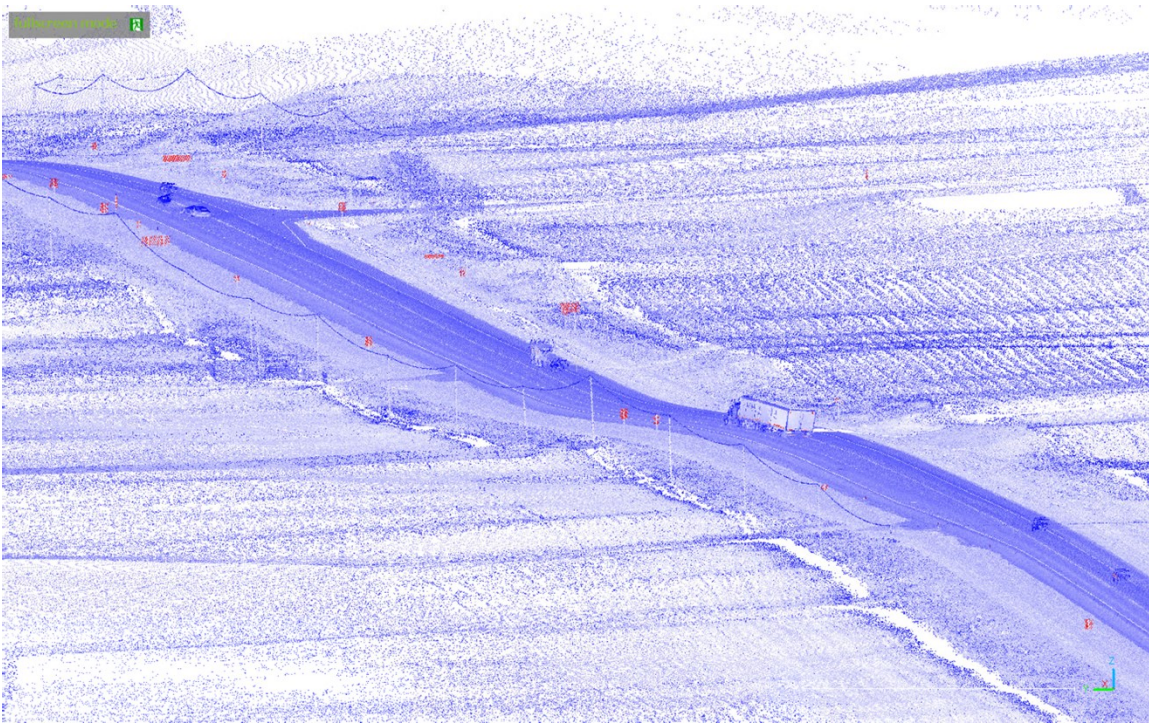
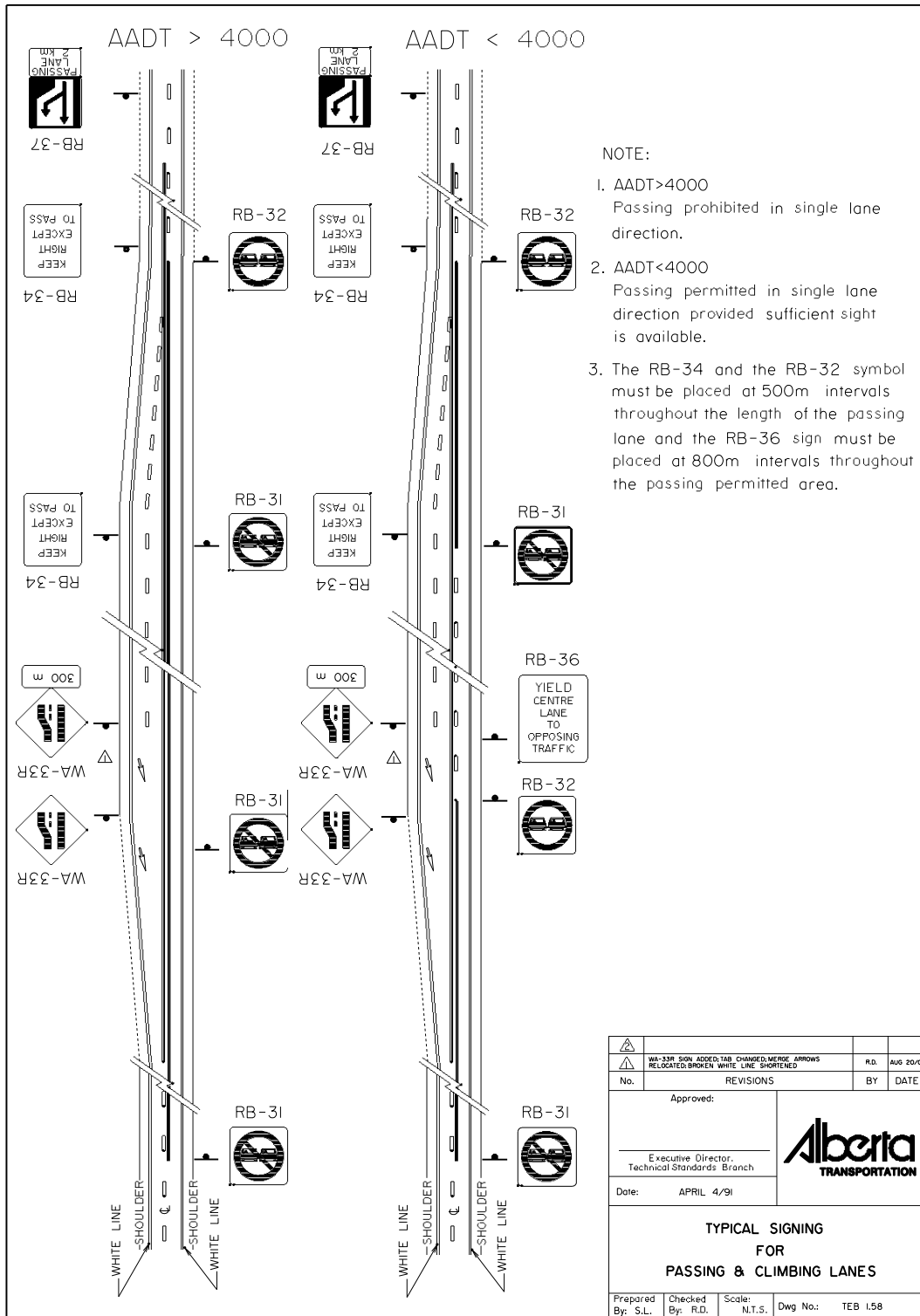


Figure 1: virtual image of the LiDAR point cloud sample for a passing lane

A passing lane, also referred to as an overtaking lane or a fast lane, is a designated portion of a roadway or highway that allows vehicles to overtake or pass slower vehicles legally. Its purpose is to facilitate smoother traffic flow and enhance safety by providing an extra lane for faster vehicles to pass slower ones without disrupting the overall traffic movement. Figure 2 displays the Passing and Climbing Lanes signage sourced from Alberta Transportation.








Graphics File: 1ebm058.sgn

Figure 2: Signing for Passing and Climbing Lanes

Table 2 presents the traffic signs utilized in the study, along with their corresponding descriptions and shapes.

Table 2: Traffic Signs

| Traffic Sign Name | Description               | Shape   |
|-------------------|---------------------------|---|
| RB-34             | KEEP RIGHT EXCEPT TO PASS |    |
| RB-37             | PASSING LANE AHEAD        |    |
| WA-33R            | RIGHT LANE ENDS           |    |
| RB-31             | DO NOT PASS               |    |
| RB-32             | PASSING PERMITTED         |  |

The study utilized LiDAR data specifically acquired for Highway 3 and Highway 9 in the province of Alberta. The objective was to assess the effectiveness of a method on various passing lanes, each exhibiting distinct characteristics, and across different highways. The subsequent sections provide detailed descriptions of each of these highways.

### **3.1 Highway 3**

Alberta Provincial Highway No. 3, also known as the Crowsnest Highway, is a provincial road in Alberta, Canada, spanning approximately 324 kilometres (201 miles) as it crosses the province's southern region. In 1985, there was an announcement regarding the construction of passing lanes on Highway 3 between Monarch and Fort Macleod, which consisted of a two-lane configuration. For analysis, segments of this highway, each measuring 4 kilometres, were selected. These specific segments, including passing lanes, were chosen from the highway's original two-lane, two-way configuration. There were 14 passing lanes considered on this highway, and the average length of these passing lanes was 2 kilometers in total

### **3.2 Highway 9**

Alberta Provincial Highway No. 9, located in the south-central region of Alberta, Canada, serves as a crucial connection between Calgary and Saskatoon, Saskatchewan, via Drumheller, in partnership with Saskatchewan Highway 7. In our analysis, we focused on 4 km sections of this highway. These sections, which feature passing lanes, are part of a two-way, two-lane road. Our examination revealed the presence of two passing lanes within these segments and their average length measures approximately 1.85 kilometers.

# Chapter 4

## Research Methodology

### 4.1 Vehicle Trajectory Calculation

In this study, the vehicle utilized for the data collection process was equipped with two LiDAR scanners that were symmetrically positioned. The LiDAR scanners played a vital role in deriving the vehicle's trajectory during the data collection phase. Data points located directly underneath it with a scanning angle of zero were utilized to obtain the trajectory of each scanner. This information was used to calculate the trajectory of each scanner. Subsequently, the overall trajectory of the vehicle was obtained by averaging the trajectories of the two scanners while using GPS time as a reference. This method of trajectory calculation ensured that the vehicle's movements were accurately captured and could be utilized in further analysis. Using two scanners positioned symmetrically on the vehicle provided a more comprehensive view of the surroundings, enhancing the precision of the trajectory calculations. The equation for the calculation of the line is provided below:

$$LinePoints = \frac{SA_1 + SA_2}{2} + \frac{T_1 + T_2}{2} \quad (1)$$

SA(x) denotes the scan angle of the LiDAR scanner, while T(x) is the GPS time recorded during data collection. S<sub>1</sub> and S<sub>2</sub> refer to the sets of trajectory points for scanner 1 and scanner 2, respectively. To obtain the trajectory of the vehicle, the indices i and j are used to reference the points in sets S<sub>1</sub> and S<sub>2</sub>, respectively. The equation considers all these factors and produces a line accurately representing the vehicle's overall trajectory during data collection.

## 4.2 Point Filtration

Point cloud information, collected in the LAS (laser) format, requires conversion to ASCII text format for easier data filtering. A three-step filtering process detects lane markings and traffic signs in a LiDAR point cloud. The first filter identifies the points close to the expected vehicle trajectory, which is determined by analyzing the scanning angle of the LiDAR data within a certain buffer zone. By extracting the points located near the trajectory points, which cover the limits of travel lanes and roadside, the algorithm can optimize the number of points processed, reducing the computational load. According to the prescribed guidelines, the shoulder adjacent to a passing lane should be no less than 1.5 meters wide or equal to the standard shoulder-width designated for that particular highway design, whichever is smaller. Hence, this thesis assumes a maximum shoulder width of 2 meters to account for potential design errors. To keep the point clouds covering the centerline lane markings and signs on two-lane two-way highways with lane widths ranging from 3.5m ( $\approx 11.48$  ft) to 5.0m ( $\approx 16.40$  ft), the filter is set to keep the points located at a distance between 4.5m ( $\approx 14.76$  ft) and 12.0m ( $\approx 39.37$  ft) from the vehicle trajectory.

The following filter to extract lane markings eliminated those with high z-gradient values, which typically correspond to roadside features and buildings, and only preserved the road boundaries for further analysis. It's important to note that, in contrast, low z-gradient values were removed while extracting traffic signs. z-gradient is determined using the subsequent method:

$$\nabla f_{\%} = \frac{\sum_{i=1}^k (f(P_i) - f(P))}{k} \quad (2)$$

The z-value of point x is denoted by  $f(x)$ , where P represents the point for which the gradient is calculated.  $P_i$  refers to the points in a group of k neighbouring points evenly sampled within a radius around the given point.

The third filtering step involves using an intensity-based filter that takes advantage of the information provided by the LiDAR data. In particular, the LiDAR data contains information about each point's position, elevation, and intensity in the point cloud. A heuristic approach was adopted to determine the optimal intensity threshold for filtering. The threshold is gradually reduced until lane markings and most traffic signs are detected, even if other objects are retained. Highly reflective objects, such as traffic signs and lane markings, have high-intensity readings compared

to other points. Traffic signs must be painted with retroreflective material to meet the visibility requirements of the MUTCD under poor lighting conditions. As a result, by filtering LiDAR points by intensity, high-reflectivity points, such as traffic signs and lane markings, can be preserved. Thus, the intensity filter is applied to isolate traffic signs and lane markings from other objects in the point cloud data. Since the traffic signs and lane markings are the highly reflective objects among the previously filtered group of points, the filter successfully separates the traffic signs and lane markings from other points. As shown below, the process of removing outlying points is carried out using statistical outlier removal (SOR), defined by Equations 3-6.

To initiate the process, Equation 3 is employed to compute the average squared Euclidean distance  $\bar{d}_+$  to the  $k$  nearest neighbouring points for every point  $m_i \in M$ . Then, based on proximity, each point  $m_i$  is added to a local cluster of points  $C_L \in C$ , where  $C$  denotes the complete set of point clusters.

$$\bar{d}_+ = \frac{\sum_{+} Ndist(k, m_+)}{J} \quad (3)$$

The squared Euclidean distance of the  $k$ -th closest neighbour to  $m_i \in M$  is represented by  $Ndist(k, m_i)$ . Supplementary information is computed to facilitate the elimination of outliers. This encompasses the mean distance to the nearest neighbour for all points ( $\mu$ ), as shown in Equation 4, the standard deviation of nearest neighbour distances ( $\xi$ ), as shown in Equation 5, and the aggregate number of points in all clusters utilized ( $\mu_u$ ) as shown in Equation 6.

$$\mu = \frac{\sum_{+} d_{+}}{J} \quad (4)$$

$$\xi = \sqrt{\frac{\sum_{+} (d_{+} - \mu)^2}{J}} \quad (5)$$

$$\mu_u = \frac{\sum_{+} NumberPoints(C_j)}{U} \quad (6)$$

$C_u$  denotes the used clusters, and  $U$  represents the total number of used clusters. Subsequently, points with distances greater than a predefined value ( $\alpha$ ) of standard deviations away from the mean distance are removed through a filtering process, as depicted in the following:

$$FinalPoints = \{m_+ \in M \mid \mu - \alpha\xi \leq \bar{d}_+ \leq (\mu + \alpha\xi)\} \quad (7)$$



### 4.3 Point Extraction

The next step involves utilizing the refined cloud to establish passing lane zones and extract their characteristics. Within the filtered cloud, distinct signs and lane markings are detected by clustering adjacent points into groups using Density-Based Spatial Clustering of Applications with Noise (DBSCAN). This technique groups points by proximity and number of hits, where the hit count refers to the number of points in a cluster. Proximity limits the distance between points that can be deemed as part of the same cluster, excluding small groups or points that are far apart. Suitable values for proximity and hit count were selected to yield optimal outcomes.

Typical lane markings include both dashed lines, each 3 m ( $\approx 9.84$  ft) in length and spaced 6 m ( $\approx 19.69$  ft) apart, as well as solid lines. To define clusters of dashed lines, a threshold of 3 m ( $\approx 9.84$  ft) is used, based on the geometry of the markings and the density of the LiDAR data (300 points/m<sup>2</sup>). Clusters containing between 10 and 100 points and a length of up to 3 m ( $\approx 9.84$  ft) are identified as “dashed” marking lines, while clusters with over 100 points and a length greater than 3 m ( $\approx 9.84$  ft) are classified as “solid” marking lines. Using the standard lengths of "dashed" and "solid" lane markings, the successful extraction of lane markings and identification of passing lane zones was possible for all analyzed highway segments using these criteria. These results will be used for model verification and generative design for each road segment.

A minimum hit count threshold of 17 was used to identify traffic sign clusters, meaning that any group with fewer than 17 points was not considered a cluster. Additionally, a proximity parameter threshold of 1.0 m was used, such that if the distance between adjacent points in a group was greater than 1 m, those points were not included in the same cluster. These specific thresholds were chosen because they were the most effective in minimizing the identification of other high-intensity objects, such as road markings and license plates, and in identifying only traffic sign clusters. Next, ground truth data on traffic signs along highway segments were gathered manually from Google Street View. Images were visually verified, and the name of each sign along with the number of signs on each segment was documented.

## 4.4 Transforming Point Data into 3D (or 2D) Mesh Structures

Upon completing the extraction of passing lane characteristics, we proceed to the subsequent stage of our analysis. It is important to note that although features such as intensity were beneficial in the previous step, we now exclusively focus on the XYZ columns as they contain the most relevant information. These columns are then arranged based on their direction vector along the x-axis.

When analyzing lane markings, the typical recommendation is to arrange them according to the direction vector of all points. Nevertheless, it has been noticed that the majority of these markings tend to align with the x-axis direction. This observation allows us to temporarily justify the assumption of sorting them based on the x-axis direction vector. When roads were not aligned with the x-direction, a rotation was applied to all the points within the passing lane, effectively aligning them with the x-direction. This adjustment proved highly advantageous, greatly simplifying the subsequent stages of the analysis. For the sign files, it is advisable to utilize the road direction vector and consider how the forward and backward directions of the signs are determined.

In the road representation context, addressing the abundance of points present along the road network is essential. Given the extensive length of roads, utilizing bounding shapes becomes imperative to prevent the formation of an excessively large encompassing region. To achieve this, the points are effectively partitioned into smaller groups, each containing a specified number of points denoted as  $N$ . Through experimentation,  $N$  has been determined to be 1000. In the given context, opting for a grouping size of 1000 points proves suitable due to its capacity to facilitate efficient data processing, grant control over bounding shapes, sustain an acceptable point density, and its empirical validation as an appropriate parameter for mitigating the challenges associated with the abundance of Lidar points within the road network. As previously noted, it is worth emphasizing that Lidar point densities on the road surface may exhibit variations ranging from 150 to 1000 points per square meter. By electing  $N$  as 1000, the assurance is that, on average, each group encapsulates an area equivalent to 1 square meter (calculated as 1000 points divided by 1000 points per square meter). This meticulous approach contributes to the preservation of an appropriate point density within each group, thereby enabling the accurate capture of intricate road surface details. It is worth noting that selecting an excessively large value for  $N$  would result in a single, cohesive entity, whereas opting for an excessively small value would introduce irregular

gaps and numerous shapes with a high triangle count, consequently impeding search efficiency. Consequently, each group of points is treated as an individual entity rather than being considered mere components of a single comprehensive road structure. This distinction holds significant importance and serves as a foundation for the subsequent discussion on the relationships we introduce, which will be further elaborated.

When it comes to grouping points, there are two effective strategies to consider. The first approach involves creating a bounding box, which encapsulates the points within a rectangular region. This method is beneficial for simplifying the representation of the road network. The second approach is to derive the convex hull, which determines the smallest convex polygon enclosing all the points from a top-down XY perspective. By extruding the shape based on the minimum and maximum  $Z$  values, the resulting volume captures the three-dimensional characteristics of the road.

In the case of two-dimensional scenarios where a third dimension is irrelevant, employing either the bounding box or the convex hull method is sufficient. The bounding box provides a rectangular envelope encompassing the points, while the convex hull creates a polygonal shape that tightly wraps around the points, accounting for their spatial arrangement.

The ear clipping technique is utilized to achieve a triangulated representation of the road shape. This algorithm effectively decomposes the shape into a series of triangles by progressively removing ear-like regions from the polygon until all remaining vertices are connected. The resulting triangulation facilitates efficient rendering and spatial analysis of the road geometry.

Regarding data organization, road files are labelled as "Marking" and classified under the specific type "Road." This labelling and categorization system aids in managing and identifying road-related data within the larger dataset context.

The representation of signs follows a straightforward procedure. To begin with, the sign's shape can be derived by employing either the bounding box or the convex hull method when observing it from a top-down perspective. This allows for accurate capturing of the sign's boundaries. It is extruded along the  $Z$ -axis to add depth to the sign, resulting in a three-dimensional representation.

Notably, sign objects typically do not necessitate the splitting of points, as the number of points in a sign file tends to remain below 1000. Thus, the complexity associated with point grouping and separation, often encountered in the case of roads, is significantly reduced for signs.

This streamlines the data processing pipeline, enabling more efficient handling of sign-related information.

Each sign file is named after its corresponding object to ensure systematic organisation. This naming convention facilitates easy retrieval and association of data during subsequent analysis. Additionally, the type "Sign" is assigned to these files, aiding in the classification and categorization of sign objects within the broader context of the research.

## 4.5 Rule Language

The rule language is designed to express various types of rules, including geometrical and non-geometrical properties of objects, whether actual or virtual elements and geometrical relations between pairs of elements. Additionally, the rule language allows for the definition of complex rules that involve logical compositions of the aforementioned basic rules. The design of this rule language aims to provide a flexible and comprehensive framework for describing and analyzing properties and relationships within the IFC system.

Several geometric rules were introduced in the preceding study [51], derived primarily from interior rules. It is important to note that despite these new introductions, numerous fundamental relationships, such as distance, facing, and above, remain applicable and relevant in the current context. These enduring relationships play a crucial role in the ongoing analysis. Three additional relations were introduced to enhance the rule expressiveness within the system. Firstly, the RoadPathDistance relation was implemented to address the limitations of measuring distances "as the crow flies," or the standard distance calculations, which typically consider the shortest straight-line distance between two points. Instead, RoadPathDistance accounts for the actual road network by determining the nearest road segment and corresponding point to the start point. This process is repeated iteratively, finding the closest road segment and pointing to the previous point until reaching the road segment nearest to the goal point. By incorporating road paths, the RoadPathDistance relation provides a more accurate distance measure along the road network.

Secondly, the LeftSideOf relation was introduced, which involves calculating the cross product between the vector from the centre of an object to a specific point and the object's forward direction from its centre. If the cross-product result is greater than 0, the relation evaluates to true;

otherwise, it evaluates to false. This relation helps determine whether a given point lies on the left side of an object regarding its orientation.

Conversely, the RightSideOf relation serves as the opposite of the LeftSideOf relation. It also involves calculating the cross product between the vector from the centre of an object to a point and the object's forward direction. If the cross-product result is greater than 0, the relation evaluates to true; otherwise, it evaluates to false. Table 3 presents geometric relations employed to enhance rule expressiveness.

Table 3: Geometrical Relations for Rule Expressiveness

| <b>Relation</b>  | <b>Description</b>   |
|------------------|--|
| RoadPathDistance | Calculates distance along the road network from start to goal points.                |
| LeftSideOf       | Evaluates if a point is on the left side of an object based on vector cross product. |
| RightSideOf      | Determines if a point is on the right side of an object.                             |
| IsAbove          | Determines if one object is positioned above another.                                |

Within the BIMKit's framework, an inventory of objects has been defined, encompassing various elements. Several new object types were introduced to augment the existing list as part of the expansion process. Notably, the inclusion of road-related information posed a unique challenge, as it was not originally incorporated into the IFC type list that serves as the foundation for BIMKit. The new types were categorized under the CivilElement type classification to address this. The newly added object types are as follows:

1. Road
2. Sign
3. Various Road Markings (such as RoadDivergePoint, RoadConvergePoint, and more)

These Road Markings are considered "virtual objects" in the Rule Language paper, possessing geometry despite their non-physical nature. By incorporating these new types, the BIMkit's framework expands its scope to encompass road-related elements, allowing for the formulation of rules that account for these objects' unique characteristics and interactions. This extension enhances the rule expressiveness of the framework and facilitates a more comprehensive

analysis and manipulation of road geometry within the BIM context. Table 4 presents a complete description of each object and its corresponding name utilized for the analysis.

Table 4: Object Description

| Object                        | Description  |
|-------------------------------|--|
| RB-37 (rb37)                  | Sign (PASSING LANE AHEAD)                          |
| RB-34 (rb34)                  | Sign (KEEP RIGHT EXCEPT TO PASS)                   |
| RB-32 (rb32)                  | Sign (PASSING PERMITTED)                           |
| RB-31 (rb31)                  | Sign (DO NOT PASS)                                 |
| WA-33R (wa33r)                | Sign (RIGHT LANE ENDS)                             |
| Road (road)                   | Marking  |
| RoadDivergePointStart (rdps)  | Virtual (Beginning of Divergence of Passing Lane)  |
| RoadDivergePointEnd (rdpe)    | Virtual (End of Divergence of Passing Lane)        |
| RoadConvergePointStart (rcps) | Virtual (Beginning of Convergence of Passing Lane) |
| RoadConvergePointEnd (rcpe)   | Virtual (End of Convergence of Passing Lane)       |

The lack of precise labelling for individual points presents a significant obstacle in accurately determining the exact nature of the road. This challenge is further compounded when dealing with point clouds that contain missing data, leading to irregular and unpredictable shapes. Given these limitations, the most practical approach is to analyze the road in a three-dimensional context and manually assign markings to the points based on a combination of road layout knowledge and visual inspection.

To facilitate this process, the BIMkit editor plays a crucial role, offering the capability to incorporate dummy objects into the object catalogue. This functionality enables users to manually add the necessary markings, thereby enhancing the interpretation of the road shape and contributing to a more comprehensive understanding of the entire road network.

## 4.6 Model Checking

The rule-based model compliance checking process consists of four essential stages [51]: rule interpretation, model preparation, rule execution, and reporting the checking results. In the first stage, natural language design constraints are transformed into a rule language that computers can understand, enabling the automation of rule interpretation. This step is crucial for ensuring the rule language can be processed effectively.

This study's interpretation phase involves manually interpreting the rules' logic into the appropriate rule language using a rule editor interface. Once all the rules have been created, they are exported to a file that the model check application can read. The rules utilized in this study have been extracted from the Highway Geometric Design Guide of Transportation Alberta, and can be found in Table 5.

A systematic approach is employed for writing the rules to accommodate the absence of road splitting based on direction. The rules are developed and evaluated separately for each direction of the road. Initially, the focus is on checking the road signs positioned on the right side of the road. Once this evaluation is complete, the direction of the road is flipped, and the rules are applied to assess the other side of the road. This sequential methodology acknowledges the current road configuration and ensures that rule considerations align with the specific direction of the road. Although the issue of road splitting remains unaddressed due to its inherent complexity, it is recognized that modifying the rules and introducing additional properties may be necessary if road splitting were to be implemented.

Table 5: Rules

| Rule Name        | Description  | Logical Expression   |
|------------------|--|--|
| RB-34 Location 1 | All<br>RoadDivergePointStart<br>(Passing Lane Taper), Any<br>RB-34 | ALL rdps = RoadDivergePointStart<br>ANY rb34 = Sign with {Name<br>CONTAINS RB-34}<br>(rdps and rb34 MUST_HAVE<br>FacingAngleTo EQUAL 90DEG)  |
| RB-34 Location 2 | All<br>RoadDivergePointEnd,<br>Any RB-34                           | ALL rdpe = RoadDivergePointEnd<br>ANY rb34 = Sign with {Name<br>CONTAINS RB-34}<br>(rdpe and rb34 MUST_HAVE<br>FacingAngleTo EQUAL 90DEG)  |
| RB-34 road side  | All RB-34, Any Road,<br>RightOf = True                             | ALL rb34 = Sign with {Name<br>CONTAINS RB-34}<br>ANY road = Road<br>(rb34 and road MUST_HAVE<br>RightSideOfXY EQUAL True AND<br>rb34 and road MUST_HAVE<br>Distance<br>LESS_THAN_OR_EQUAL 3.5M<br>AND<br>rb34 and road MUST_HAVE<br>Distance<br>GREATER_THAN_OR_EQUAL<br>1.8M) |
| RB-37 Location   | All<br>RoadDivergePointStart,<br>Any RB-37, Distance = 2<br>Km     | ALL rdps = RoadDivergePointStart<br>ANY rb37 = Sign with {Name<br>CONTAINS RB-37}<br>(rdps and rb37 MUST_HAVE<br>RoadPathDistance EQUAL 2000M)   |



|                  |   |  |
|------------------|---|--|
| RB-37 road side  | All RB-37, Any Road,<br>RightOf = True                            | ALL rb37 = Sign with {Name<br>CONTAINS RB-37}<br>ANY road = Road<br>(rb37 and road MUST_HAVE<br>RightSideOfXY EQUAL True AND<br>rb37 and road MUST_HAVE<br>Distance<br>LESS_THAN_OR_EQUAL 3.5M<br>AND<br>rb37 and road MUST_HAVE<br>Distance<br>GREATER_THAN_OR_EQUAL<br>1.8M) |
| RB-31 Location 1 | All<br>RoadDivergePointEnd,<br>Any RB-31                          | ALL rdpe = RoadDivergePointEnd<br>ANY rb31 = Sign with {Name<br>CONTAINS RB-31}<br>(rdpe and rb31 MUST_HAVE<br>FacingAngleTo EQUAL 90DEG)  |
| RB-31 Location 2 | All<br>RoadConvergePointStart,<br>Any RB-31, Distance <=<br>120 m | ALL rcps = RoadConvergePointStart<br>ANY rb31 = Sign with {Name<br>CONTAINS RB-31}<br>(rcps and rb31 MUST_HAVE<br>RoadPathDistance<br>LESS_THAN_OR_EQUAL 120M)   |
| RB-31 Location 3 | All<br>RoadConvergePointEnd,<br>Any RB-31                         | ALL rcpe = RoadConvergePointEnd<br>ANY rb31 = Sign with {Name<br>CONTAINS RB-31}<br>(rcpe and rb31 MUST_HAVE<br>FacingAngleTo EQUAL 90DEG)   |
| RB-31 road side  | All RB-31, Any Road,<br>LeftOf = True                             | ALL rb31 = Sign with {Name<br>CONTAINS RB-31}  |

|                 |   |   |
|-----------------|---|---|
|                 |   | <p>ANY road = Road<br/>         (rb31 and road MUST_HAVE LeftSideOfXY EQUAL True AND<br/>         rb31 and road MUST_HAVE Distance<br/>         LESS_THAN_OR_EQUAL 3.5M<br/>         AND<br/>         rb31 and road MUST_HAVE Distance<br/>         GREATER_THAN_OR_EQUAL 1.8M)</p>   |
| RB-32 Location  | All RoadDivergePointStart (Shoulder Taper), Any RB-32 | <p>ALL rdps = RoadDivergePointStart<br/>         ANY rb32 = Sign with {Name CONTAINS RB-32}<br/>         (rdps and rb32 MUST_HAVE FacingAngleTo EQUAL 90DEG)</p>  |
| RB-32 road side | All RB-32, Any Road, LeftOf = True                    | <p>ALL rb32 = Sign with {Name CONTAINS RB-32}<br/>         ANY road = Road<br/>         (rb32 and road MUST_HAVE LeftSideOfXY EQUAL True AND<br/>         rb32 and road MUST_HAVE Distance<br/>         LESS_THAN_OR_EQUAL 3.5M<br/>         AND<br/>         rb32 and road MUST_HAVE Distance<br/>         GREATER_THAN_OR_EQUAL 1.8M)</p> |

|                       |   |   |
|-----------------------|---|---|
| Road Split Length     | The length of the split road segment should be between 1.5 and 2 km | ALL rdps = RoadDivergePointStart<br>ALL rcpe = RoadConvergePointEnd<br>(rdps and rcpe MUST_HAVE RoadPathDistance GREATER_THAN_OR_EQUAL 1500M AND rdps and rcpe MUST_HAVE RoadPathDistance LESS_THAN_OR_EQUAL 2000M) |
| Sign Road Dist        | Sign distance to roadside   | ALL sign = Sign<br>ANY road = Road<br>(sign and road MUST_HAVE Distance LESS_THAN_OR_EQUAL 3.5M AND sign and road MUST_HAVE Distance GREATER_THAN_OR_EQUAL 1.8M)  |
| Sign Road Rule        | All Sign, All Road, IsAbove = False                                 | ALL sign = Sign<br>ALL road = Road<br>(sign and road MUST_HAVE IsAbove EQUAL False)   |
| Sign to Sign Distance | Equal signs   | ALL s1 = Sign<br>ALL s2 = Sign<br>(s1 and s2 MUST_HAVE Distance GREATER_THAN 1M)  |
| WA-33R Location 1     | All RoadConvergePointStart, Any WA-33R, Distance = 300 m            | ALL rcps = RoadConvergePointStart<br>ANY wa33r = Sign with {Name CONTAINS WA-33R}   |

|                   |  |   |
|-------------------|--|---|
|                   |  | (rcps and wa33r MUST_HAVE RoadPathDistance EQUAL 300M)  |
| WA-33R Location 2 | All RoadConvergePointStart, Any WA-33R | ALL rcps = RoadConvergePointStart<br>ANY wa33r = Sign with {Name CONTAINS WA-33R}<br>(rcps and wa33r MUST_HAVE FacingAngleTo EQUAL 90DEG)   |
| WA-33R road side  | All WA-33R, Any Road, RightOf = True   | ALL wa33r = Sign with {Name CONTAINS WA-33R}<br>ANY road = Road<br>(wa33r and road MUST_HAVE RightSideOfXY EQUAL True AND wa33r and road MUST_HAVE Distance LESS_THAN_OR_EQUAL 3.5M AND wa33r and road MUST_HAVE Distance GREATER_THAN_OR_EQUAL 1.8M) |

In the provided table, three specific rules were designated as error-related rules (or Hard Constraint), which held utmost importance and had to be fully satisfied without compromise. These rules specifically centred around the positioning of traffic signs, with the criteria encompassing situations where a) signs were situated too close or too far from the road, b) signs were positioned above the road, and c) the requirement for maintaining a minimum distance of 1 meter between two signs to avoid duplications.

Notably, these error-related rules were non-negotiable and required strict adherence in the context of generative design. These rules were deemed critical as they directly influenced the effectiveness and safety of the passing lane. Any deviation or failure to comply with these rules would be considered a substantial error and necessitate corrective action.

Conversely, the remaining rules were classified as warning-related rules (Soft Constraint). These warning-related rules encompassed a broader range of important criteria to consider but carried a lesser degree of severity regarding their impact on the passing lane's functionality and safety. Although these rules demanded attention and compliance, they were comparatively less critical than error-related ones.

The second stage involves dealing with the information contained within the model. Sometimes, this information may be disorganized or not explicitly defined, resulting in slow and laborious checking procedures. To address this, the second stage focuses on organizing and summarizing the model's information, making it easier and more efficient to perform the compliance checks. It has been observed that the efficiency of the rule checks significantly improves when the road and signs are represented in a 2D format. This involves adjusting the Z value of the points to zero and eliminating the extrusion process. The number of triangles comprising the objects is reduced by transforming the road and signs into a 2D representation, thereby accelerating the rule evaluation process. This simplification technique potentially reduces the overall check time by approximately one-third. Consequently, the system benefits from improved computational efficiency, enabling faster and more streamlined rule assessments.

During the rule execution stage, the organized model information is used to evaluate each rule sequentially. The compliance checking process can determine whether each rule is satisfied or violated by applying the rule-based approach based on the available model data.

Finally, the last stage involves providing the user with a comprehensive report of the checking results. This report includes a rule-by-rule evaluation, indicating the compliance assessment of the model. Additionally, it contains information about any faults or issues identified during the checking process, which were instrumental in determining the overall compliance status.

Following these four stages, rule-based model compliance checking can be conducted professionally, ensuring that design constraints are accurately interpreted, model information is effectively organized, rules are executed systematically, and detailed reports are generated to facilitate compliance evaluation.

## 4.7 Generative Design

Enhancing the design of passing lanes can prove to be a demanding endeavour, primarily due to the many design restrictions that must be considered. However, by harnessing the power of computational methods to generate and assess various design alternatives, the time required for this process can be significantly reduced [52]. The generative design process necessitates the inclusion of three key components: a Performance Metric, a Configuration Variation method, and a Decision-Making Response.

In assessing the quality of each stage within the generative design process, the method proposes the adoption of rule-based compliance checking as the performance metric. The previously described model-checking approach is employed, albeit with specific adjustments to the four stages involved. The first alteration occurs during the model preparation stage, adding missing traffic signs. While static model objects do not necessitate property recalculation, the addition or movement of an object requires recalculating all its relationships with other objects. The second alteration occurs during the execution stage. While a binary true or false value suffices for model-checking purposes, it is advantageous in generative design to scale the outcome of the rules. Boolean and string properties only yield a true or false result, corresponding to values of 1 or 0, respectively. However, a numeric property check can be formulated to produce a result within the range of  $[0, 1]$ . A value of 1 signifies full compliance with the rules, whereas any value less than 1 indicates varying degrees of rule violation.

In the context of configuration variation, the generative design approach requires three inputs: a Building Information Modeling (BIM) model representing an empty space, functioning as the passing lane layout, a set of objects consisting of traffic signs to be integrated, and a predefined set of design rules. This method utilizes these inputs to generate fresh configurations of the model. The procedure involves identifying suitable objects to include and determining their optimal placement locations within the design. Notably, in this specific case, the objects in focus pertain exclusively to traffic signs. Furthermore, it is noteworthy that during the generative design process, adjustments to the orientation or location Z value are deliberately omitted due to their typically apparent and self-evident nature on-site.

The decision-making process is characterized by a meticulous evaluation of various configuration changes, each undergoing thorough scrutiny. Subsequently, a selection is made based

on these evaluations to identify the most suitable configuration for further progression. On the other hand, the generative design approach adopts a greedy strategy, wherein it systematically chooses the configuration with the most favourable evaluation and iteratively continues the process from that chosen point.

Moreover, the process doesn't merely involve a single round of evaluation; instead, it is an ongoing and iterative procedure. As new information becomes available or the project progresses, the decision-making process may adapt to incorporate new considerations or reevaluate existing choices.

# Chapter 5

## Results & Discussion

To evaluate the effectiveness of the generative design methodology, experiments were conducted on 16 real-world passing lane scenarios. The approach involved applying model-checking techniques to the available passing lane samples. Initially, the point cloud data was transformed into a 3D mesh representation, creating a model of the existing lanes. By leveraging the features of these lanes and the generated model, the model-check evaluation method from the model-check library was used to calculate scores for each road segment.

The outcomes of the model-checking procedure provided pass or fail results for each utilized rule. These rule outcomes included boolean values and corresponding references with detailed rules descriptions. Additionally, the results encompassed information about each rule instance and its outcome, ensuring a thorough evaluation and analysis of individual rule performance.

The generative design methodology's effectiveness and accuracy in generating passing lane designs that deviate from the guidelines were assessed through this evaluation process. The flexibility and adaptability of this methodology in addressing unique requirements in passing lane design were demonstrated by generating designs that differed from existing norms.

The subsequent sections describe each passing lane scenario before and after applying the generative design approach. The results of each design iteration are presented, showcasing the outcomes achieved through the generative design process.



## 5.1 Passing Lane 1

The primary task involves comparing the first passing lane design generated by the system and real-world passing lane design. Specifically, the passing lane is on Highway 3, more commonly called Crowsnest Highway. Spanning a distance of 1.9 kilometres, the passing lane extends from coordinates 49.873347, -111.09544 to 49.873364, -111.068725.

The passing lane in question has been assessed for its compatibility with the existing guidelines, yielding a compatibility score of 60.580%. This score indicates that out of the 12 rules applied to evaluate the passing lane, the total score of these rules amounted to 7.270. It is important to note that this score of 7.270 does not necessarily mean that seven rules passed. The evaluation revealed that, apart from three rules that received a perfect score of 1 and passed, all others scored below 1. For example, the "WA-33R Location 2" rule received a score of 0.48. Breaking it down further, within this set of rules, the score for error-related rules amounted to 2.598 out of 3, suggesting a high level of compliance. Two of these three rules received a score of 1, but the "Sign Road Dist." rule failed, obtaining a score of 0.6. However, when considering the warning-related rules, the score was 4.672 out of 9, revealing that the total failure score for rule-compliances in this passing lane is 4.328.

Regarding signage, the passing lane exhibits an additional RB-34 sign but lacks three RB-31 signs and one RB-32 sign. To rectify this issue, necessary adjustments were implemented to ensure the inclusion of the correct number of signs and the incorporation of any missing signs into the model. The generative design runtime for this passing lane amounted to 02:37:59<sup>1</sup>, involving a comprehensive check count of 21,580.

After implementing the generative design approach, there has been a notable increase in the compatibility score of this passing lane, reaching an impressive 93.151%. This substantial improvement indicates that out of the 18 rules considered in the evaluation, a significant majority of 16.767 rules were successfully satisfied by this passing lane.

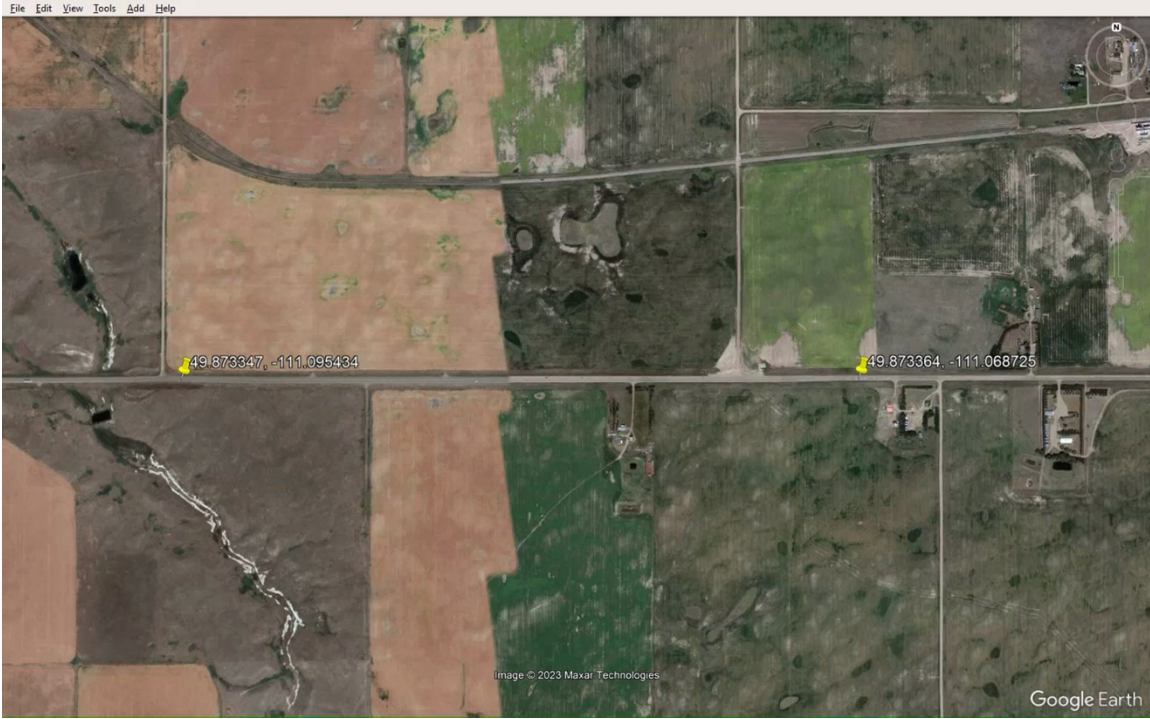
It is worth noting that all three error-related rules were met within this set of rules, demonstrating a flawless adherence to those specific guidelines. Furthermore, when it comes to

---

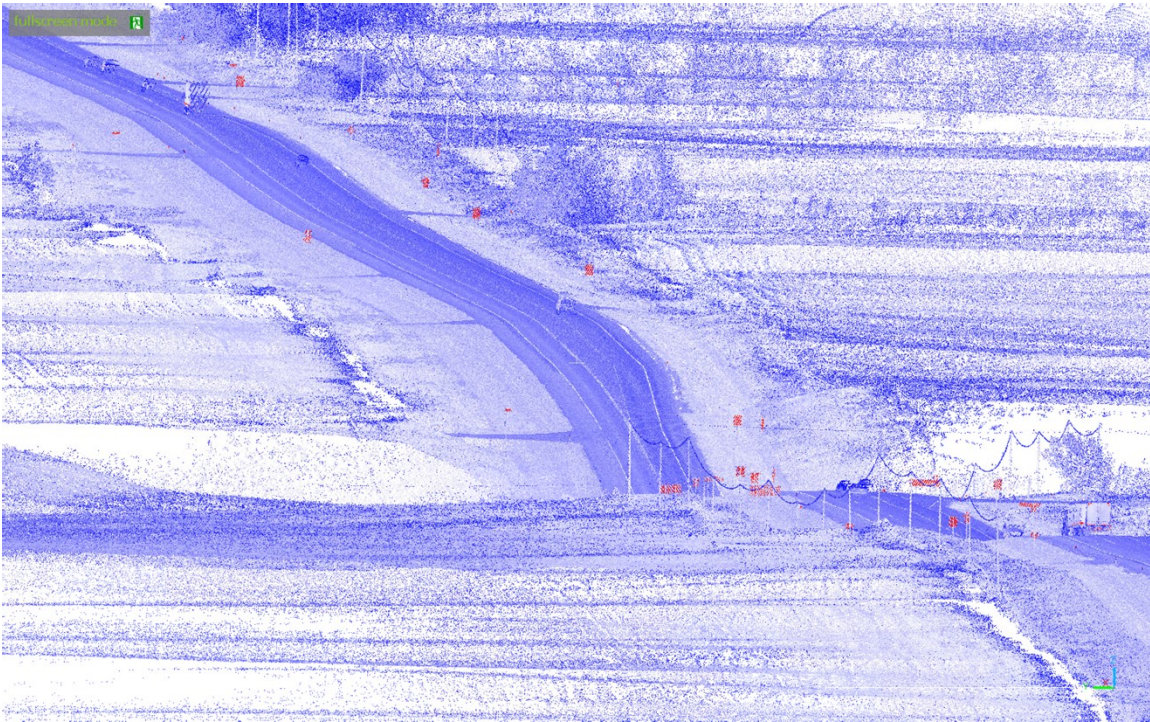
<sup>1</sup> The device used for analysis is equipped with a 12th Gen Intel(R) Core(TM) i9-12900KF processor running at 3.19 GHz, 64.0 GB of installed RAM (63.8 GB usable), and operates on a 64-bit system with no pen or touch input available for its display.

the warning-related rules, this passing lane exhibited compatibility with 13.767 out of the total 15, leaving only 1.233 rules that have not been fully met. This achievement highlights the high level of compliance achieved by the passing lane regarding the warning-related criteria, with room for further optimization to fully satisfy all the rules.

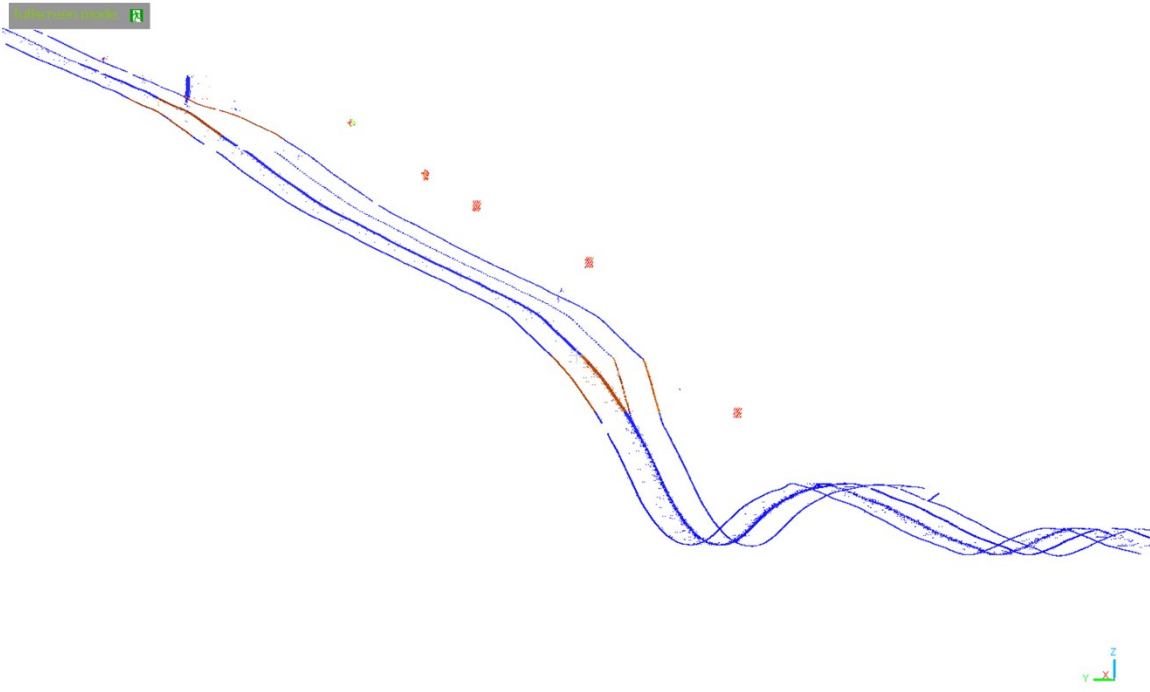
By undertaking the generative design process and making necessary adjustments, the passing lane achieved notable enhancements in overall score and adherence to guidelines. To provide a visual representation of this passing lane and its associated data, Figure 3 serves as a point of reference. The figure comprises several parts that offer valuable insights into the passing lane's characteristics. Part a of the figure showcases the precise location of the passing lane within the context of Google Earth. Part b presents the raw point-cloud file corresponding to this passing lane, while part c showcases the extracted features and characteristics specific to this particular passing lane. Finally, part d illustrates the design of the passing lane after applying the generative design process.



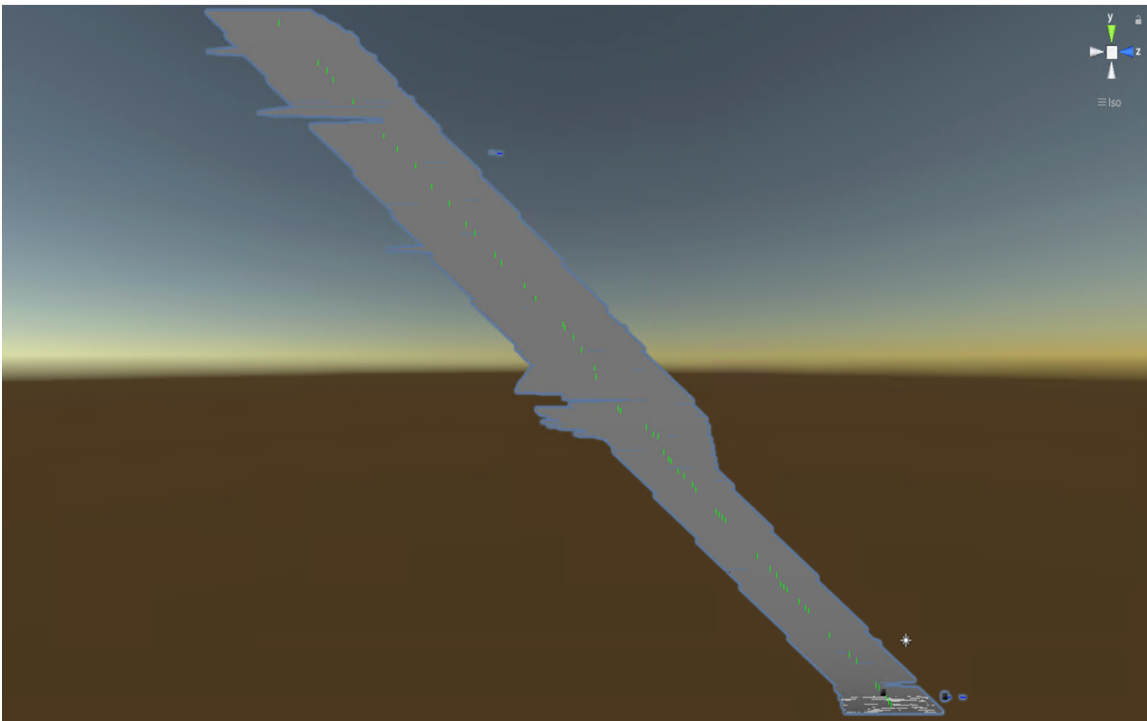
(a) Satellite Image Location



(b) Raw point-cloud



(c) Filtered point-cloud



(d) Generative Design Result

Figure 3: Results for passing lane 1 on Highway 3

## 5.2 Passing Lane 2

A comprehensive evaluation was carried out to compare the next passing lane design generated by the system with an existing real-world passing lane design. This analysis specifically focused on a passing lane on Highway 3, spanning 1.8 kilometres. The passing lane stretches between coordinates 49.873359, -111.106667 and 49.873380, -111.132048.

Upon evaluating the passing lane against the existing guidelines, it obtained a compatibility score of 58.699%. This score indicates that out of the 12 rules applied during the assessment, a total of 7.044 rules were successfully met. Further analysis revealed that the passing lane strongly complies with error-related rules, scoring 2.595 out of 3. However, there is room for improvement in satisfying warning-related rules, as the score was 4.449 out of 9, indicating that 4.551 rules were not fully satisfied.

Regarding signage, it was observed that the passing lane lacked three RB-31 signs and one RB-32 sign. Appropriate adjustments were made to ensure the correct number of signs and incorporate any missing signs into the design to address this issue. The generative design process for this passing lane took a runtime of 02:21:13 and involved a thorough check count of 19,818.

Following the implementation of the generative design approach, there was a remarkable improvement in the compatibility score, reaching an impressive 94.197%. This substantial increase indicates that out of the 18 rules considered in the evaluation, a significant majority of 16.956 rules were successfully satisfied by the passing lane.

Notably, all three error-related rules were met, showcasing a flawless adherence to those guidelines. Additionally, regarding the warning-related rules, the passing lane demonstrated compatibility with 13.956 out of the total 15, with only 1.044 rules remaining to be fully met. This achievement emphasizes the passing lane's high level of compliance with warning-related criteria while suggesting the potential for further optimization to satisfy all the rules fully.

Significant improvements were achieved in the passing lane's overall performance and adherence to guidelines by implementing the generative design process and necessary adjustments. To provide a visual representation of this passing lane and its associated data, Figure 4 serves as a valuable point of reference.

In part a of the figure, the precise location of the passing lane is depicted within the broader context of Google Earth, providing a clear understanding of its geographical placement. Part b

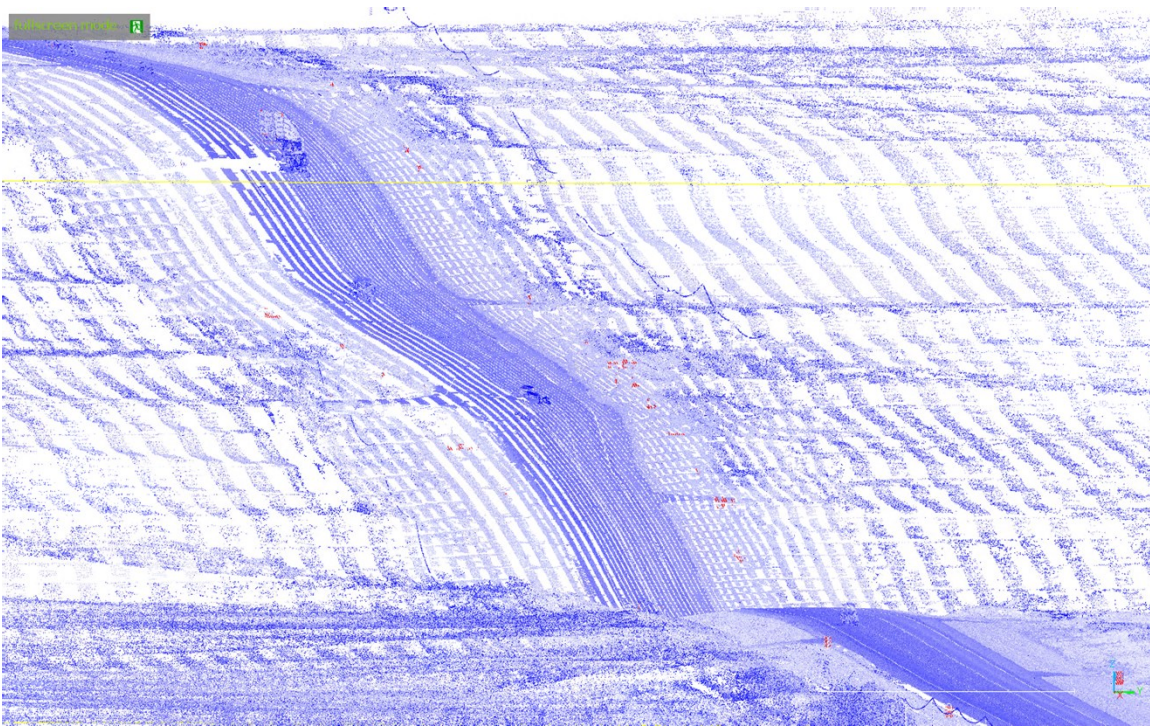
showcases the raw point-cloud file corresponding to this passing lane, providing a comprehensive visual representation of the war point-cloud data.

Moving to part c, the figure presents the extracted features and characteristics specific to this passing lane. This section offers detailed insights into the various elements and attributes of the passing lane that were analyzed during the evaluation process.

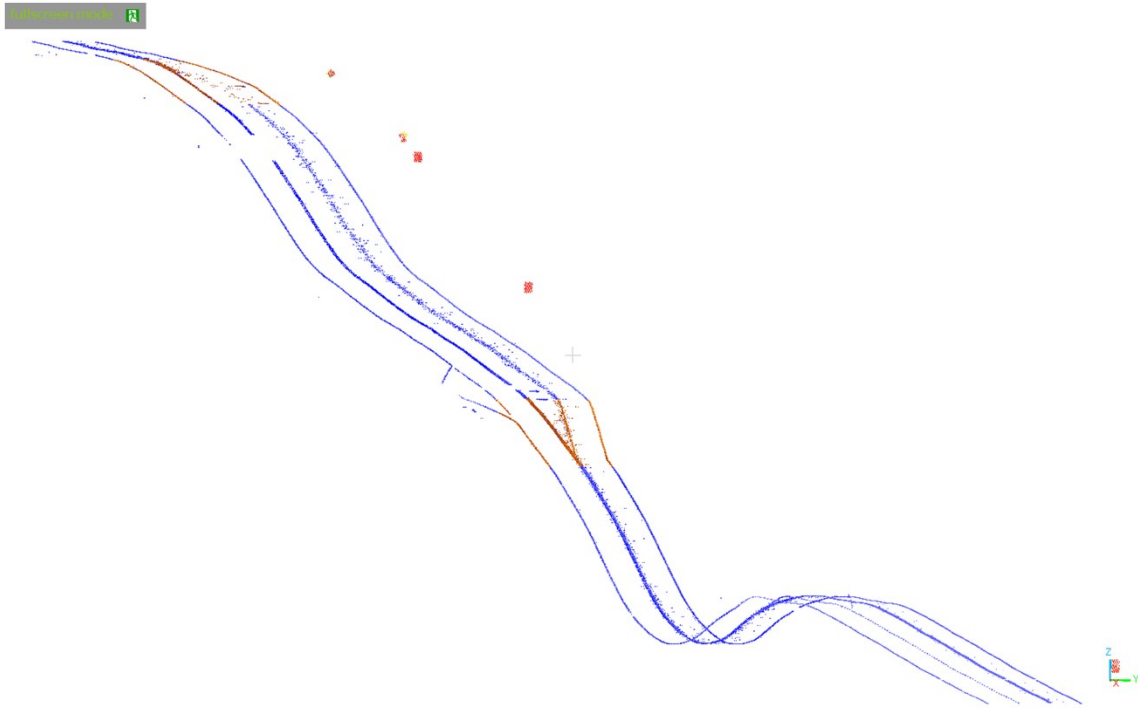
Finally, in part d of the figure, the passing lane's design is illustrated after applying the generative design process. This visual representation showcases the optimized design resulting from the integration of generative design techniques, highlighting the enhancements made to the passing lane's overall layout and functionality.



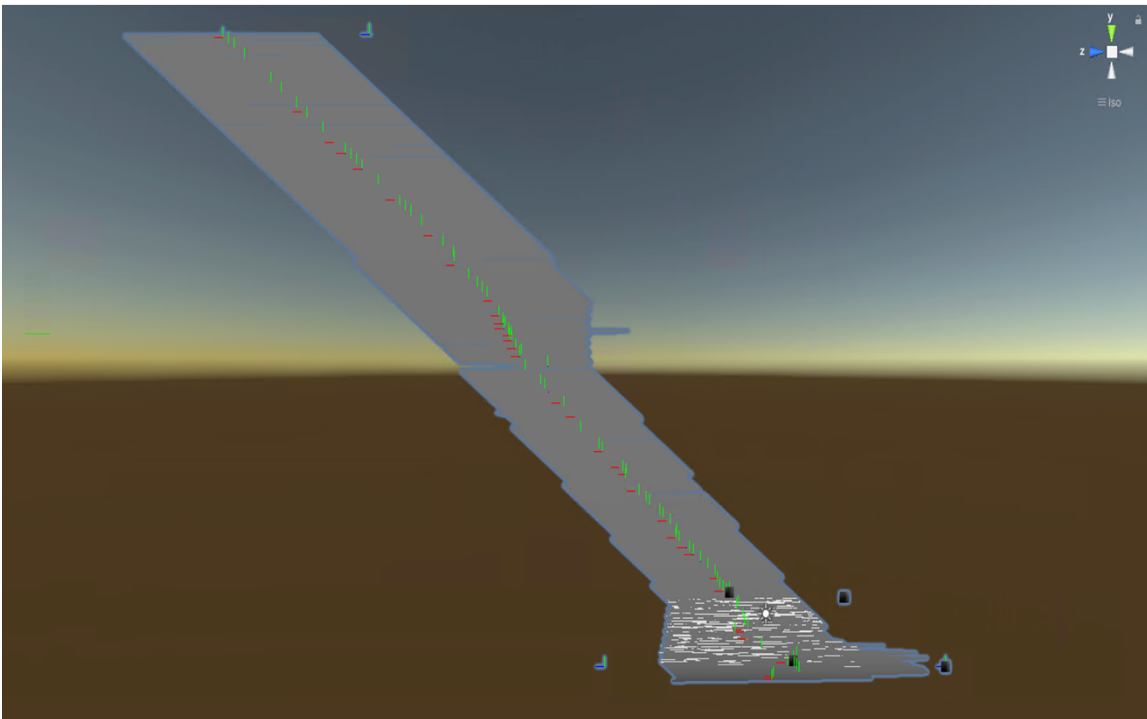
(a) Satellite Image Location



(b) Raw point-cloud



(c) Filtered point-cloud



(d) Generative Design Result

Figure 4: Results for passing lane 2 on Highway 3



### 5.3 Passing Lane 3

A thorough evaluation was conducted to compare the design of the next passing lane generated by the system with an existing real-world passing lane. This analysis focused on a specific passing lane on Highway 3, spanning 2.6 kilometres. The passing lane extends between coordinates 49.873443, -111.292349 and 49.873448, -111.255783.

The passing lane was assessed against established guidelines during the evaluation process, resulting in a compatibility score of 67.640%. This score indicates that out of the 12 rules considered, 8.117 rules were successfully met. Further examination revealed that the passing lane demonstrated strong compliance with error-related rules, achieving a score of 2.592 out of 3. However, there is room for improvement in meeting warning-related rules, as the score was 5.524 out of 9, indicating that 3.476 rules were not fully satisfied.

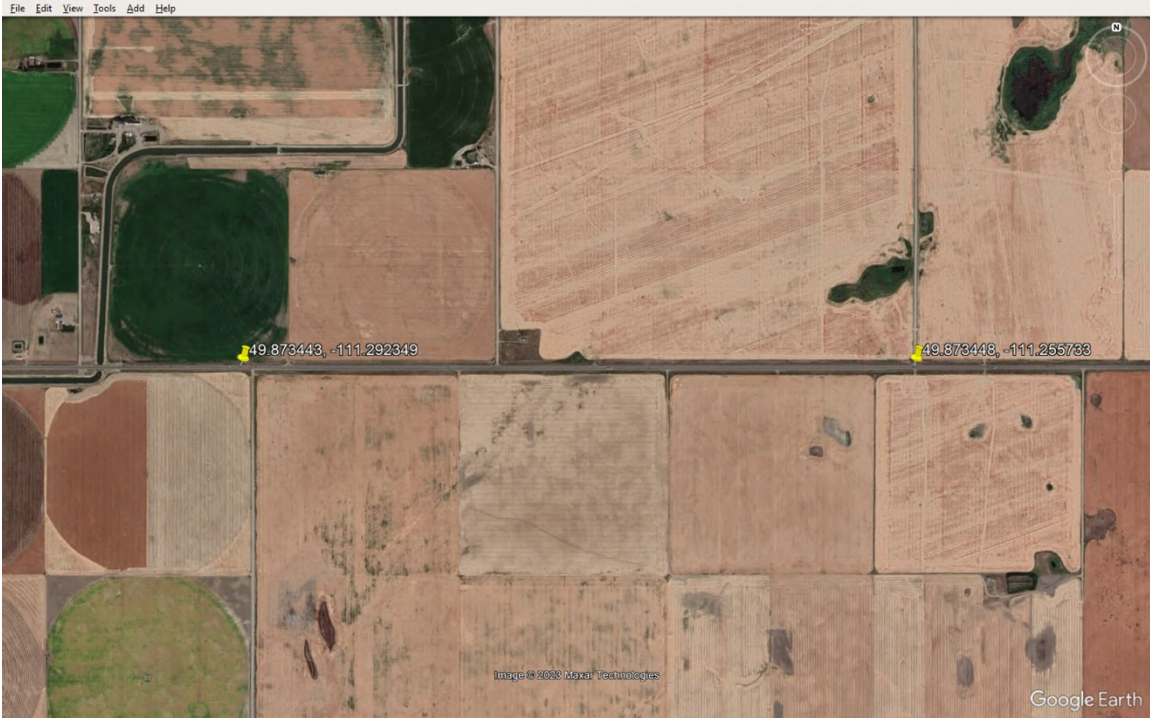
In terms of signage, it was observed that the passing lane had three additional RB-34 signs, but it lacked three RB-31 signs and one RB-32 sign. Appropriate adjustments were made to ensure the correct number of signs and incorporate any missing signs into the design to rectify this issue. The generative design process for this passing lane had a runtime of 07:06:25 and involved a comprehensive check count of 26,544.

After implementing the generative design approach, a remarkable improvement in the compatibility score was achieved, reaching an impressive 95.44%. This substantial increase indicates that out of the 18 rules considered, a significant majority of 17.18 rules were successfully satisfied by the passing lane.

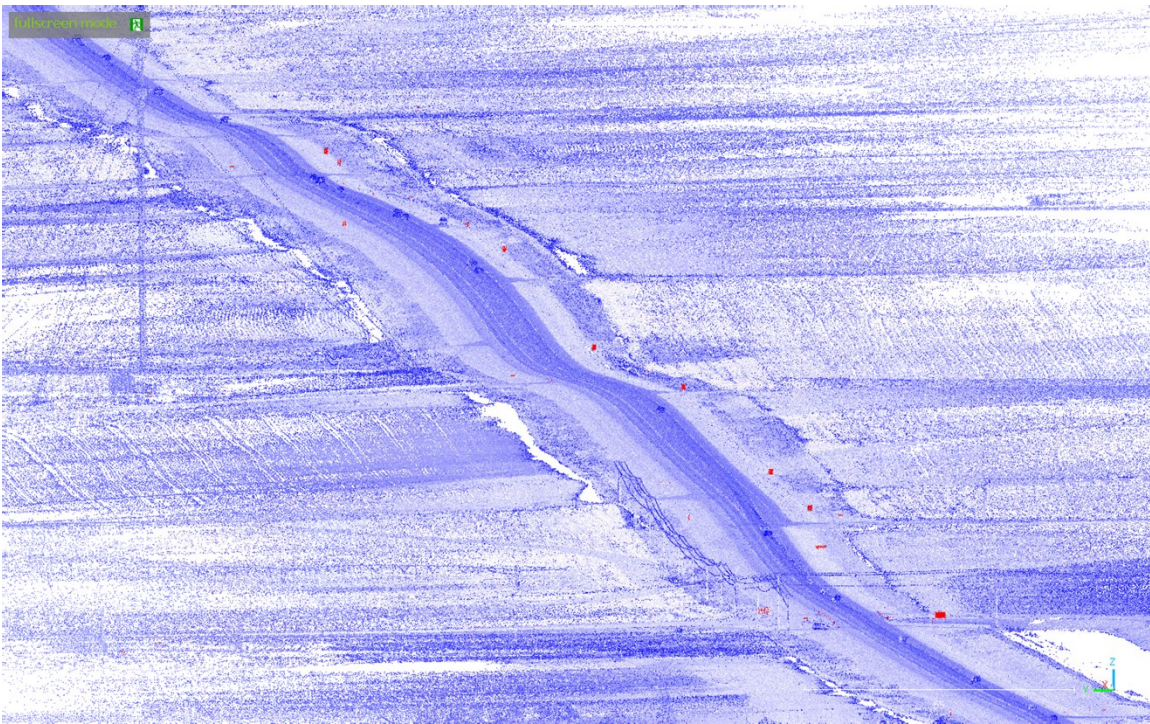
Notably, all three error-related rules were fully met, demonstrating flawless adherence to those guidelines. Moreover, concerning the warning-related rules, the passing lane exhibited compatibility with 14.18 out of the total 15, with only 0.82 rules remaining to be fully satisfied. This achievement underscores the passing lane's high level of compliance with warning-related criteria while also indicating the potential for further optimization to meet all the rules fully.

To provide a visual representation of the passing lane and its associated data, Figure 5 serves as a valuable reference. In part a of the figure, the precise location of the passing lane is depicted within the broader context of Google Earth, offering clarity on its geographical placement. Part b showcases the raw point-cloud file, providing a comprehensive visual representation of the collected data.

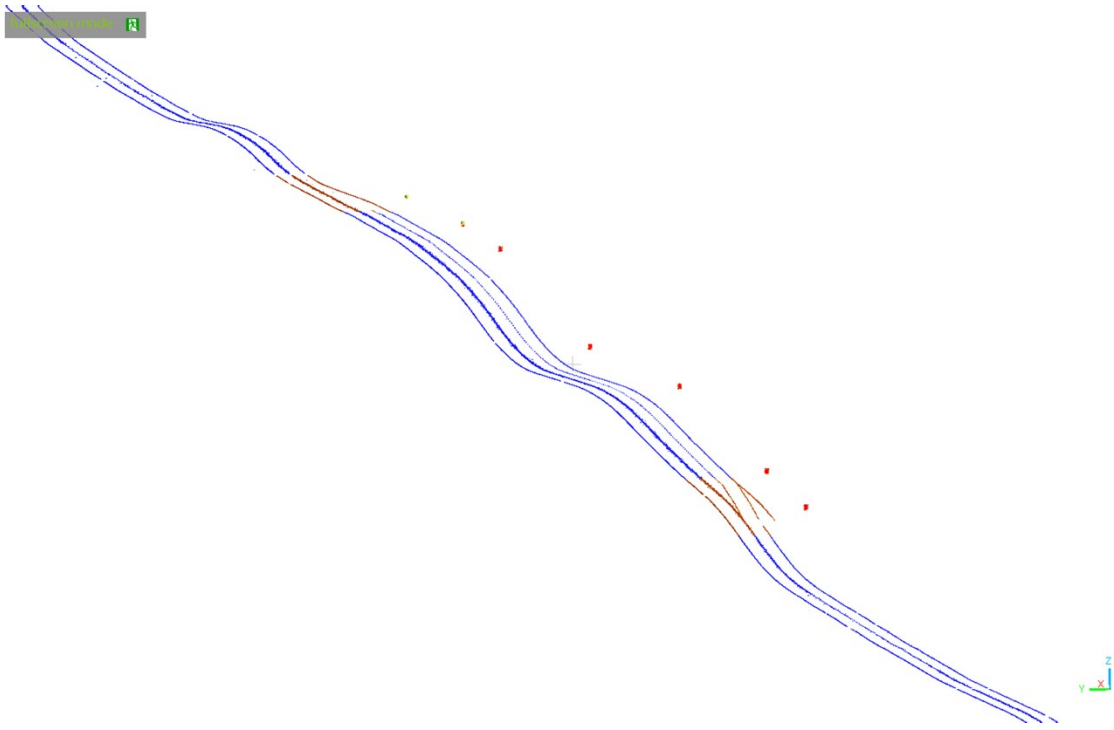
Moving to part c, the figure presents the extracted features and characteristics specific to this passing lane, providing detailed insights into the various elements analyzed during the evaluation process. Lastly, part d illustrates the passing lane's design after incorporating generative design techniques, highlighting the optimized layout and improved functionality resulting from this approach.



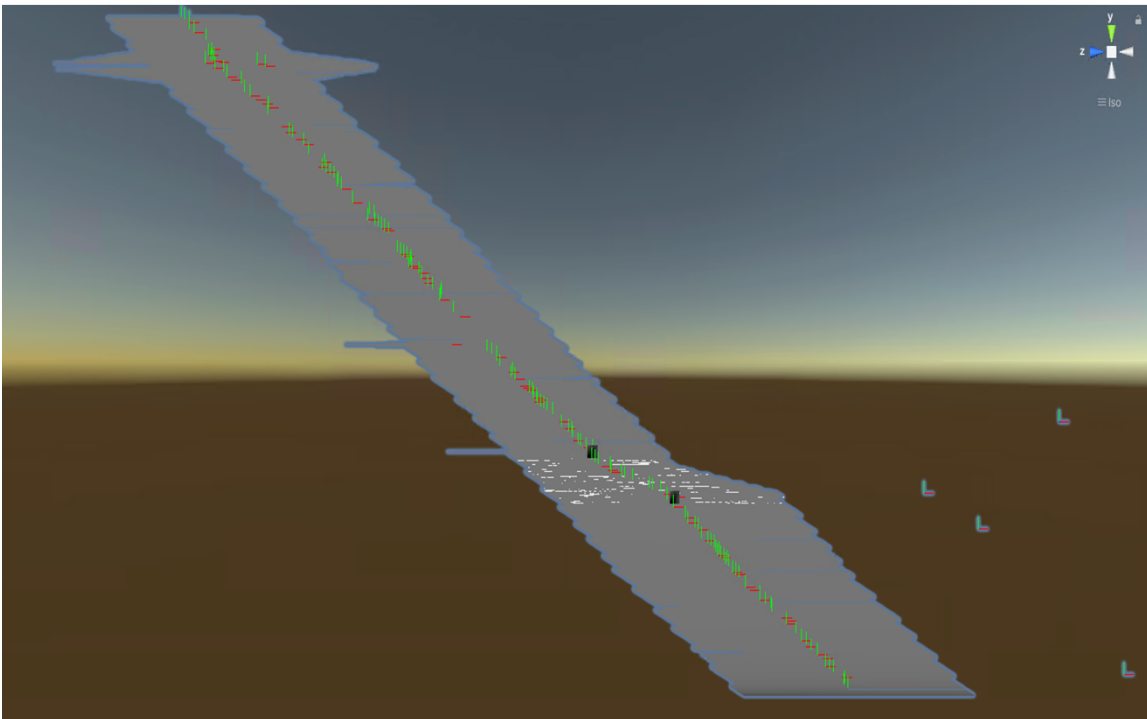
(a) Satellite Image Location



(b) Raw point-cloud



(c) Filtered point-cloud



(d) Generative Design Result

Figure 5: Results for passing lane 3 on Highway 3

## 5.4 Passing Lane 4

A thorough evaluation was conducted to compare the design of the next passing lane generated by the system with an existing real-world passing lane. This analysis focused on a specific passing lane on Highway 3, spanning a distance of 1.6 kilometres. The passing lane extends between coordinates 49.827715, -111.630585 to 49.827404, -111.607892.

The passing lane underwent a comprehensive assessment based on established guidelines during the evaluation process, resulting in a compatibility score of 66.725%. This score indicates that out of the 12 rules considered, a total of 8.007 rules were successfully met. Further analysis revealed that the passing lane strongly complies with error-related rules, scoring 2.601 out of 3. However, there is room for improvement in meeting warning-related rules, as the score was 5.406 out of 9, indicating that 3.594 rules were not fully satisfied.

Regarding signage, it was observed that the passing lane had an additional RB-34 sign, while lacking three RB-31 signs and one RB-32 sign. Appropriate adjustments were made to ensure the correct number of signs and incorporate any missing signs into the design to rectify this discrepancy. The generative design process for this passing lane had a runtime of 01:38:46 and involved a comprehensive check count of 22,060.

After implementing the generative design approach, a significant improvement in the compatibility score was achieved, reaching an impressive 95.580%. This substantial increase indicates that out of the 18 rules considered, the passing lane successfully satisfied a majority of 17.204 rules.

It is worth noting that all three error-related rules were fully met, demonstrating a flawless adherence to those specific guidelines. Furthermore, regarding the warning-related rules, the passing lane exhibited compatibility with 14.204 out of the total 15, with only 0.796 rules remaining to be fully satisfied. This achievement highlights the passing lane's high level of compliance with warning-related criteria signalling the potential for further optimization to meet all the rules fully.

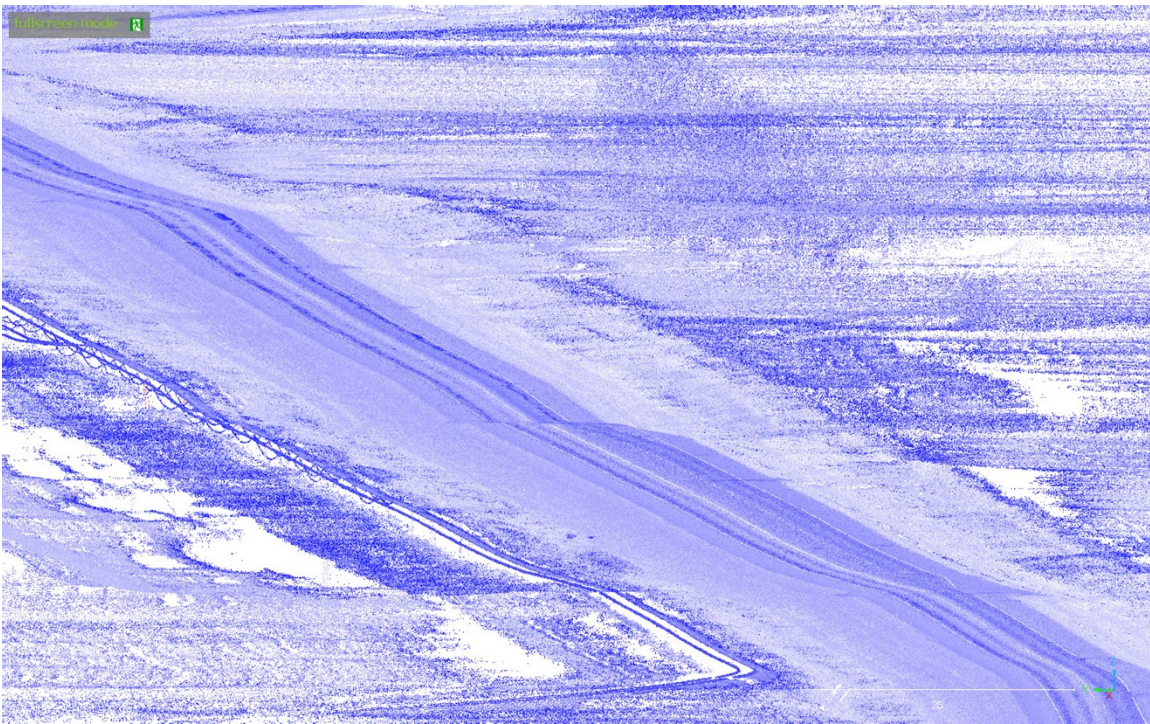
To provide a visual representation of the passing lane and its associated data, Figure 6 serves as a valuable reference. Part a of the figure showcases the precise location of the passing lane within the broader context of Google Earth, providing a clear understanding of its

geographical placement. Part b presents the raw point-cloud file, offering a comprehensive visual representation of the collected data.

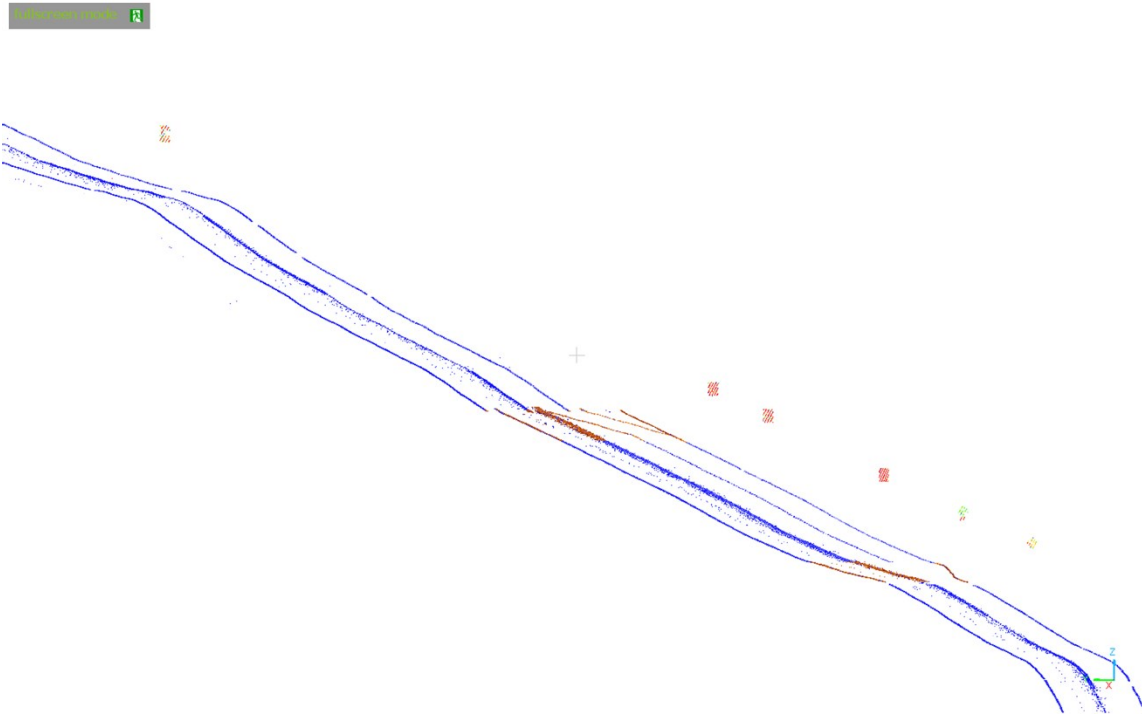
Moving on to part c, the figure presents the extracted features and characteristics specific to this passing lane, providing detailed insights into the various elements analyzed during the evaluation process. Finally, part d illustrates the passing lane's design after incorporating generative design techniques, highlighting the optimized layout and improved functionality resulting from this approach.



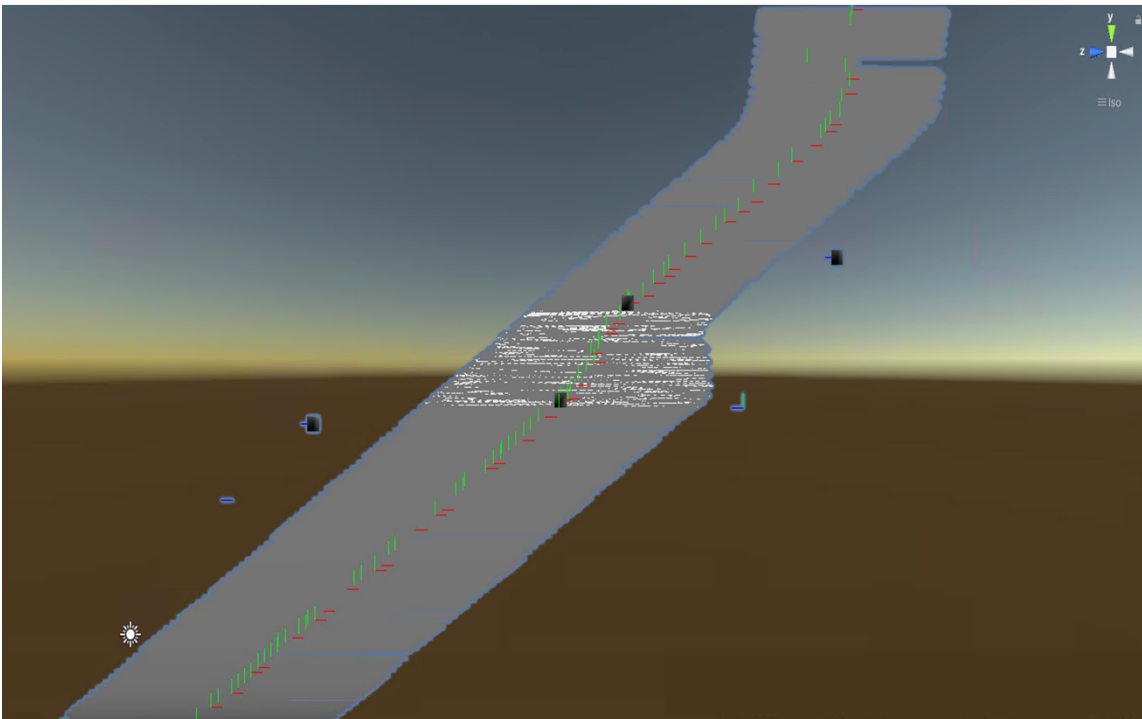
(a) Satellite Image Location



(b) Raw point-cloud



(c) Filtered point-cloud



(d) Generative Design Result

Figure 6: Results for passing lane 4 on Highway 3



## 5.5 Passing Lane 5

A comprehensive evaluation was conducted to compare the design of the next passing lane generated by the system with an existing real-world passing lane. This analysis focused on a specific passing lane on Highway 3, spanning a distance of 1.7 kilometres. The passing lane extends between coordinates 49.821330, -111.788630 to 49.817916, -111.811857.

The passing lane underwent a thorough assessment based on established guidelines during the evaluation process, resulting in a compatibility score of 59.478%. This score indicates that out of the 16 rules considered, a total of 9.517 rules were successfully met. Further analysis revealed that the passing lane strongly complies with error-related rules, scoring 2.603 out of 3. However, there is room for improvement in meeting warning-related rules, as the score was 6.914 out of 13, indicating that 6.086 rules were not fully satisfied.

In terms of signage, it was observed that the passing lane lacked one RB-34 sign, one RB-31 sign, and one RB-32 sign. Appropriate adjustments were made to ensure the correct number of signs and incorporate any missing signs into the design to address this discrepancy. The generative design process for this passing lane had a runtime of 01:32:57 and involved a comprehensive check count of 20,018.

Following the implementation of the generative design approach, a significant improvement in the compatibility score was achieved, reaching an impressive 90.467%. This substantial increase indicates that out of the 18 rules considered, the passing lane successfully satisfied a majority of 16.284 rules.

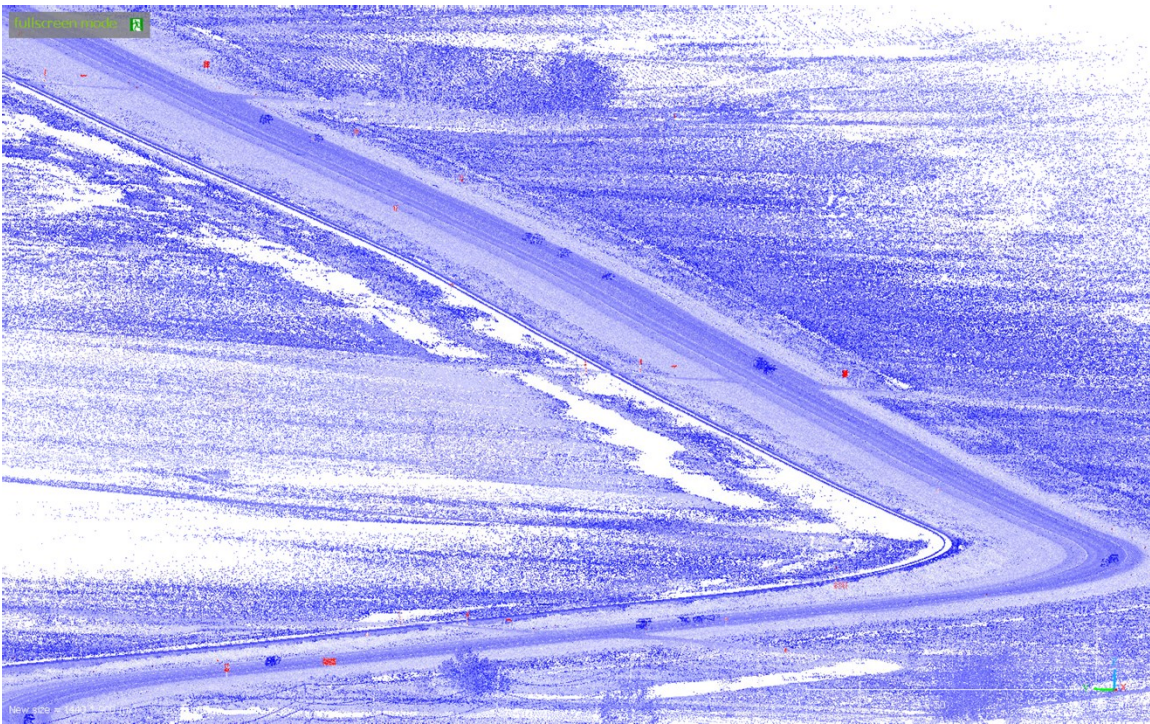
Notably, all three error-related rules were fully met, demonstrating a flawless adherence to those guidelines. Furthermore, regarding the warning-related rules, the passing lane exhibited compatibility with 13.284 out of the total 15, with only 1.716 rules remaining to be fully satisfied. This achievement highlights the passing lane's high level of compliance with warning-related criteria while also indicating the potential for further optimization to meet all the rules fully.

To provide a visual representation of the passing lane and its associated data, Figure 7 serves as a valuable reference. Part a of the figure showcases the precise location of the passing lane within the broader context of Google Earth, providing a clear understanding of its geographical placement. Part b presents the raw point-cloud file, offering a comprehensive visual representation of the collected data.

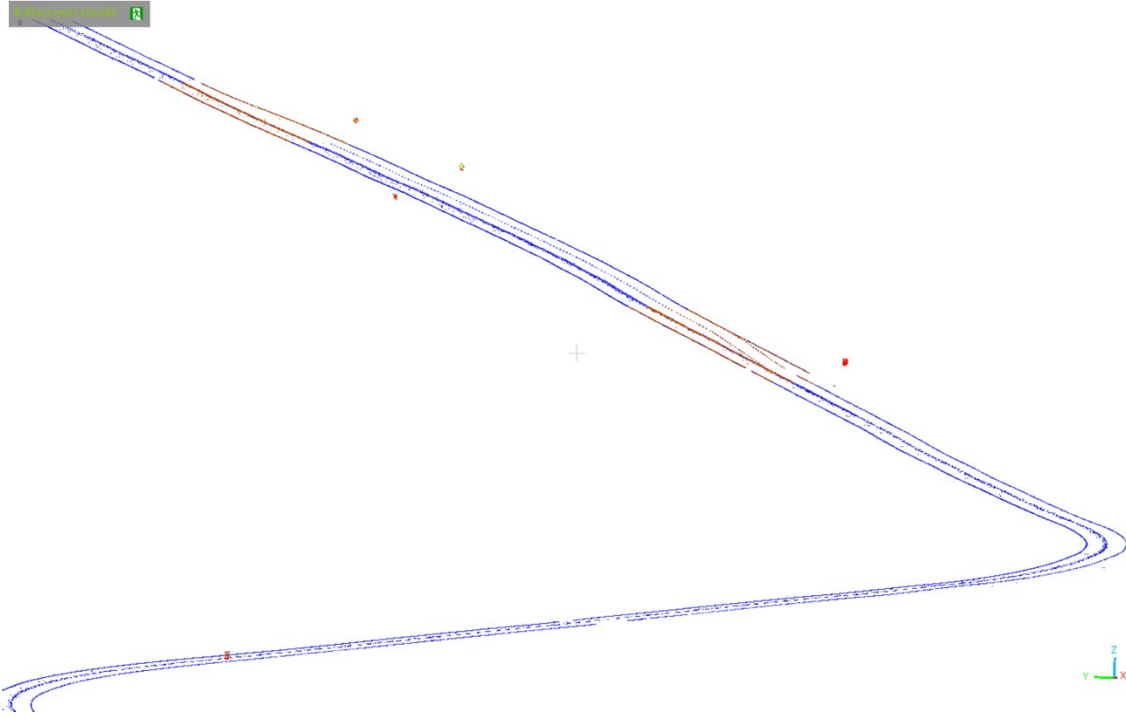
Moving on to part c, the figure presents the extracted features and characteristics specific to this passing lane, providing detailed insights into the various elements analyzed during the evaluation process. Finally, part d illustrates the passing lane's design after incorporating generative design techniques, highlighting the optimized layout and improved functionality resulting from this approach.



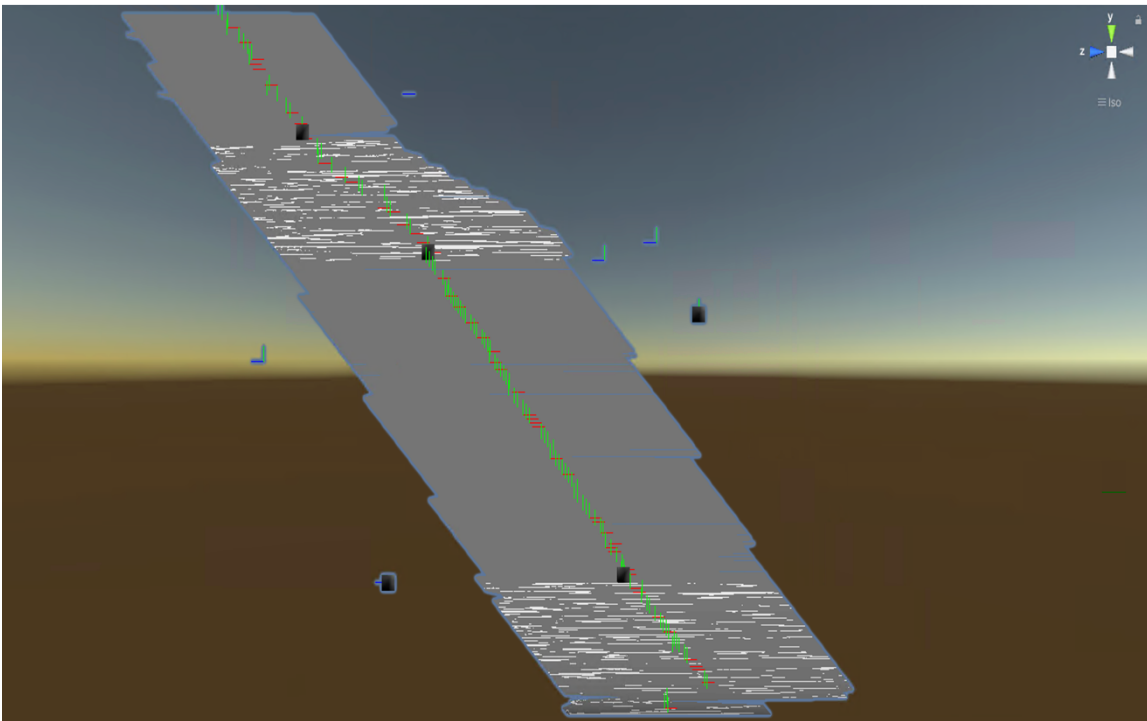
(a) Satellite Image Location



(b) Raw point-cloud



(c) Filtered point-cloud



(d) Generative Design Result

Figure 7: Results for passing lane 5 on Highway 3

## 5.6 Passing Lane 6

A comprehensive assessment was conducted to compare the design of the next passing lane generated by the system with an existing real-world passing lane. The evaluation focused on a specific passing lane located on Highway 3, with a length of 1.6 kilometres between coordinates 49.815091, -111.923428 and 49.815087, -111.945266.

The passing lane underwent a thorough analysis based on established guidelines during the evaluation process. The resulting compatibility score was 56.997%, indicating that out of the 16 rules considered, 9.119 rules were successfully met. Further examination revealed strong compliance with error-related rules, achieving a score of 2.593 out of 3. However, improvement is needed in meeting warning-related rules, with a score of 6.527 out of 13, indicating that 6.473 rules were not fully satisfied.

In terms of signage, it was observed that the passing lane had an additional RB-31 sign, but was missing one RB-32 sign and one RB-34 sign. Adjustments were made to address these discrepancies and ensure the correct number of signs in the design. The generative design process for this passing lane had a runtime of 02:53:53 and involved a comprehensive check count of 23,640.

Following the implementation of the generative design approach, a significant improvement in the compatibility score was achieved, reaching an impressive 81.989%. This indicates that out of the 18 rules considered, a majority of 14.758 rules were successfully satisfied by the passing lane.

It is important to note that all three error-related rules were fully met, demonstrating adherence to those specific guidelines. Moreover, concerning the warning-related rules, the passing lane exhibited compatibility with 11.758 out of the total 15, with only 3.242 rules remaining to be fully satisfied. This achievement underscores the passing lane's high level of compliance with warning-related criteria while also suggesting the potential for further optimization to meet all the rules fully.

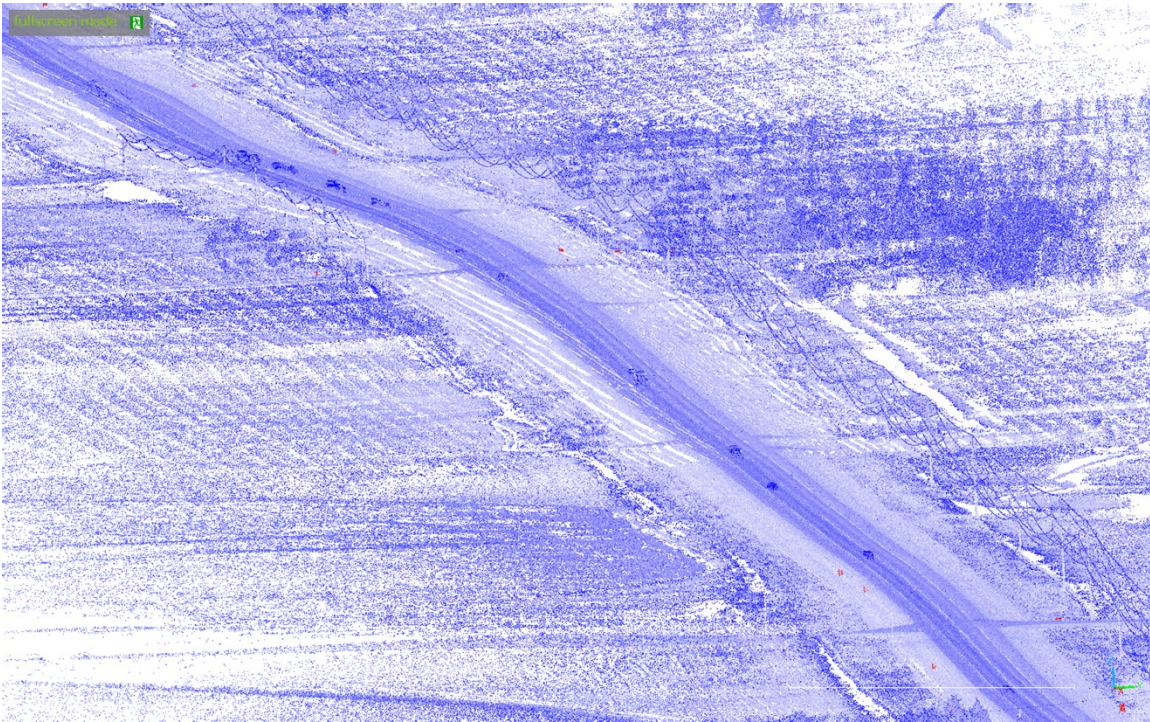
To provide a visual representation of the passing lane and its associated data, Figure 8 serves as a valuable reference. Part a of the figure showcases the precise location of the passing lane within the broader context of Google Earth, offering a clear understanding of its geographical

placement. Part b presents the raw point-cloud file, providing a comprehensive visual representation of the collected data.

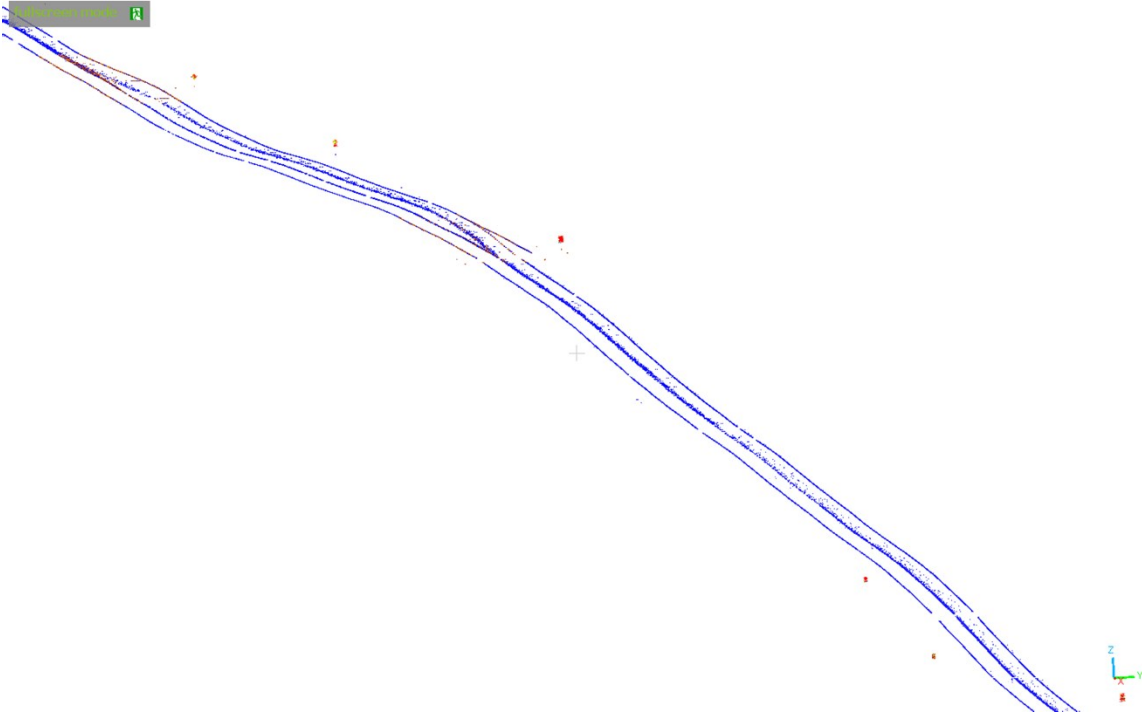
Moving on to part c, the figure presents the extracted features and characteristics specific to this passing lane, offering detailed insights into the various elements analyzed during the evaluation process. Finally, part d illustrates the passing lane's design after incorporating generative design techniques, highlighting the optimized layout and improved functionality resulting from this approach.



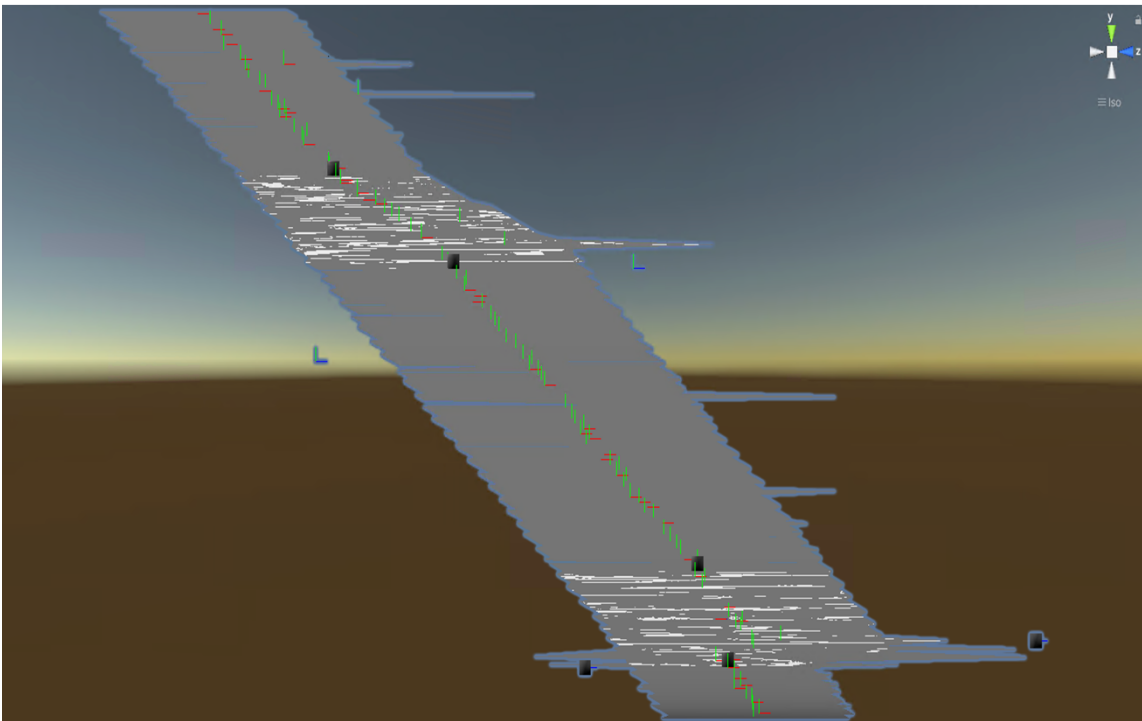
(a) Satellite Image Location



(b) Raw point-cloud



(c) Filtered point-cloud



(d) Generative Design Result

Figure 8: Results for passing lane 6 on Highway 3



## 5.7 Passing Lane 7

A thorough evaluation was conducted to compare the design of the next passing lane generated by the system with an existing real-world passing lane. This analysis focused on a specific passing lane on Highway 3, spanning a length of 1.8 kilometres between coordinates 49.922426, -110.854962 to 49.908842, -110.867662.

The passing lane underwent a comprehensive assessment based on established guidelines during the evaluation process. The resulting compatibility score was 58.611%, indicating that out of the 18 rules considered, 10.550 rules were successfully met. Further examination revealed strong compliance with error-related rules, scoring 2.615 out of 3. However, there is room for improvement in meeting warning-related rules, with a score of 7.935 out of 15, indicating that 7.065 rules were not fully satisfied.

Concerning signage, it was noted that the passing lane had an additional RB-34 sign while lacking one RB-31 sign. Adjustments were made to address these discrepancies and ensure the correct number of signs in the design. The generative design process for this passing lane had a runtime of 02:41:38 and involved a comprehensive check count of 21,840.

Following the implementation of the generative design approach, a significant improvement in the compatibility score was achieved, reaching an impressive 93.196%. This indicates that out of the 18 rules considered, the passing lane successfully satisfied a majority of 16.775 rules.

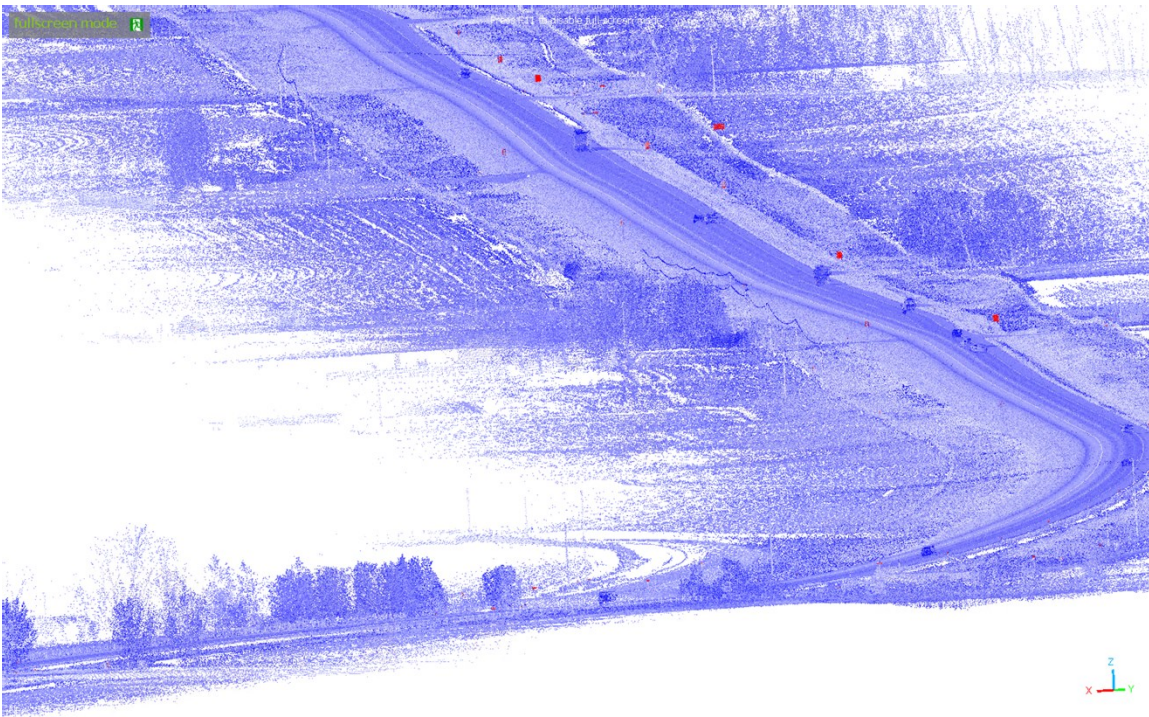
It is essential to highlight that all three error-related rules were fully met, demonstrating adherence to those guidelines. Furthermore, regarding the warning-related rules, the passing lane exhibited compatibility with 13.775 out of the total 15, with only 1.225 rules remaining to be fully satisfied. This accomplishment underscores the passing lane's high level of compliance with warning-related criteria while also suggesting the potential for further optimization to meet all the rules fully.

To provide a visual representation of the passing lane and its associated data, Figure 9 serves as a valuable reference. Part a of the figure depicts the precise location of the passing lane within the broader context of Google Earth, enabling a clear understanding of its geographical placement. Part b showcases the raw point-cloud file, offering a comprehensive visual representation of the collected data.

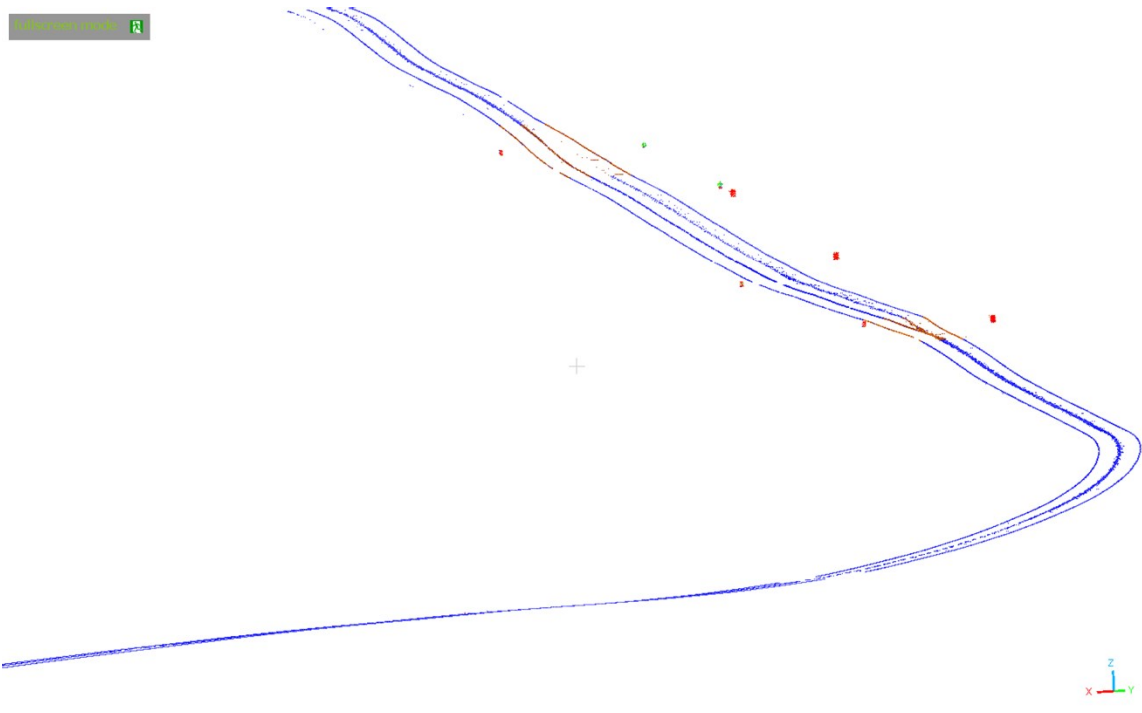
Moving on to part c, the figure presents the extracted features and characteristics specific to this passing lane, providing detailed insights into the various elements analyzed during the evaluation process. Finally, part d illustrates the passing lane's design after incorporating generative design techniques, highlighting the optimized layout and improved functionality resulting from this approach.



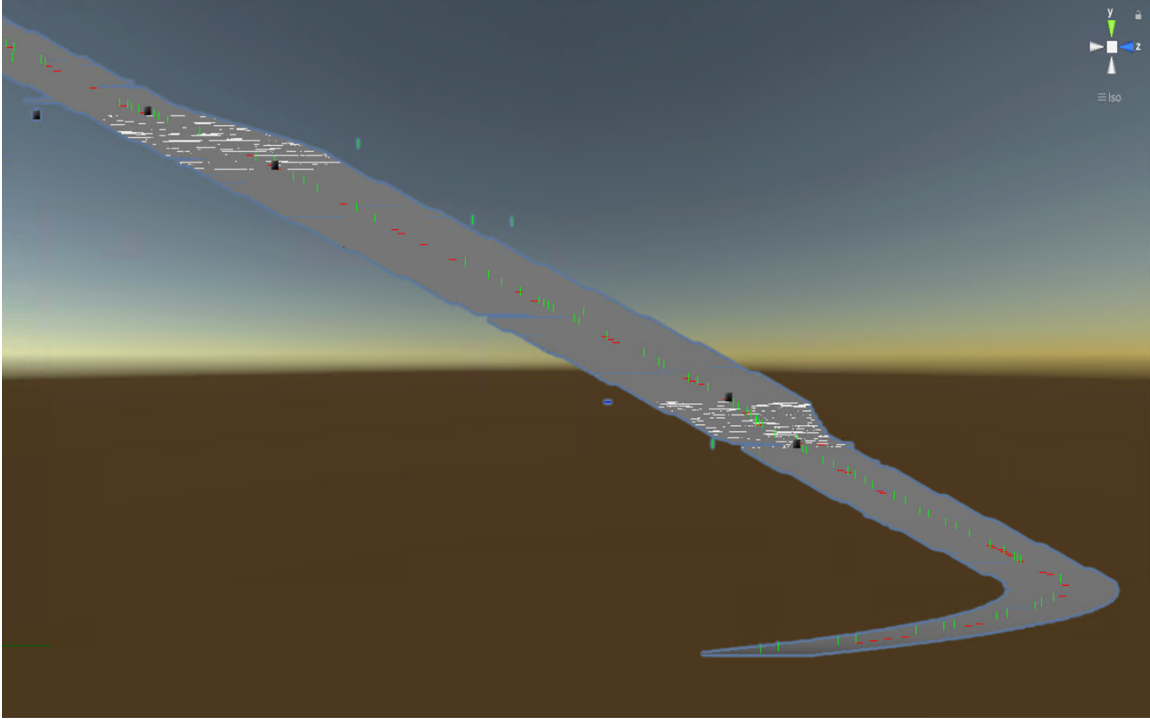
(a) Satellite Image Location



(b) Raw point-cloud



(c) Filtered point-cloud



(d) Generative Design Result

Figure 9: Results for passing lane 7 on Highway 3

## 5.8 Passing Lane 8

A comprehensive evaluation was conducted to compare the design of the next passing lane generated by the system with an existing real-world passing lane. This analysis focused on a specific passing lane located on Highway 3, spanning a length of 1.7 kilometres between coordinates 49.883389, -110.898671 to 49.894096, -110.881434.

The passing lane underwent a thorough assessment based on established guidelines during the evaluation process. The resulting compatibility score was 69.458%, indicating that out of the 14 rules considered, 9.724 rules were successfully met. Further examination revealed strong compliance with error-related rules, scoring 2.642 out of 3. However, there is room for improvement in meeting warning-related rules, with a score of 7.082 out of 11, indicating that 3.918 rules were not fully satisfied.

Regarding signage, it was noted that the passing lane had three additional RB-31 signs while lacking one RB-34 sign, one RB-37 sign, and one RB-32 sign. Adjustments were made to address these discrepancies and ensure the correct number of signs in the design. The generative design process for this passing lane had a runtime of 14:42:07 and involved a comprehensive check count of 26,124.

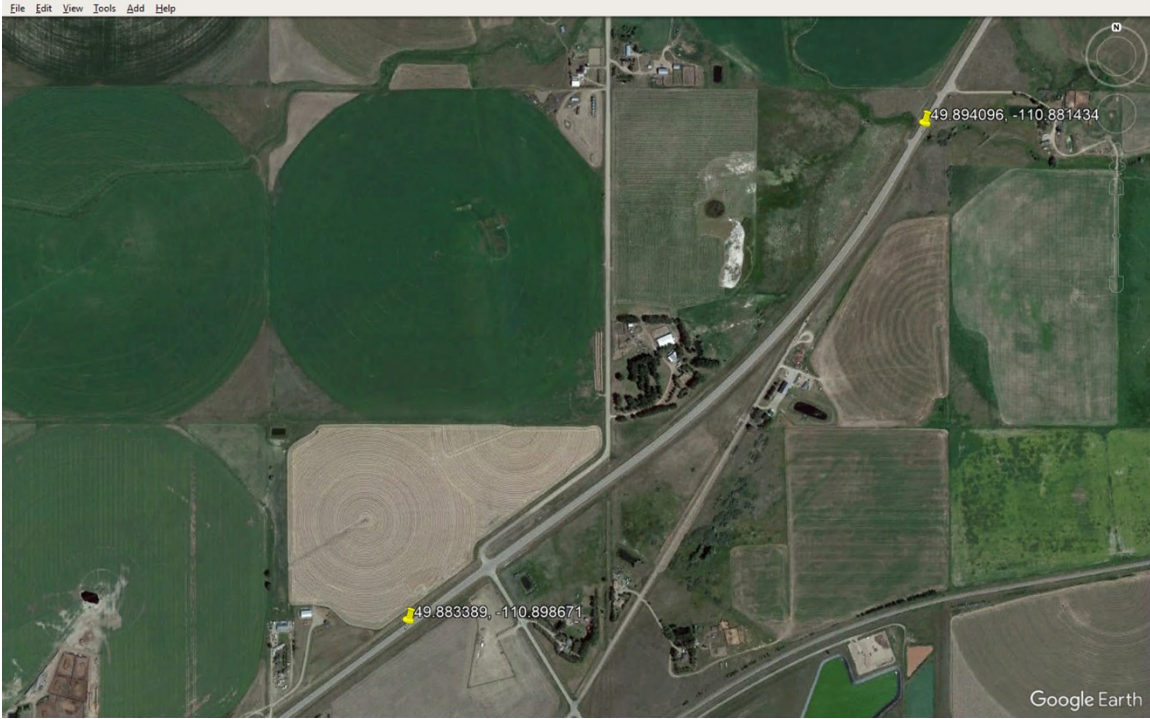
Following the implementation of the generative design approach, a significant improvement in the compatibility score was achieved, reaching an impressive 95.03%. This indicates that out of the 18 rules considered, the passing lane successfully satisfied a majority of 17.11 rules.

It is important to highlight that all three error-related rules were fully met, demonstrating adherence to those guidelines. Furthermore, regarding the warning-related rules, the passing lane exhibited compatibility with 14.11 out of the total 15, with only 0.89 rules remaining to be fully satisfied. This accomplishment underscores the passing lane's high level of compliance with warning-related criteria while also suggesting the potential for further optimization to meet all the rules fully.

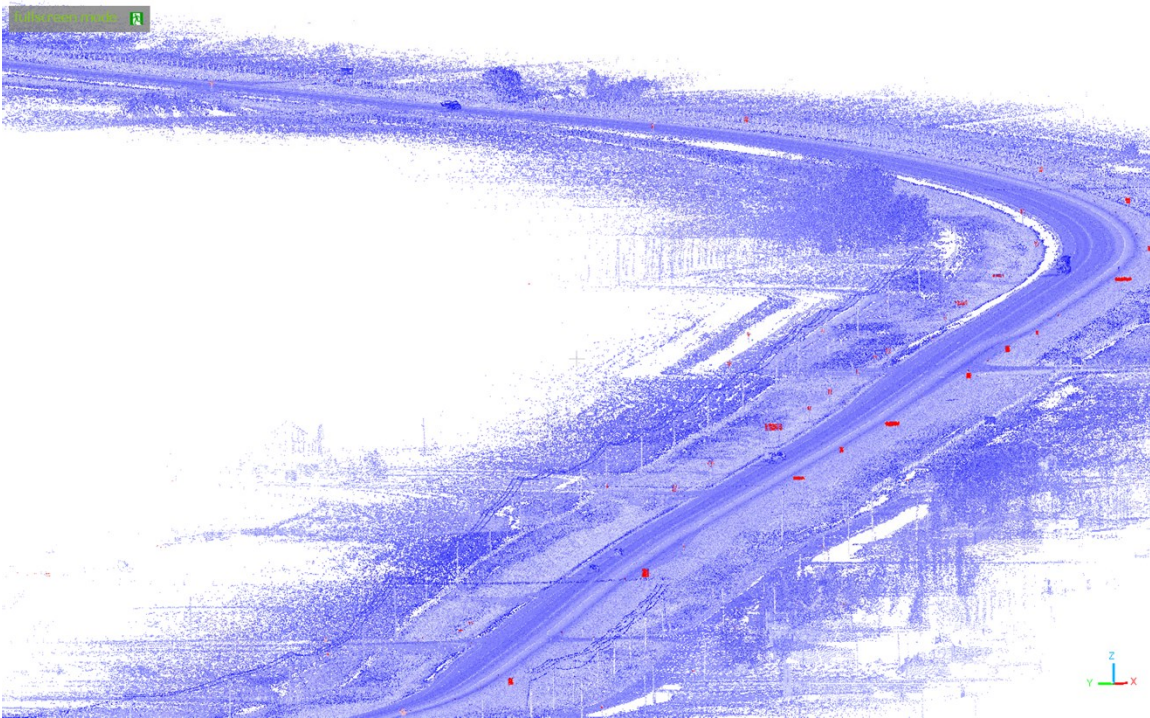
To provide a visual representation of the passing lane and its associated data, Figure 10 serves as a valuable reference. Part a of the figure depicts the precise location of the passing lane within the broader context of Google Earth, providing a clear understanding of its geographical

placement. Part b showcases the raw point-cloud file, offering a comprehensive visual representation of the collected data.

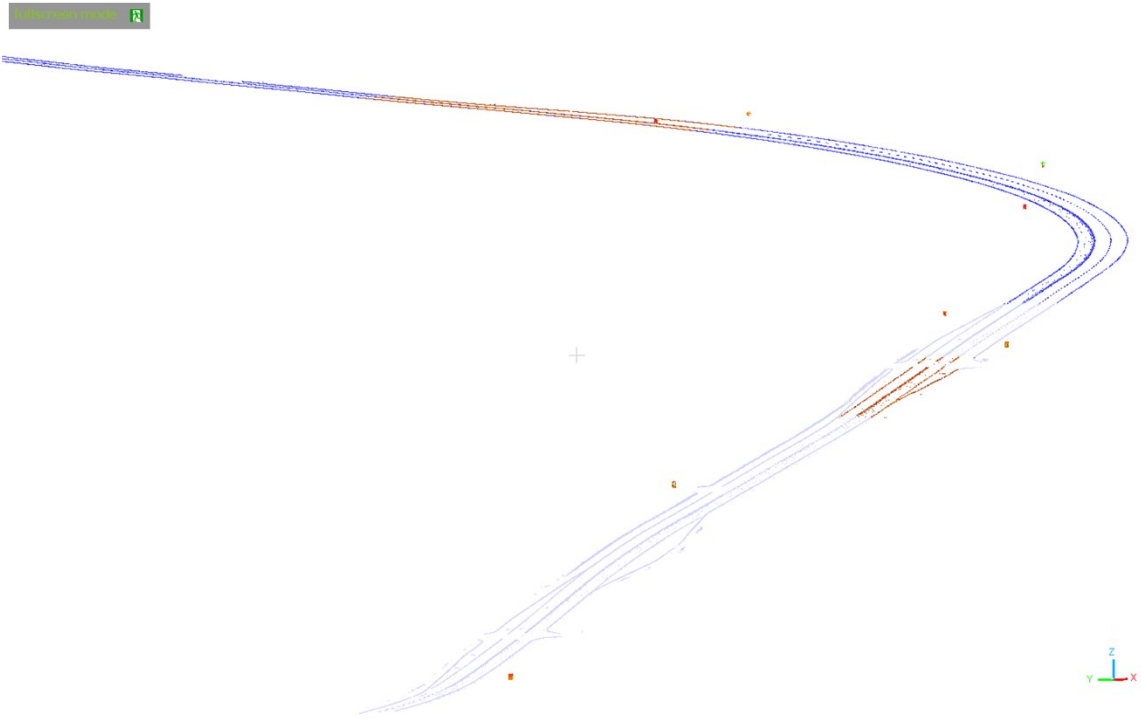
Moving on to part c, the figure presents the extracted features and characteristics specific to this passing lane, providing detailed insights into the various elements analyzed during the evaluation process. Finally, part d illustrates the passing lane's design after incorporating generative design techniques, highlighting the optimized layout and improved functionality resulting from this approach.



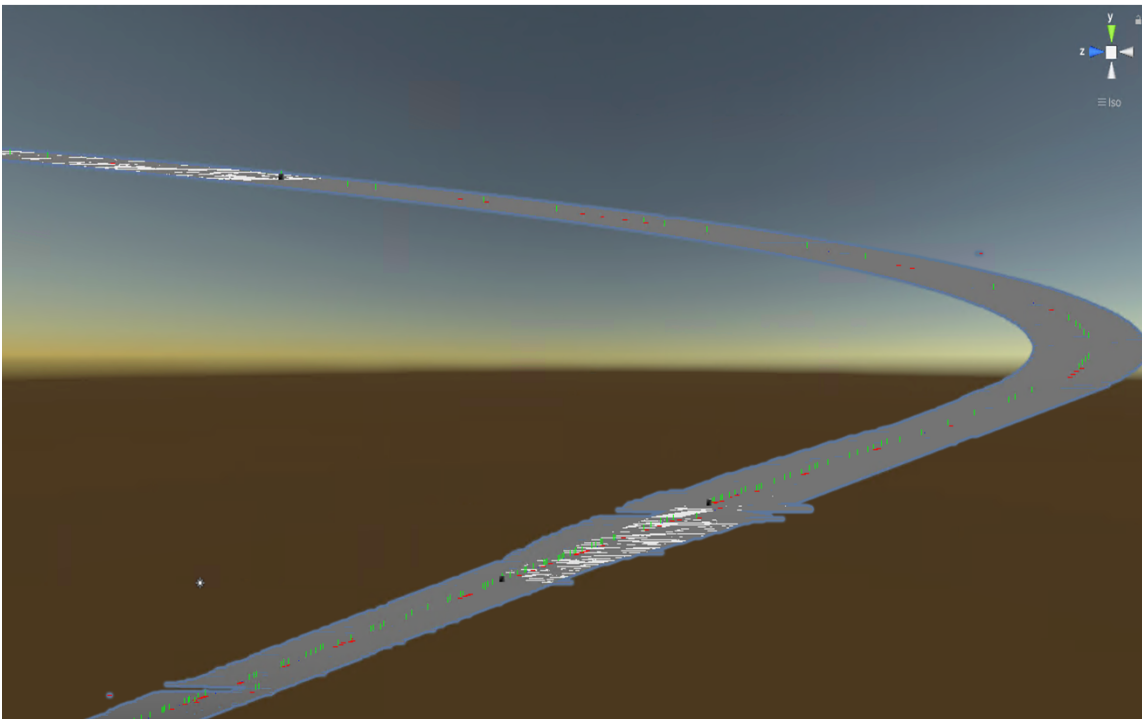
(a) Satellite Image Location



(b) Raw point-cloud



(c) Filtered point-cloud



(d) Generative Design Result

Figure 10: Results for passing lane 8 on Highway 3



## 5.9 Passing Lane 9

A comprehensive evaluation was undertaken to compare the design of the next passing lane generated by the system with an existing real-world passing lane. The analysis focused on a specific passing lane on Highway 9, spanning a distance of 1.6 kilometres between coordinates 51.648965, -112.675161 to 51.648960, -112.652072.

The passing lane underwent a rigorous assessment based on established guidelines during the evaluation. The resulting compatibility score was 63.156%, indicating that out of the 16 rules considered, 9.724 rules were successfully met. Further analysis revealed strong compliance with error-related rules, scoring 2.719 out of 3. However, there is room for improvement in meeting warning-related rules, with a score of 7.386 out of 13, indicating that 5.614 rules were not fully satisfied.

Concerning signage, it was identified that the passing lane was missing one RB-34 sign, one RB-31 sign, one RB-32 sign, and one WA-33R sign. Appropriate adjustments were made to address these discrepancies and ensure the correct number of signs in the design. The generative design process for this passing lane had a runtime of 00:58:37 and involved a comprehensive check count of 19,418.

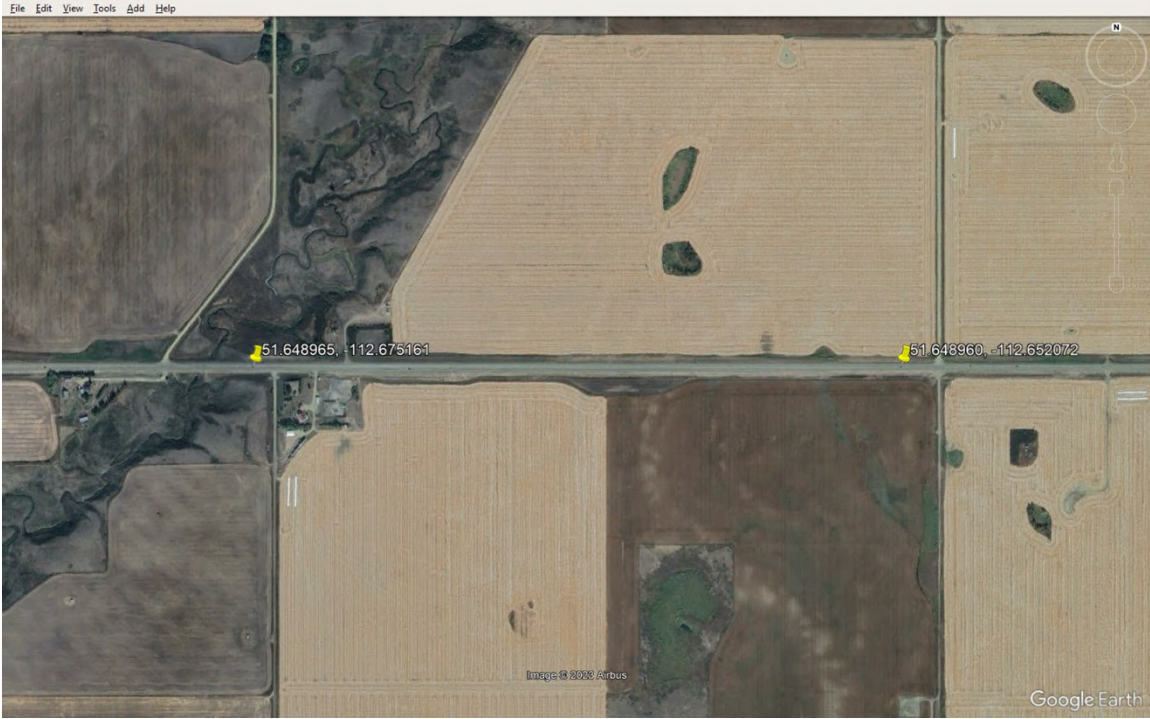
Following the implementation of the generative design approach, a significant improvement in the compatibility score was achieved, reaching an impressive 87.372%. This indicates that out of the 18 rules considered, the passing lane successfully satisfied a majority of 15.727 rules.

It is worth highlighting that all three error-related rules were fully met, demonstrating adherence to those specific guidelines. Furthermore, regarding the warning-related rules, the passing lane exhibited compatibility with 12.727 out of the total 15, with only 2.273 rules remaining to be fully satisfied. This achievement underscores the passing lane's high level of compliance with warning-related criteria while also suggesting the potential for further optimization to meet all the rules fully.

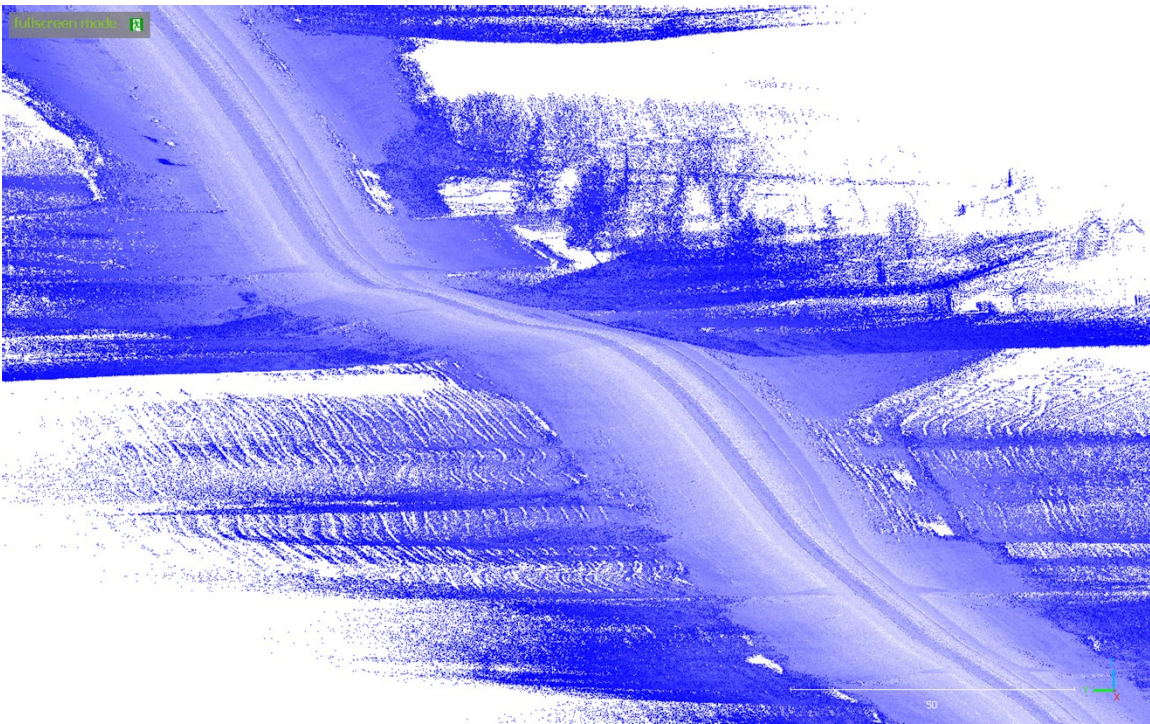
To provide a visual representation of the passing lane and its associated data, Figure 11 serves as a valuable reference. Part a of the figure illustrates the precise location of the passing lane within the broader context of Google Earth, offering a clear understanding of its geographical

placement. Part b showcases the raw point-cloud file, providing a comprehensive visual representation of the collected data.

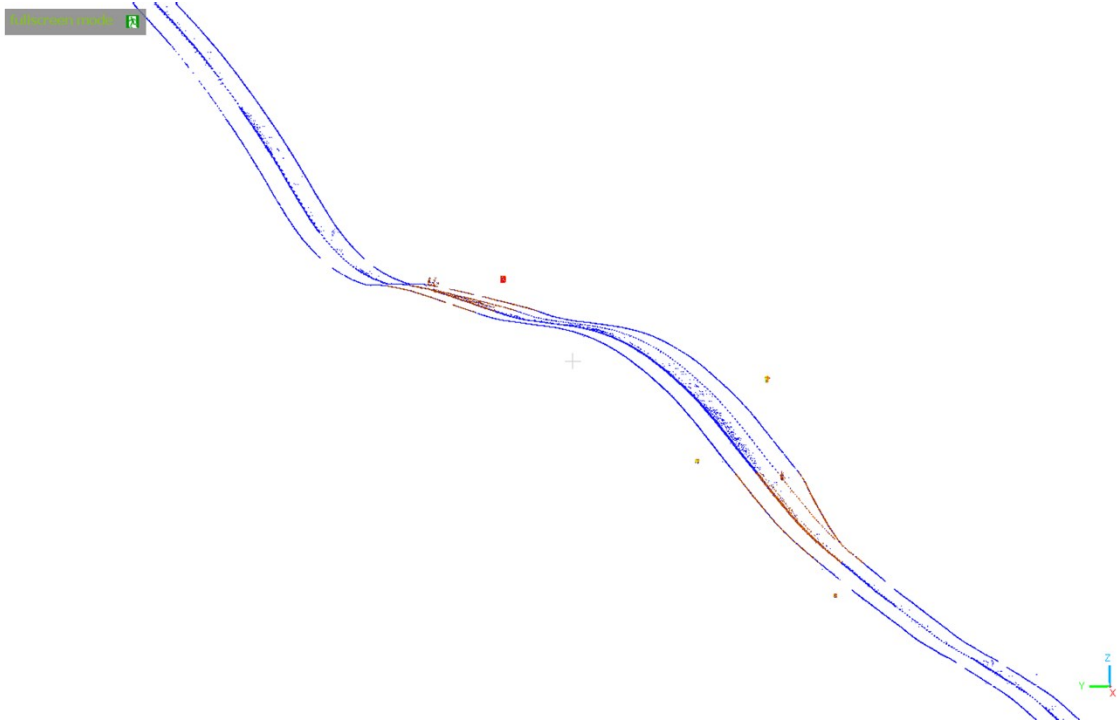
Moving on to part c, the figure presents the extracted features and characteristics specific to this passing lane, offering detailed insights into the various elements analyzed during the evaluation process. Finally, part d depicts the passing lane's design after incorporating generative design techniques, highlighting the optimized layout and improved functionality resulting from this approach.



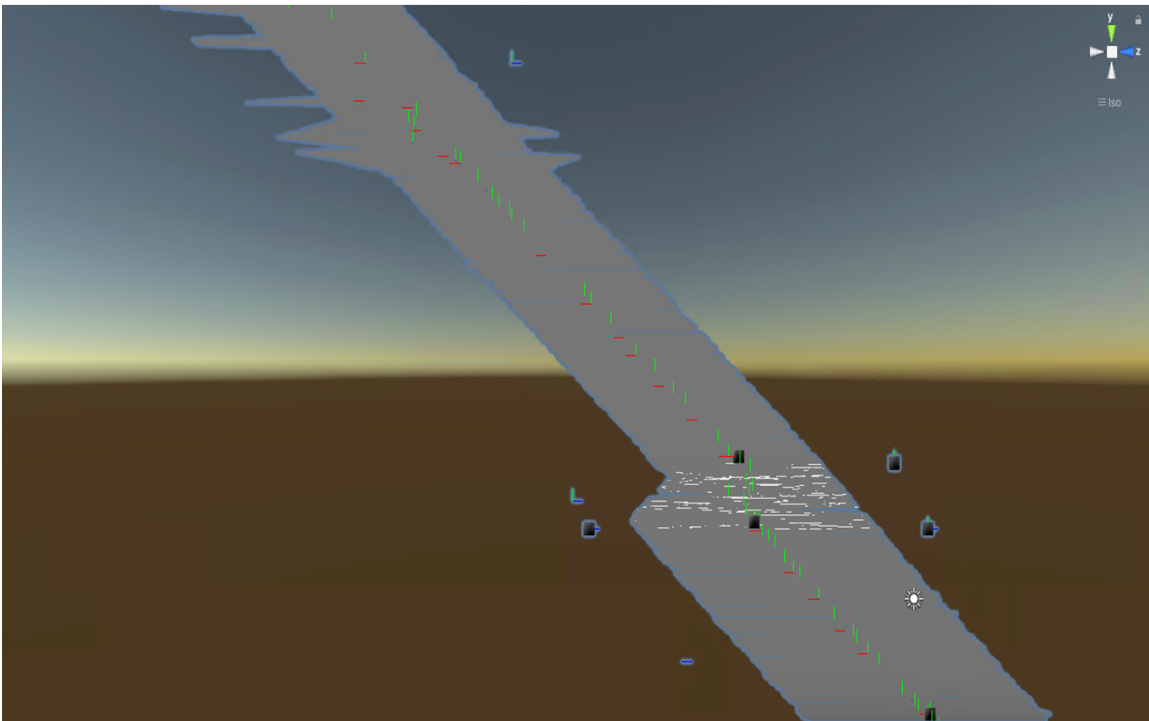
(a) Satellite Image Location



(b) Raw point-cloud



(c) Filtered point-cloud



(d) Generative Design Result

Figure 11: Results for passing lane 9 on Highway 9

## 5.10 Passing Lane 10

A comprehensive evaluation was conducted to compare the design of the next passing lane generated by the system with an existing real-world passing lane. The assessment focused on a specific passing lane on Highway 9, spanning a distance of 2.1 kilometres between coordinates 51.649030, -112.279487 to 51.649029, -112.310567.

The passing lane underwent a rigorous assessment based on established guidelines during the evaluation process. The resulting compatibility score was 45.665%, indicating that 8.220 of the 18 rules were successfully met. Further analysis revealed strong adherence to error-related rules, scoring 2.625 out of 3. However, improvement is needed in meeting warning-related rules, with a score of 5.594 out of 15, indicating that 9.406 rules were not fully satisfied.

Regarding signage, it was identified that the passing lane lacked one RB-34 sign, one RB-31 sign, and one WA-33R sign. Appropriate adjustments were made to address these discrepancies and ensure the correct number of signs in the design. The generative design process for this passing lane took 01:04:44 and involved a comprehensive check count of 20,958.

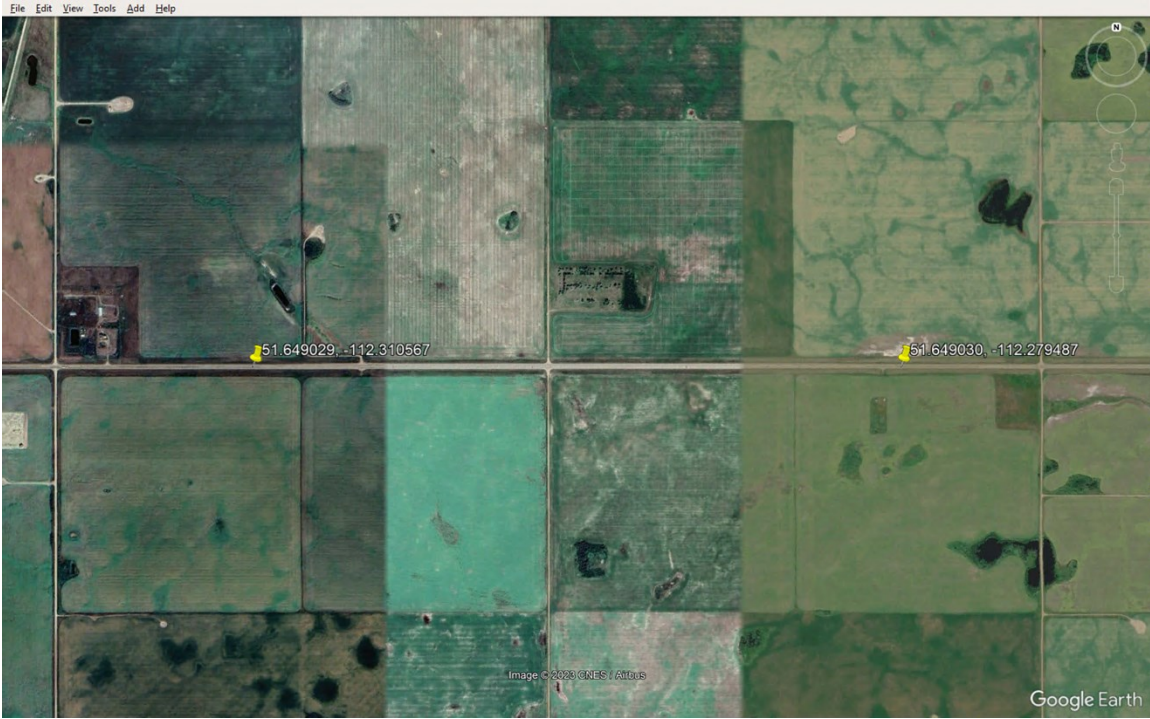
Following the implementation of the generative design approach, a significant improvement in the compatibility score was achieved, reaching an impressive 86.599%. This indicates that the passing lane successfully satisfied a majority of 15.588 out of the 18 rules.

All three error-related rules were fully met, demonstrating adherence to those guidelines. Regarding the warning-related rules, the passing lane exhibited compatibility with 12.588 out of the total 15, leaving only 2.412 rules fully satisfied. This accomplishment underscores the passing lane's high level of compliance with warning-related criteria while also suggesting the potential for further optimization to meet all the rules fully.

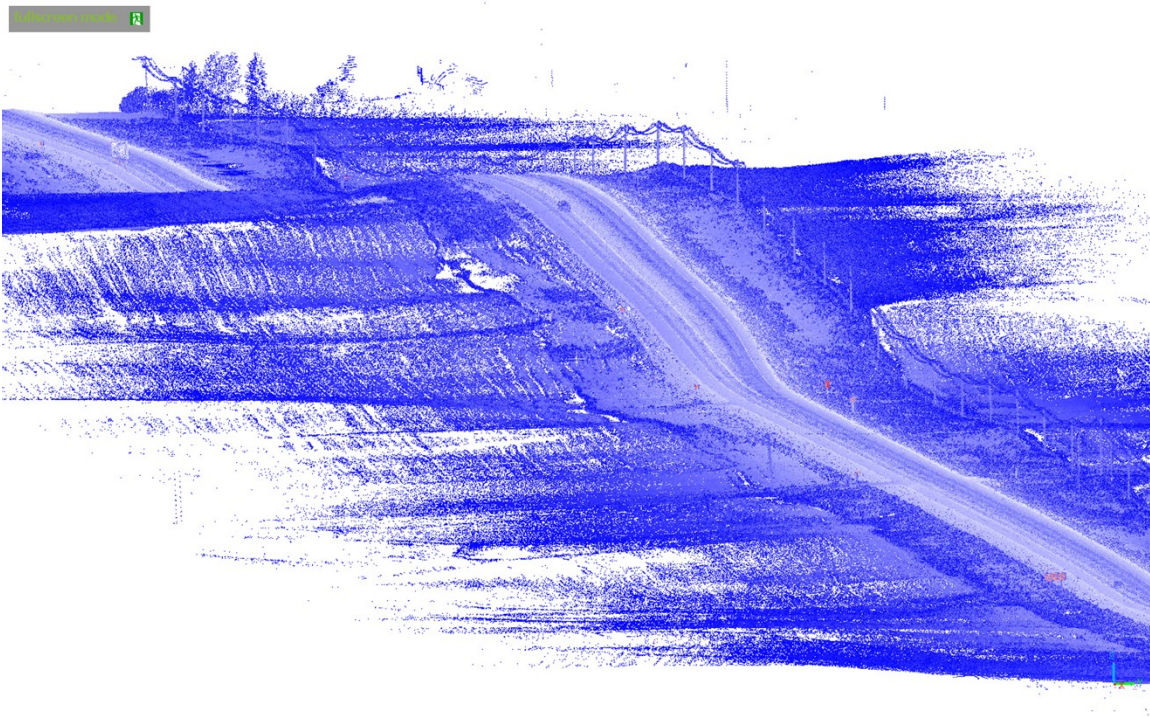
To provide a visual representation of the passing lane and its associated data, Figure 12 serves as a valuable reference. Part a of the figure illustrates the precise location of the passing lane within the broader context of Google Earth, offering a clear understanding of its geographical placement. Part b showcases the raw point-cloud file, providing a comprehensive visual representation of the collected data.

Moving on to part c, the figure presents the extracted features and characteristics specific to this passing lane, offering detailed insights into the various elements analyzed during the evaluation process. Finally, part d depicts the passing lane's design after incorporating generative

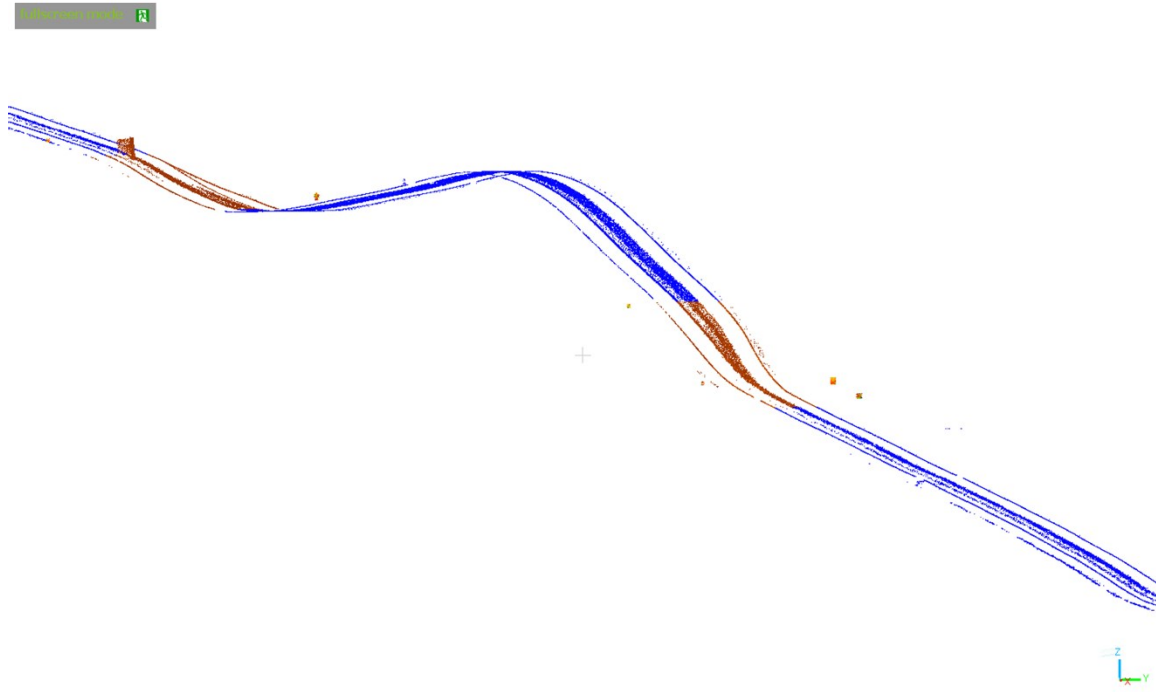
design techniques, highlighting the optimized layout and improved functionality resulting from this approach.



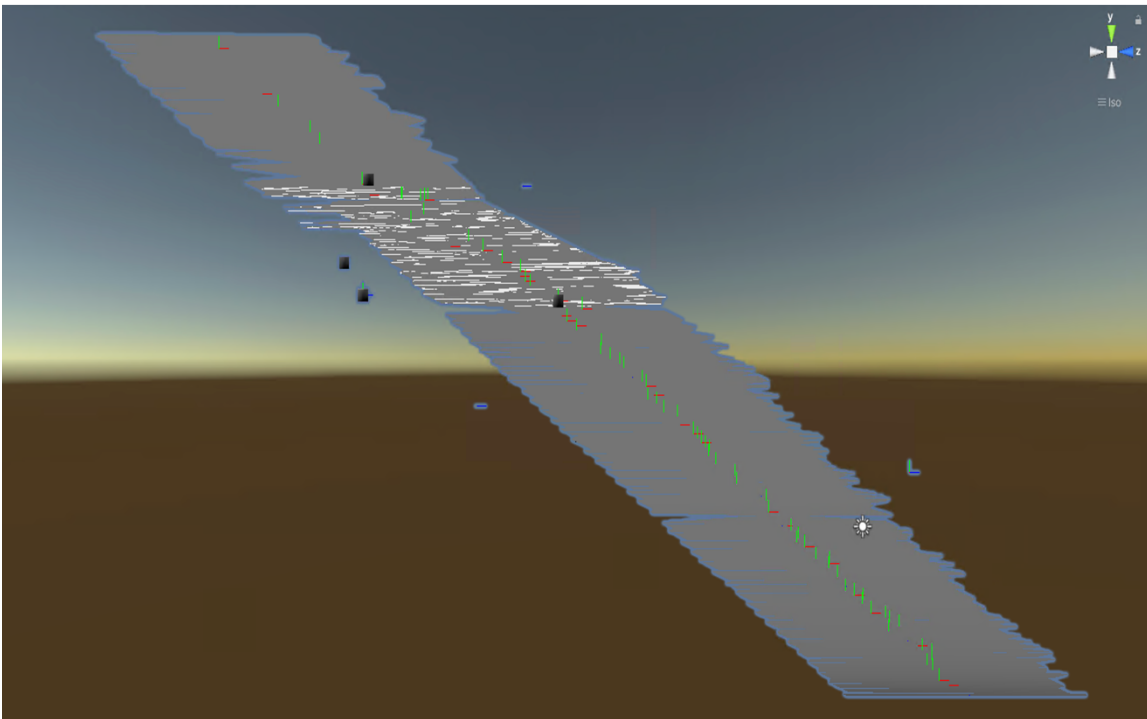
(a) Satellite Image Location



(b) Raw point-cloud



(c) Filtered point-cloud



(d) Generative Design Result

Figure 12: Results for passing lane 10 on Highway 9



## 5.11 Passing Lane 11

A comprehensive evaluation was conducted to compare the design of the next passing lane generated by the system with an existing real-world passing lane. The assessment focused on a specific passing lane on Highway 3, spanning a distance of 3.1 kilometres between coordinates 49.546383, -113.799089 to 49.542439, -113.840776.

The passing lane underwent a rigorous assessment based on established guidelines during the evaluation process. The resulting compatibility score was 66.009%, indicating that 10.561 of the 16 rules were successfully met. Further analysis revealed strong adherence to error-related rules, scoring 2.629 out of 3. However, improvement is needed in meeting warning-related rules, with a score of 7.933 out of 13, indicating that 5.067 rules were not fully satisfied.

Regarding signage, it was identified that the passing lane had three additional RB-34 signs and three additional RB-31 signs while lacking one RB-32 sign. Appropriate adjustments were made to address these discrepancies and ensure the correct number of signs in the design. The generative design process for this passing lane took 4 hours, 33 minutes, and 42 seconds and involved a comprehensive check count of 33,510.

Following the implementation of the generative design approach, a significant improvement in the compatibility score was achieved, reaching an impressive 95.468%. This indicates that the passing lane successfully satisfied 17.184 out of the 18 rules.

All three error-related rules were fully met, demonstrating adherence to those guidelines. Regarding the warning-related rules, the passing lane exhibited compatibility with 14.184 out of the total 15, leaving only 0.816 rules remaining to be fully satisfied. This accomplishment underscores the passing lane's high level of compliance with warning-related criteria while also suggesting the potential for further optimization to meet all the rules fully.

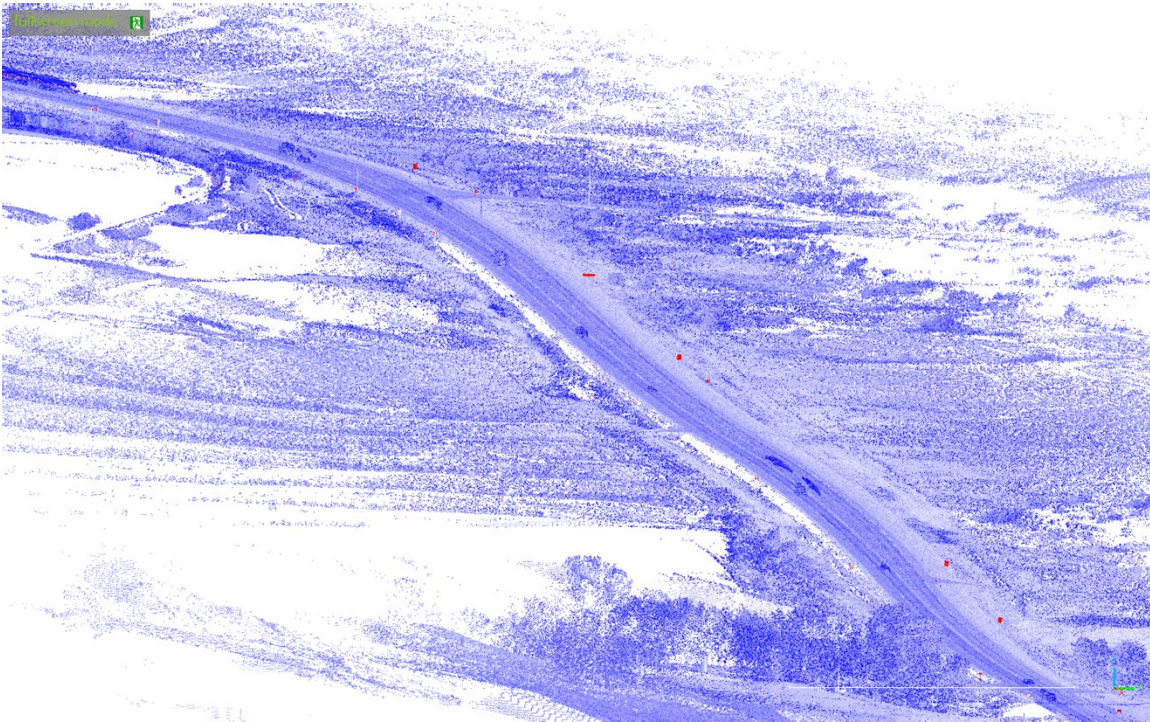
To provide a visual representation of the passing lane and its associated data, Figure 13 serves as a valuable reference. Part a of the figure illustrates the precise location of the passing lane within the broader context of Google Earth, offering a clear understanding of its geographical placement. Part b showcases the raw point-cloud file, providing a comprehensive visual representation of the collected data.

Moving on to part c, the figure presents the extracted features and characteristics specific to this passing lane, offering detailed insights into the various elements analyzed during the

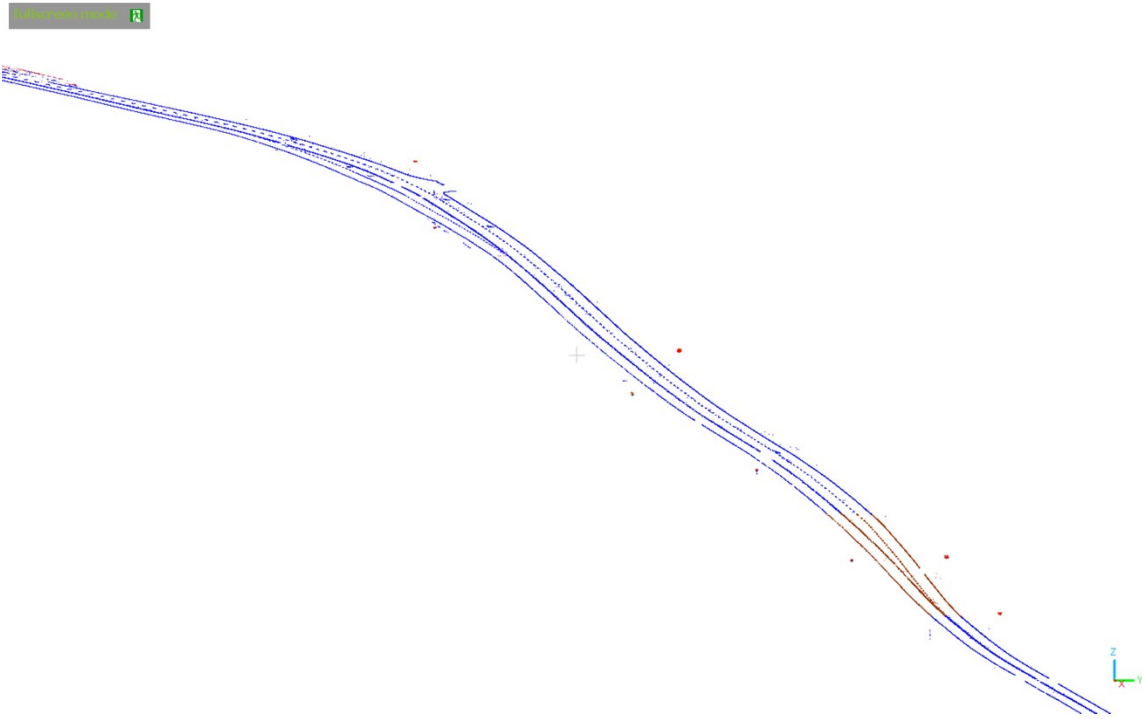
evaluation process. Finally, part d depicts the passing lane's design after incorporating generative design techniques, highlighting the optimized layout and improved functionality resulting from this approach.



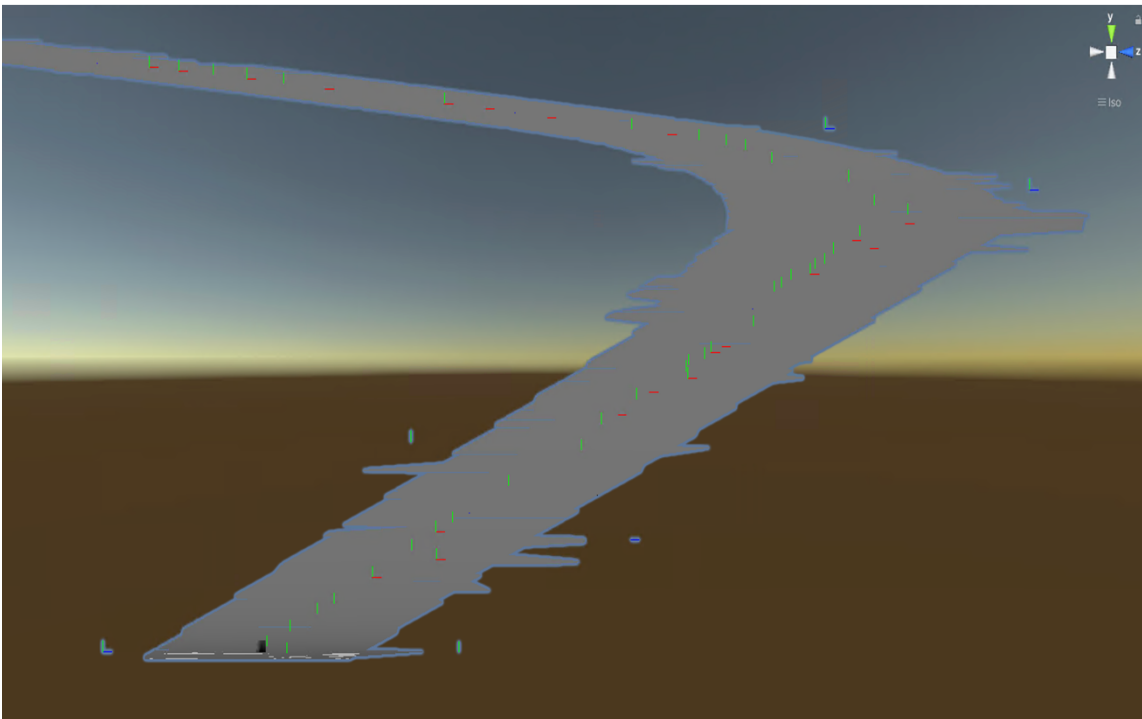
(a) Satellite Image Location



(b) Raw point-cloud



(c) Filtered point-cloud



(d) Generative Design Result

Figure 13: Results for passing lane 11 on Highway 3

## 5.12 Passing Lane 12

An extensive evaluation was conducted to compare the design of the next passing lane generated by the system with an existing real-world passing lane. The assessment focused on a particular passing lane on Highway 3, covering a distance of 1.5 kilometres between coordinates 49.546620, -113.790790 to 49.547616, -113.772923.

The passing lane underwent a rigorous assessment based on established guidelines during the evaluation process. The resulting compatibility score was 58.704%, indicating that 10.567 of the 18 rules were successfully met. Further analysis revealed strong compliance with error-related rules, scoring 2.630 out of 3. However, there is room for improvement in meeting warning-related rules, as the score was 7.937 out of 15, signifying that 7.063 rules were not fully satisfied.

Concerning signage, it was identified that the passing lane had one additional RB-34 sign while lacking one RB-31 sign. Appropriate adjustments were made to rectify these discrepancies and ensure the correct number of signs in the design. The generative design process for this passing lane took 1 hour, 41 minutes, and 55 seconds and involved a comprehensive check count of 21,980.

Following the implementation of the generative design approach, a remarkable improvement in the compatibility score was achieved, reaching an impressive 90.552%. This indicates that the passing lane successfully satisfied 16.299 out of the 18 rules.

All three error-related rules were fully met, demonstrating adherence to those guidelines. Furthermore, regarding the warning-related rules, the passing lane exhibited compatibility with 13.299 out of the total 15, with only 1.701 rules remaining to be fully satisfied. This accomplishment emphasizes the passing lane's high level of compliance with warning-related criteria while suggesting the potential for further optimization to meet all the rules fully.

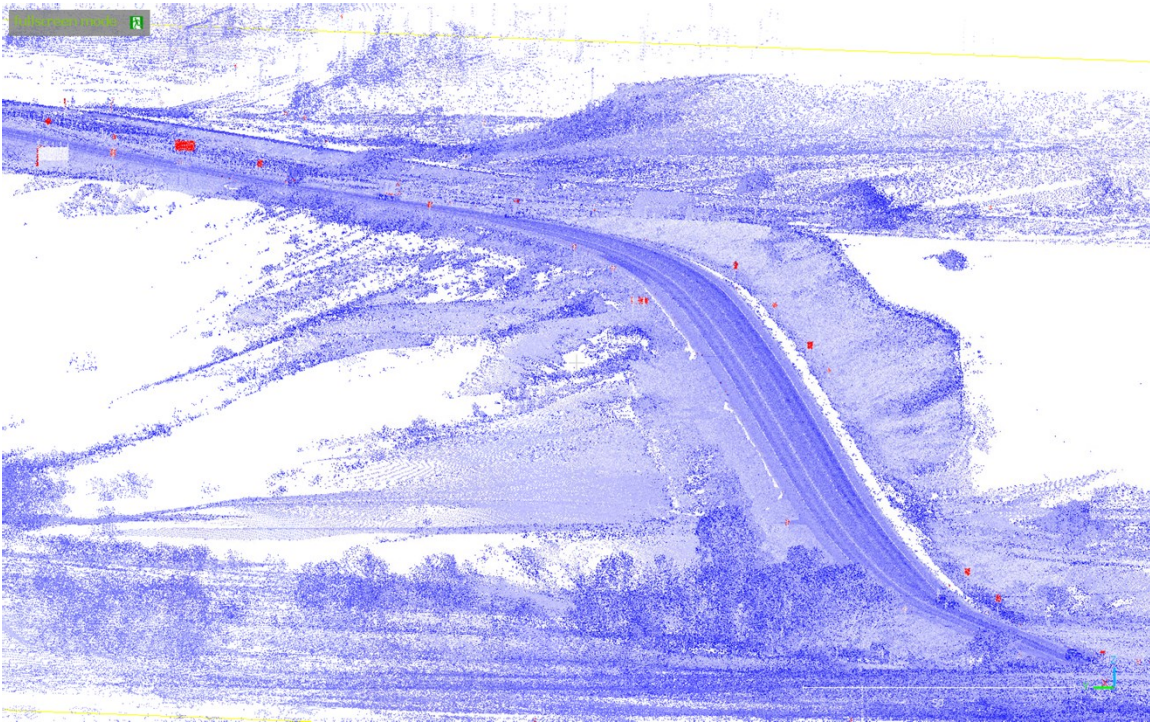
To provide a visual representation of the passing lane and its associated data, Figure 14 serves as a valuable reference. Part a of the figure illustrates the precise location of the passing lane within the broader context of Google Earth, offering a clear understanding of its geographical placement. Part b showcases the raw point-cloud file, providing a comprehensive visual representation of the collected data.

Moving on to part c, the figure presents the extracted features and characteristics specific to this passing lane, offering detailed insights into the various elements analyzed during the evaluation process. Finally, part d depicts the passing lane's design after incorporating generative

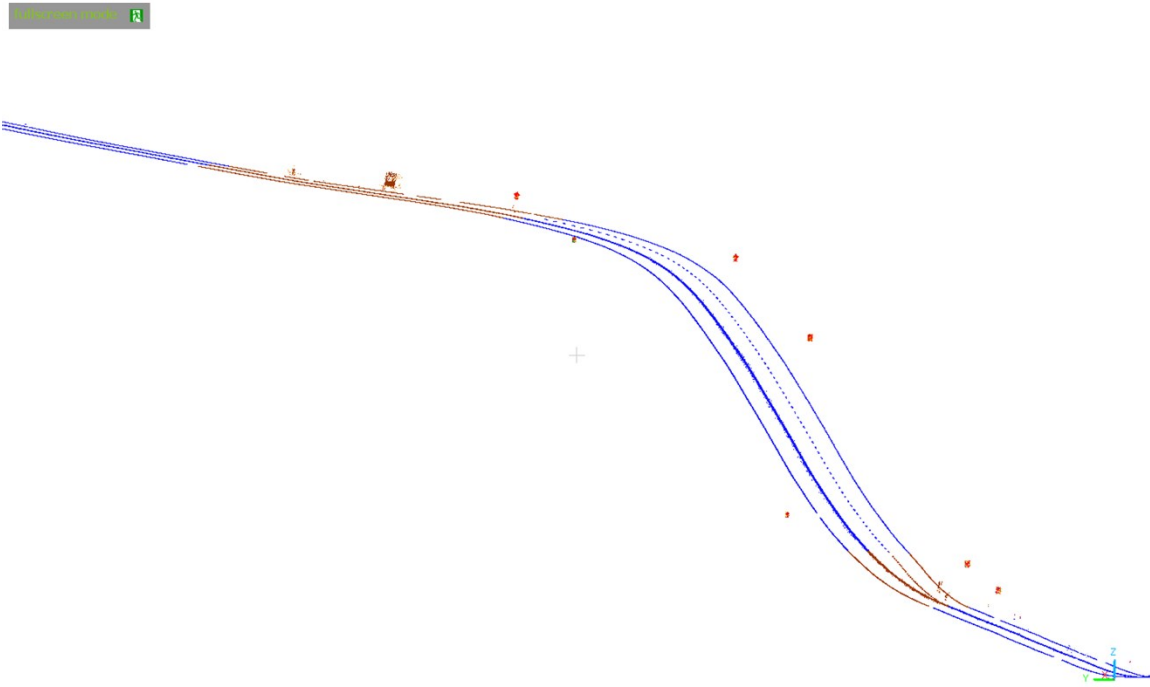
design techniques, highlighting the optimized layout and improved functionality resulting from this approach.



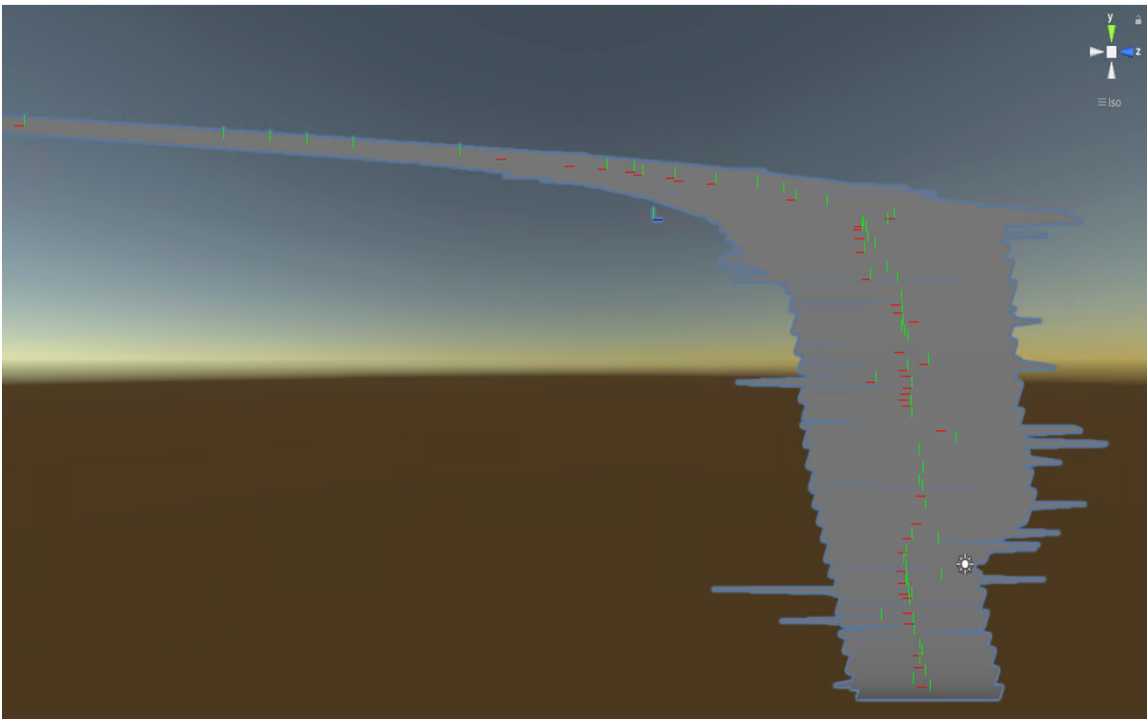
(a) Satellite Image Location



(b) Raw point-cloud



(c) Filtered point-cloud



(d) Generative Design Result

Figure 14: Results for passing lane 12 on Highway 3



### 5.13 Passing Lane 13

A comprehensive evaluation was undertaken to compare the design of the next passing lane generated by the system with an existing real-world passing lane. The analysis focused on a specific passing lane located on Highway 3, spanning a distance of 2.2 kilometres between coordinates 49.576055, -113.698865 to 49.587529, -113.673550.

The passing lane underwent a thorough evaluation based on established guidelines during the assessment process. The resulting compatibility score was 66.934%, indicating that 10.710 of the 16 rules were successfully met. Further examination revealed strong adherence to error-related rules, scoring 2.680 out of 3. However, there is room for improvement in meeting warning-related rules, with a score of 8.029 out of 13, signifying that 4.971 rules were not fully satisfied.

Regarding signage, it was observed that the passing lane had one additional RB-34 sign and two additional RB-31 signs, while lacking one RB-32 sign. Appropriate adjustments were made to rectify these discrepancies and ensure the correct number of signs in the design. The generative design process for this passing lane took 2 hours, 18 minutes, and 8 seconds and involved a comprehensive check count of 26,344.

Following the implementation of the generative design approach, a remarkable improvement in the compatibility score was achieved, reaching an impressive 91.406%. This indicates that the passing lane successfully satisfied 16.453 out of the 18 rules.

All three error-related rules were fully met, demonstrating adherence to those guidelines. Furthermore, regarding the warning-related rules, the passing lane exhibited compatibility with 13.453 out of the total 15, with only 1.547 rules remaining to be fully satisfied. This accomplishment emphasizes the passing lane's high level of compliance with warning-related criteria while suggesting the potential for further optimization to meet all the rules fully.

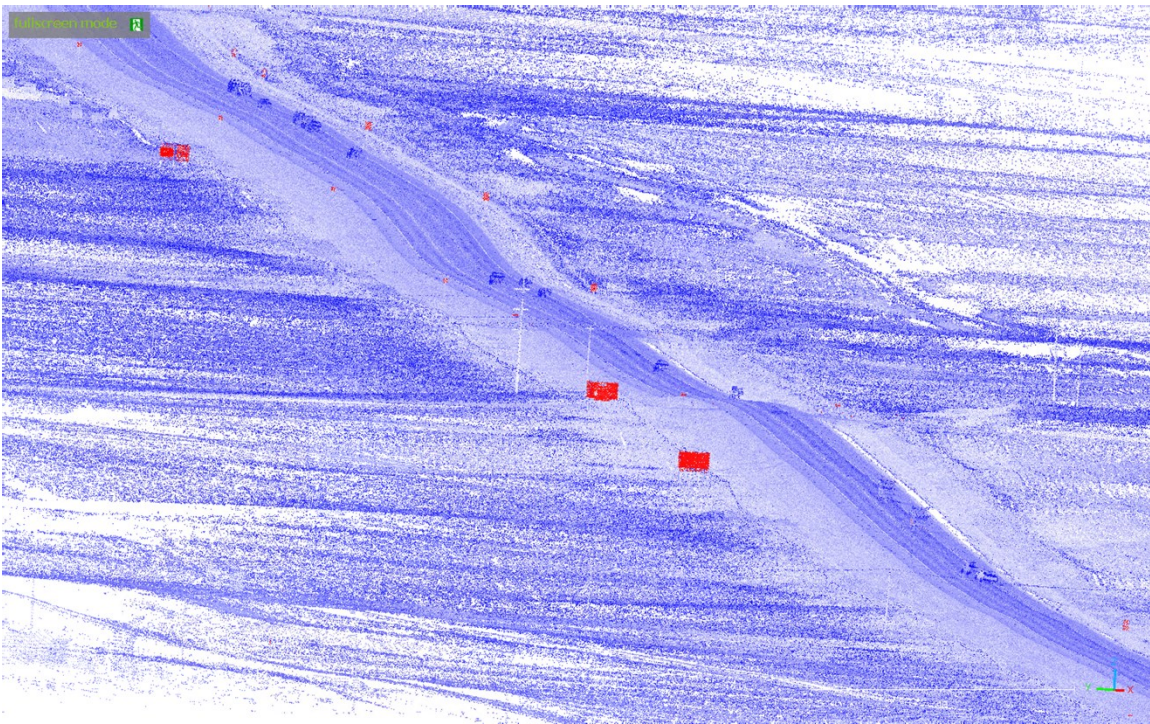
To provide a visual representation of the passing lane and its associated data, Figure 15 serves as a valuable reference. Part a of the figure illustrates the precise location of the passing lane within the broader context of Google Earth, offering a clear understanding of its geographical placement. Part b showcases the raw point-cloud file, providing a comprehensive visual representation of the collected data.

Moving on to part c, the figure presents the extracted features and characteristics specific to this passing lane, offering detailed insights into the various elements analyzed during the

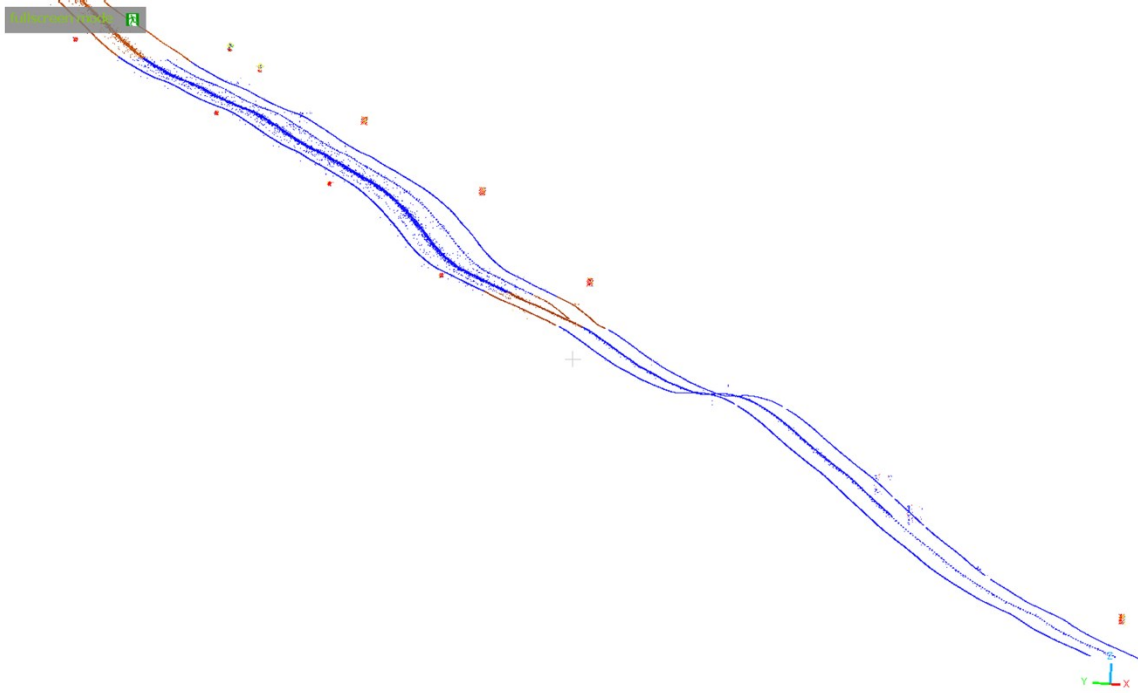
evaluation process. Finally, part d depicts the passing lane's design after incorporating generative design techniques, highlighting the optimized layout and improved functionality resulting from this approach.



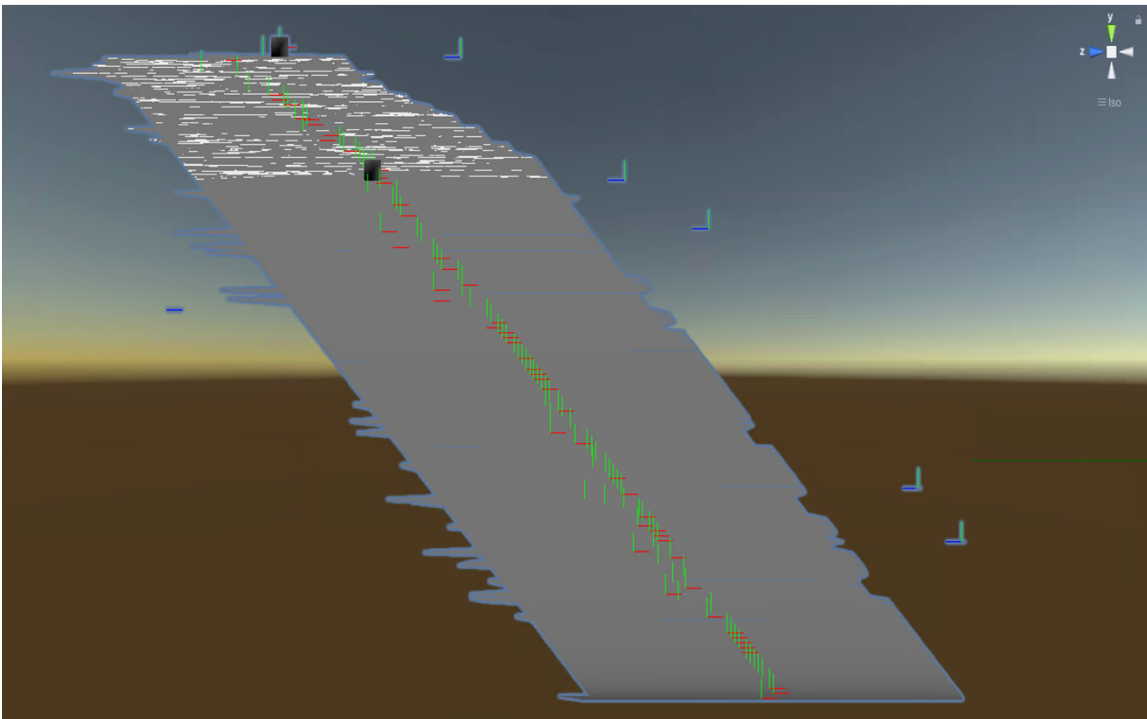
(a) Satellite Image Location



(b) Raw point-cloud



(c) Filtered point-cloud



(d) Generative Design Result

Figure 15: Results for passing lane 13 on Highway 3

## 5.14 Passing Lane 14

A comprehensive assessment was conducted to compare the design of the next passing lane generated by the system with an existing real-world passing lane. This analysis focused on a specific passing lane on Highway 3, spanning a distance of 1.8 kilometres between coordinates 49.596760, -113.653177 to 49.587637, -113.673313.

The passing lane underwent a thorough examination based on established guidelines during the evaluation process. The resulting compatibility score was 64.772%, indicating that 9.068 of the 14 rules were successfully met. Further analysis revealed strong adherence to error-related rules, scoring 2.658 out of 3. However, there is room for improvement in meeting warning-related rules, with a score of 6.410 out of 11, signifying that 4.590 rules were not fully satisfied.

Regarding signage, it was observed that the passing lane had two additional RB-34 signs and two additional RB-31 signs while lacking one RB-37 sign and one RB-32 sign. Appropriate adjustments were made to rectify these discrepancies and ensure the correct number of signs in the design. The generative design process for this passing lane took 01:12:11 and involved a comprehensive check count of 27,926.

Following the implementation of the generative design approach, a remarkable improvement in the compatibility score was achieved, reaching an impressive 94.068%. This indicates that the passing lane successfully satisfied most of 16.932 out of the 18 rules.

All three error-related rules were fully met, demonstrating adherence to those guidelines. Furthermore, regarding the warning-related rules, the passing lane exhibited compatibility with 13.932 out of the total 15, with only 1.068 rules remaining to be fully satisfied. This accomplishment emphasizes the passing lane's high level of compliance with warning-related criteria while suggesting the potential for further optimization to meet all the rules fully.

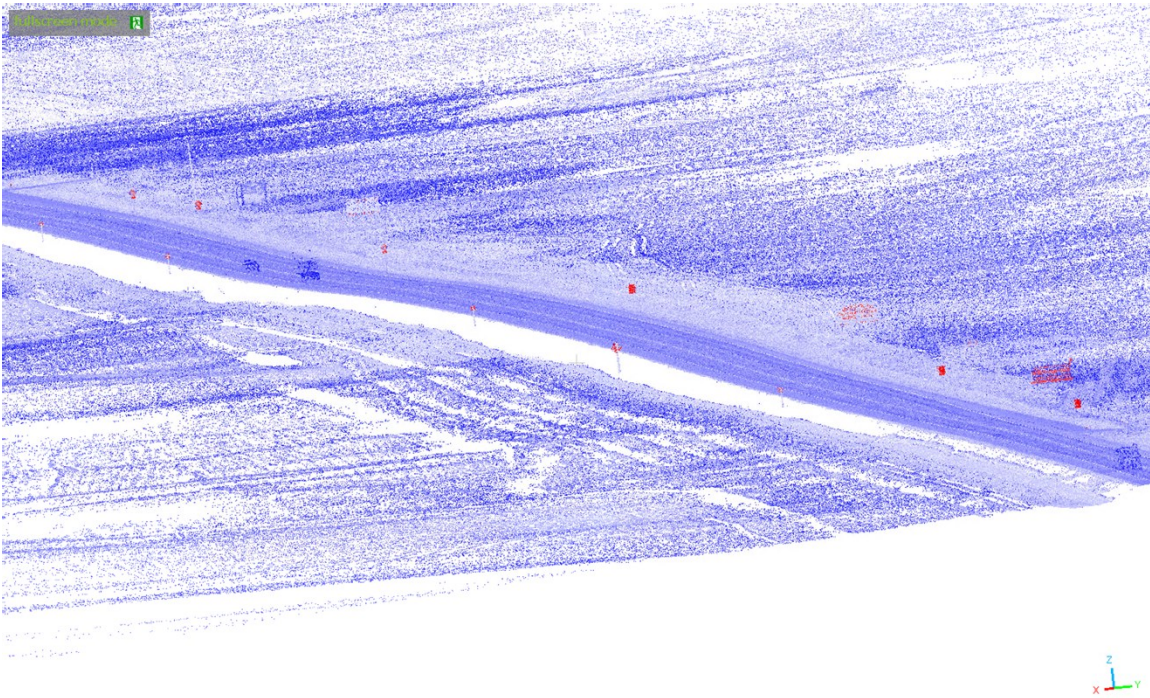
To provide a visual representation of the passing lane and its associated data, Figure 16 serves as a valuable reference. Part a of the figure illustrates the precise location of the passing lane within the broader context of Google Earth, offering a clear understanding of its geographical placement. Part b showcases the raw point-cloud file, providing a comprehensive visual representation of the collected data.

Moving on to part c, the figure presents the extracted features and characteristics specific to this passing lane, offering detailed insights into the various elements analyzed during the

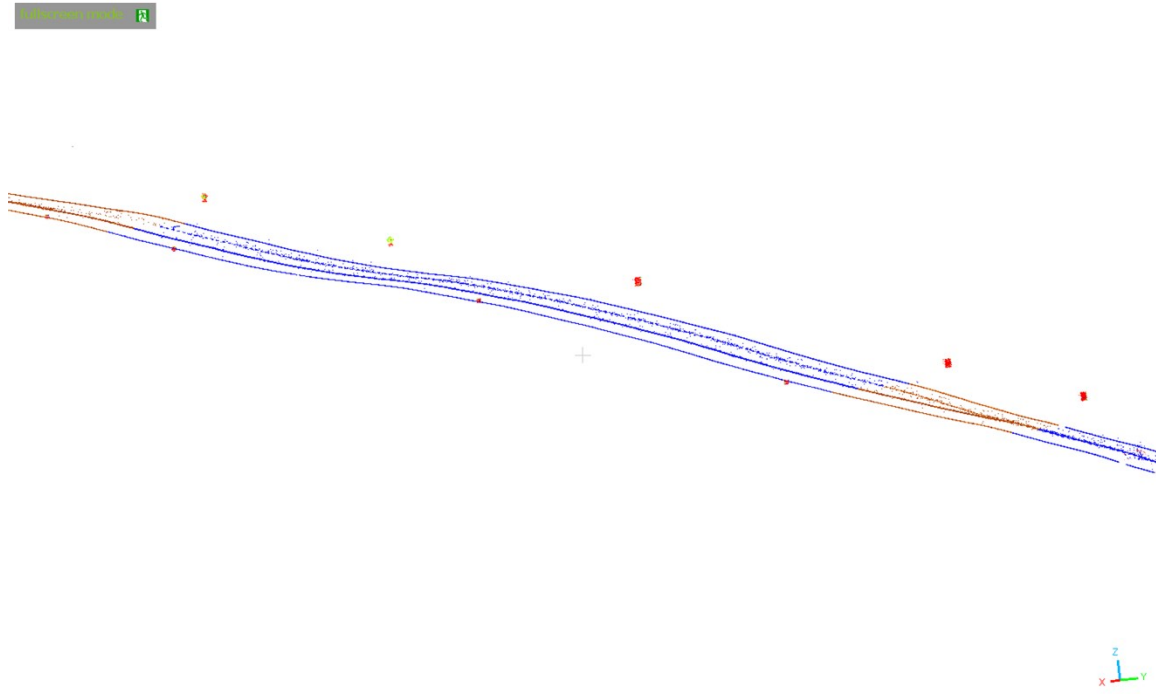
evaluation process. Finally, part d depicts the passing lane's design after incorporating generative design techniques, highlighting the optimized layout and improved functionality resulting from this approach.



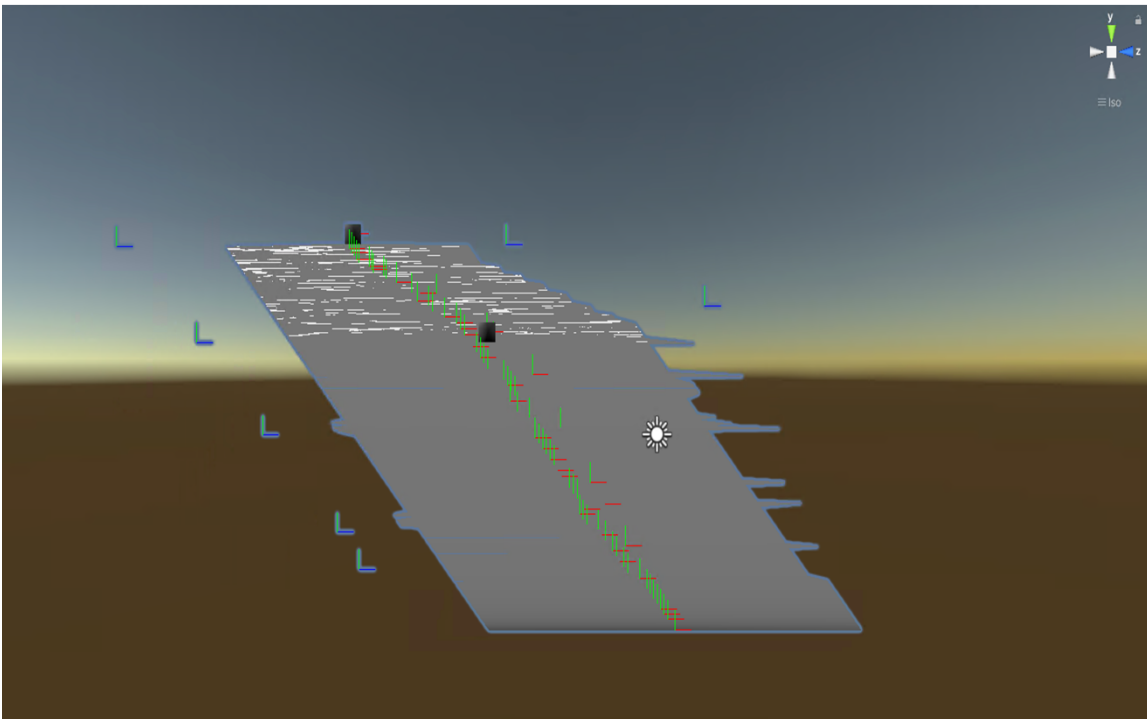
(a) Satellite Image Location



(b) Raw point-cloud



(c) Filtered point-cloud



(d) Generative Design Result

Figure 16: Results for passing lane 14 on Highway 3



## 5.15 Passing Lane 15

A comprehensive evaluation was conducted to compare the design of the next passing lane generated by the system with an existing real-world passing lane. This analysis focused on a specific passing lane on Highway 3, spanning a distance of 2.4 kilometres between coordinates 49.624402, -113.602590 to 49.641090, -113.580770.

The passing lane underwent a thorough examination based on established guidelines during the assessment. The resulting compatibility score was 62.995%, indicating that 10.079 of the 16 rules were successfully met. Further analysis revealed strong adherence to error-related rules, scoring 2.623 out of 3. However, there is room for improvement in meeting warning-related rules, with a score of 7.456 out of 13, signifying that 5.544 rules were not fully satisfied.

Regarding signage, it was observed that the passing lane had two additional RB-34 signs and three additional RB-31 signs, while lacking one RB-37 sign. Appropriate adjustments were made to rectify these discrepancies and ensure the correct number of signs in the design. The generative design process for this passing lane took 02:45:00 and involved a comprehensive check count of 30,948.

Following the implementation of the generative design approach, a remarkable improvement in the compatibility score was achieved, reaching an impressive 86.541%. This indicates that the passing lane successfully satisfied a majority of 15.577 out of the 18 rules.

All three error-related rules were fully met, demonstrating adherence to those guidelines. Furthermore, regarding the warning-related rules, the passing lane exhibited compatibility with 12.577 out of the total 15, with only 2.423 rules remaining to be fully satisfied. This accomplishment underscores the passing lane's high level of compliance with warning-related criteria while also suggesting the potential for further optimization to meet all the rules fully.

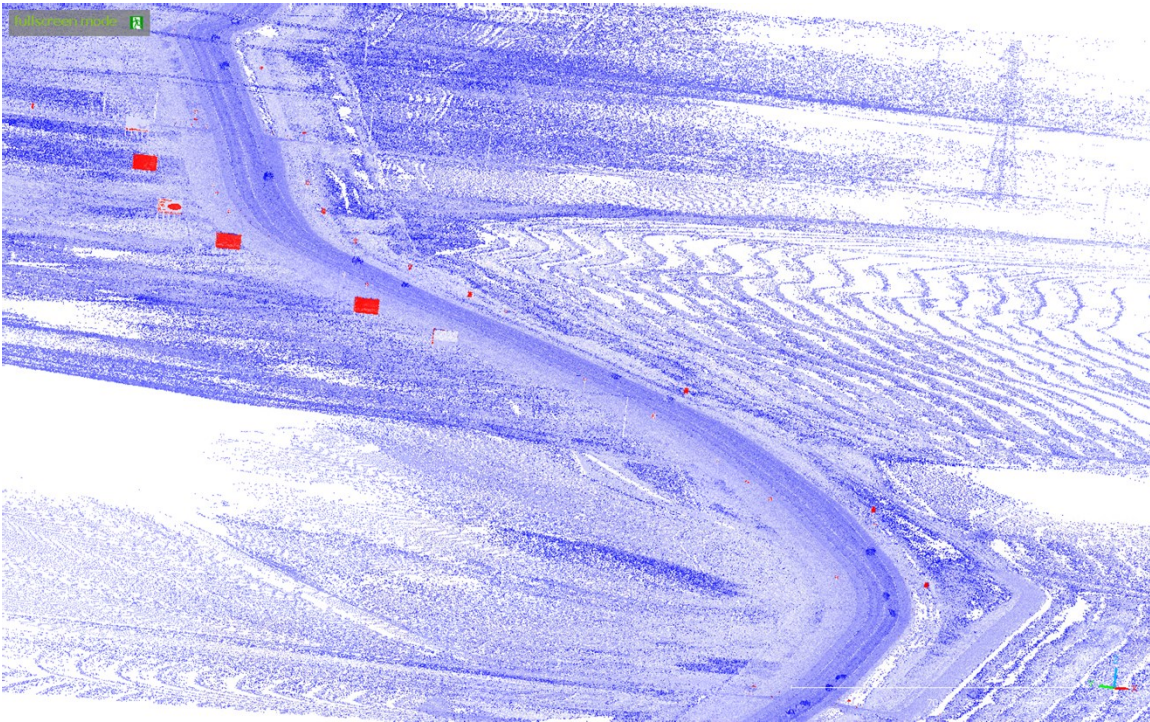
To provide a visual representation of the passing lane and its associated data, Figure 17 serves as a valuable reference. Part a of the figure illustrates the precise location of the passing lane within the broader context of Google Earth, offering a clear understanding of its geographical placement. Part b showcases the raw point-cloud file, providing a comprehensive visual representation of the collected data.

Moving on to part c, the figure presents the extracted features and characteristics specific to this passing lane, offering detailed insights into the various elements analyzed during the

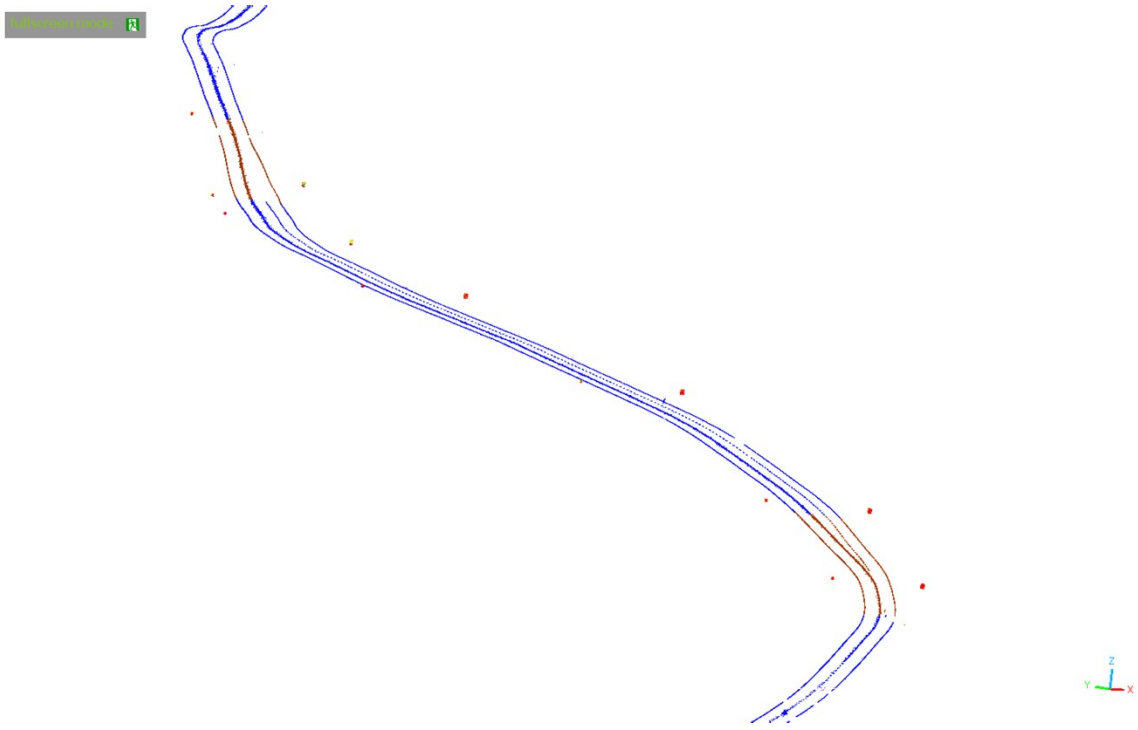
evaluation process. Finally, part d depicts the passing lane's design after incorporating generative design techniques, highlighting the optimized layout and improved functionality resulting from this approach.



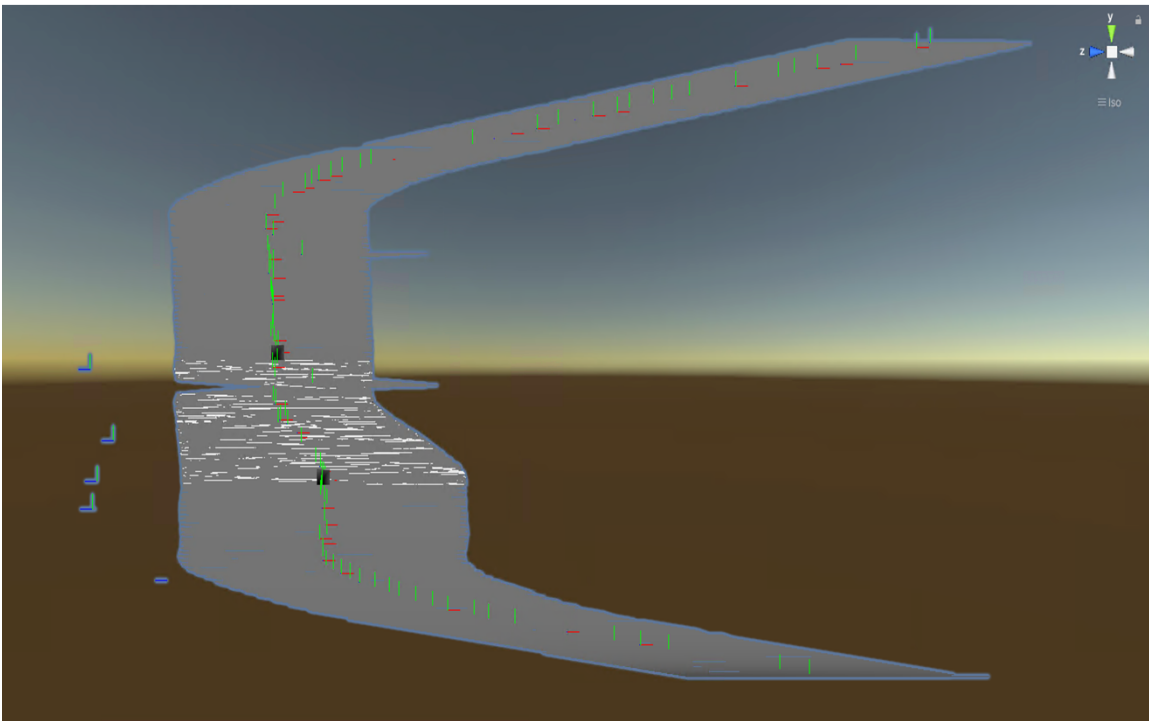
(a) Satellite Image Location



(b) Raw point-cloud



(c) Filtered point-cloud



(d) Generative Design Result

Figure 17: Results for passing lane 15 on Highway 3

## 5.16 Passing Lane 16

An extensive evaluation was undertaken to compare the design of the next passing lane generated by the system with an existing real-world passing lane. The analysis centred on a specific passing lane on Highway 3, covering a distance of 2.2 kilometres between coordinates 49.688709, -113.501620 to 49.675341, -113.524406.

The passing lane underwent a comprehensive examination based on established guidelines throughout the assessment. The resulting compatibility score was 62.679%, indicating that 8.775 of the 14 rules were successfully met. Further scrutiny revealed strong adherence to error-related rules, scoring 2.636 out of 3. However, there is potential for improvement in meeting warning-related rules, with a score of 6.139 out of 11, indicating that 4.861 rules were not fully satisfied.

Regarding signage, it was noted that the passing lane had three additional RB-34 signs and two additional RB-31 signs while lacking one RB-37 sign and one RB-32 sign. Appropriate adjustments were made to address these discrepancies and ensure the correct number of signs in the design. The generative design process for this passing lane took 02:48:22 and involved a comprehensive check count of 30,928.

Following the implementation of the generative design approach, a significant improvement in the compatibility score was achieved, reaching an impressive 89.827%. This indicates that the passing lane successfully satisfied most of 16.169 out of the 18 rules.

All three error-related rules were fully met, demonstrating adherence to those guidelines. Furthermore, regarding the warning-related rules, the passing lane exhibited compatibility with 13.169 out of the total 15, with only 1.831 rules remaining to be fully satisfied. This accomplishment underscores the passing lane's high level of compliance with warning-related criteria while also suggesting the potential for further optimization to meet all the rules fully.

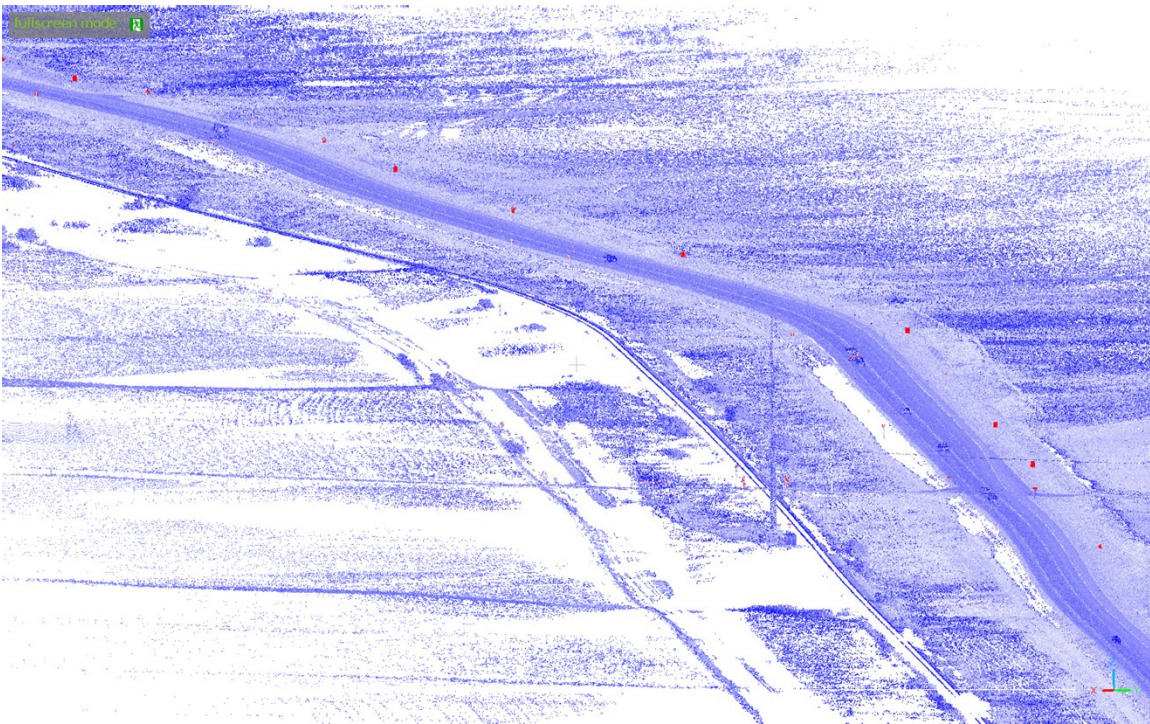
To provide a visual representation of the passing lane and its associated data, Figure 18 serves as a valuable reference. Part a of the figure illustrates the precise location of the passing lane within the broader context of Google Earth, offering a clear understanding of its geographical placement. Part b showcases the raw point-cloud file, providing a comprehensive visual representation of the collected data.

Moving on to part c, the figure presents the extracted features and characteristics specific to this passing lane, offering detailed insights into the various elements analyzed during the

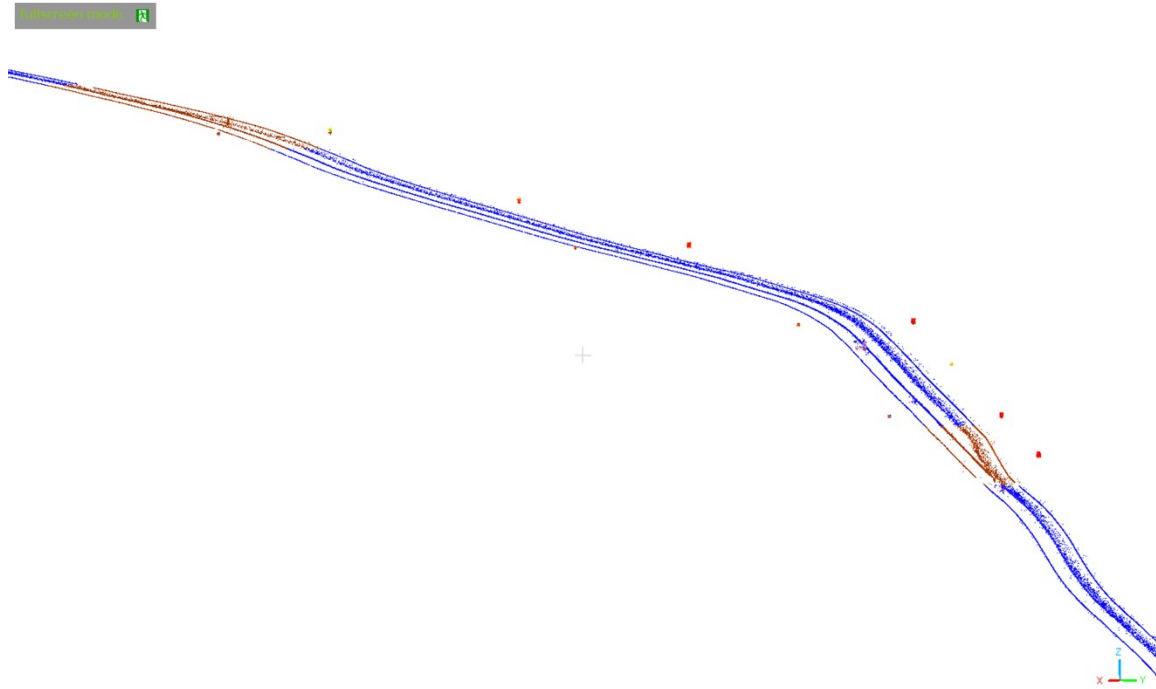
evaluation process. Finally, part d depicts the passing lane's design after incorporating generative design techniques, highlighting the optimized layout and improved functionality resulting from this approach.



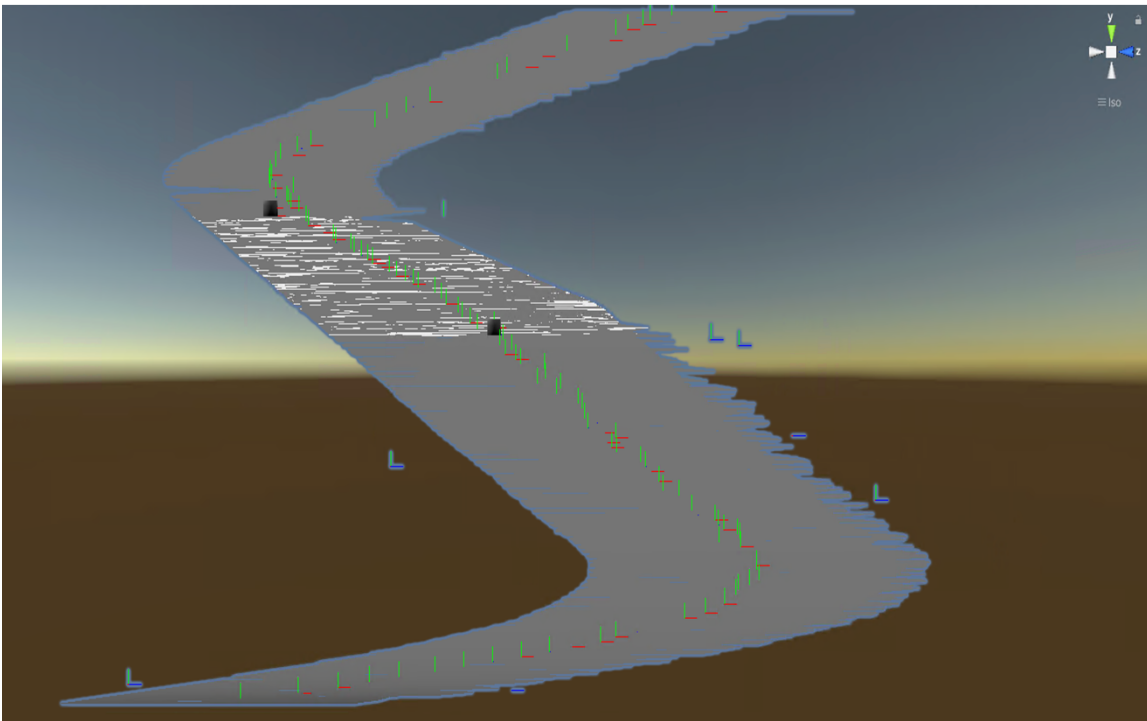
(a) Satellite Image Location



(b) Raw point-cloud



(c) Filtered point-cloud



(d) Generative Design Result

Figure 18: Results for passing lane 16 on Highway 3



## 5.17 Summary

A series of experiments were conducted on 16 real-world passing lane scenarios to assess the effectiveness of the generative design methodology. The methodology involved applying model-checking techniques to the available passing lane samples, followed by implementing generative design to reduce their level of incompatibility with established guidelines. This evaluation aimed to determine the efficacy and accuracy of the generative design methodology in producing passing lane designs that deviate from the guidelines.

For each passing lane scenario discussed, detailed information was provided, encompassing the specific highway location, precise start and end coordinates, passing lane length, initial real-world score, score after applying generative design, the runtime of the generative design process, and the number of checks performed. Visual representations were also presented, including the passing lane's location on Google Earth, the raw point-cloud data, the filtered point-cloud, and the design generated through generative design.

In this study, approximately 31.6 kilometers, which featured a total of 16 passing lanes, underwent comprehensive examination. It was observed that among the various passing lane signs, the RB-31 sign exhibited the highest incidence of missing data, followed closely by the RB-32 sign.

Furthermore, the analysis of road sign placement revealed a notable concern regarding the location of the RB-34 sign, particularly in proximity to the onset of the taper within the passing lane. This specific location exhibited a considerable failure score, indicating a deficiency in the placement of existing signs. To be more precise, the failure score for this particular road segment reached a 84 percent.

In specific numbers, the analysis revealed the absence of 17 RB-31 signs, 12 RB-32 signs, 5 RB-34 signs, 4 RB-37 signs, and 2 WA-33R signs. Interestingly, it was noted that there were additional signs beyond what was stipulated by the passing lane guidelines. Specifically, there were 18 additional RB-34 signs, possibly indicating the engineer's recognition of the need for more "KEEP RIGHT EXCEPT TO PASS" signage to enhance driver awareness of the passing lane. Additionally, there were 16 extra RB-31 signs, which serve as "DO NOT PASS" warnings, alerting drivers to potentially hazardous situations when considering a passing maneuver.

A summarized overview of the results can be found in Table 6.

Table 6: Modelling results

| <b>Passing Lane Test #</b> | <b>Initial Score</b>   | <b>Score After Generative Design</b>                                       |
|----------------------------|--|--|
| 1                          | Total Score: 7.270/12: 60.580%<br>Error: 2.598/3<br>Warning: 4.672/9   | Total Score: 16.77/18: 93.15%<br>Errors: 3.00/3.00<br>Warning: 13.77/15.00 |
| 2                          | Total Score: 7.044/12: 58.699%<br>Error: 2.595/3<br>Warning: 4.449/9   | Total Score: 16.96/18: 94.20%<br>Errors: 3.00/3.00<br>Warning: 13.96/15.00 |
| 3                          | Total Score: 8.117/12: 67.640%<br>Error: 2.592/3<br>Warning: 5.524/9   | Total Score: 17.18/18: 95.44%<br>Errors: 3.00/3.00<br>Warning: 14.18/15.00 |
| 4                          | Total Score: 8.007/12: 66.725%<br>Error: 2.601/3<br>Warning: 5.406/9   | Total Score: 17.20/18: 95.58%<br>Errors: 3.00/3.00<br>Warning: 14.20/15.00 |
| 5                          | Total Score: 9.517/16: 59.478%<br>Error: 2.603/3<br>Warning: 6.914/13  | Total Score: 16.28/18: 90.47%<br>Errors: 3.00/3.00<br>Warning: 13.28/15.00 |
| 6                          | Total Score: 9.119/16: 56.997%<br>Error: 2.593/3<br>Warning: 6.527/13  | Total Score: 14.76/18: 81.99%<br>Errors: 3.00/3.00<br>Warning: 11.76/15.00 |
| 7                          | Total Score: 10.550/18: 58.611%<br>Error: 2.615/3<br>Warning: 7.935/15 | Total Score: 16.78/18: 93.20%<br>Errors: 3.00/3.00<br>Warning: 13.78/15.00 |
| 8                          | Total Score: 9.724/14: 69.458%<br>Error: 2.642/3<br>Warning: 7.082/11  | Total Score: 17.11/18: 95.03%<br>Errors: 3.00/3.00<br>Warning: 14.11/15.00 |
| 9                          | Total Score: 10.105/16: 63.156%<br>Error: 2.719/3<br>Warning: 7.386/13 | Total Score: 15.73/18: 87.37%<br>Errors: 3.00/3.00<br>Warning: 12.73/15.00 |
| 10                         | Total Score: 8.220/18: 45.665%<br>Error: 2.625/3<br>Warning: 5.594/15  | Total Score: 15.59/18: 86.60%<br>Errors: 3.00/3.00<br>Warning: 12.59/15.00 |
| 11                         | Total Score: 10.561/16: 66.009%<br>Error: 2.629/3<br>Warning: 7.933/13 | Total Score: 17.18/18: 95.47%<br>Errors: 3.00/3.00<br>Warning: 14.18/15.00 |
| 12                         | Total Score: 10.567/18: 58.704%<br>Error: 2.630/3<br>Warning: 7.937/15 | Total Score: 16.30/18: 90.55%<br>Errors: 3.00/3.00<br>Warning: 13.30/15.00 |
| 13                         | Total Score: 10.710/16: 66.934%<br>Error: 2.680/3<br>Warning: 8.029/13 | Total Score: 16.45/18: 91.41%<br>Errors: 3.00/3.00<br>Warning: 13.45/15.00 |
| 14                         | Total Score: 9.068/14: 64.772%<br>Error: 2.658/3<br>Warning: 6.410/11  | Total Score: 16.93/18: 94.07%<br>Errors: 3.00/3.00<br>Warning: 13.93/15.00 |

|    |  |  |
|----|--|--|
| 15 | Total Score: 10.079/16: 62.995%<br>Error: 2.623/3<br>Warning: 7.456/13 | Total Score: 15.58/18: 86.54%<br>Errors: 3.00/3.00<br>Warning: 12.58/15.00 |
| 16 | Total Score: 8.775/14: 62.679%<br>Error: 2.636/3<br>Warning: 6.139/11  | Total Score: 16.17/18: 89.83%<br>Errors: 3.00/3.00<br>Warning: 13.17/15.00 |

According to Table 6, certain error-related rules pertaining to the distance of signs from the roadside received a score below one when assessed on existing roads and before implementing the generative design process. This indicates that the placement of certain traffic signs either exceeds or falls short of the prescribed distance limit from the roadside, thus highlighting deviations from the required standards.

The analysis of the passing lanes revealed substantial enhancements in the overall score and adherence to guidelines due to implementing the generative design process and making necessary adjustments. Before employing generative design, the average initial compatibility of the considered passing lanes was 61.82%. However, this compatibility significantly increased to 91.31% after leveraging generative design techniques.

An important observation from the analysis is that all three error-related rules were fully satisfied when using the generative design approach, attaining a perfect score of 3 out of 3. This achievement highlights the effectiveness and reliability of generative design in addressing crucial safety and compliance aspects of highway infrastructure design. The generative design process effectively eliminated any violations of error-related rules, ensuring a high level of safety and adherence to standards.

While the passing lanes successfully met the error-related criteria, the analysis indicates that further optimization is required to meet warning-related rules. Despite achieving a remarkable overall score, specific warning-related aspects have room for improvement. Addressing these areas through iterative refinements in the generative design process can lead to even greater compliance with guidelines, ultimately enhancing the safety and functionality of passing lanes on highways.

The findings underscore the significance of incorporating generative design in the transportation domain. By leveraging advanced algorithms and computational methods, generative design can significantly improve infrastructure planning and design efficiency and effectiveness. It offers a powerful tool to design engineers, enabling them to create innovative and compliant solutions for highway projects.

The success of generative design in enhancing the passing lanes' designs demonstrates its potential to revolutionize highway infrastructure planning, ensuring better compliance with guidelines and promoting safer and more efficient roadways. As the technology continues to advance, its integration into transportation projects is expected to become more prevalent, leading to smarter and more sustainable highway systems. Embracing generative design in the transportation sector has the potential to shape the future of highway infrastructure, fostering safer, more efficient, and environmentally conscious road networks.

## Chapter 6

### Conclusion & Recommendations

Highway elements' improper design is a significant contributor to traffic collisions. To tackle this issue, engineers rely on guidelines and regulations as valuable references to create compliant and safe highway models. Conventional manual methods for highway design are found inadequate for modern transportation networks, necessitating the exploration of alternative solutions.

The adoption of generative design, harnessing algorithms and computational methods, emerges as a promising approach to address the challenges in highway design. It enables engineers to analyze numerous scenarios and identify efficient and cost-effective solutions. Integrating Building Information Modeling (BIM) further facilitates the creation of comprehensive and precise highway models.

The specific focus of the research was on applying generative design techniques to evaluate 16 existing passing lane designs situated on Highway 3 and Highway 9 in Alberta. A series of experiments were conducted on real-world passing lane scenarios to assess the efficacy and accuracy of the generative design methodology. The initial step involved extracting the features and characteristics of the passing lanes from the available LiDAR data. Subsequently, the evaluation process commenced, which included model-checking techniques applied to the existing passing lanes. The purpose was to assess their compatibility with established guidelines. Generative design was applied to improve the passing lane designs' compliance with the guidelines. This involved using algorithms and computational methods to generate alternative designs that adhere to the recommended guidelines. By implementing generative design, the research aimed to determine its efficacy in producing passing lane designs that meet the established criteria.

Detailed information was provided for each passing lane scenario, including highway location, start and end coordinates, passing lane length, initial real-world score, score after generative design implementation, the runtime of the generative design process, and the number of checks performed. Visual representations were also presented, such as the passing lane's location on Google Earth, raw point-cloud data, filtered point-cloud, and the generative design-generated model.

The findings demonstrated substantial improvements in compliance with design guidelines after employing generative design. The implementation of generative design led to a remarkable increase in compatibility, elevating the initial 61.82% to an impressive 91.31%. This success validated the effectiveness of the generative design approach. While the generative design method effectively addressed error-related criteria, areas for further optimization were identified concerning warning-related rules.

## **6.1 Research Contributions**

An innovative approach has been developed, utilizing automated techniques to evaluate designs and provide recommendations for improved compliance, leveraging LiDAR data. This methodology has been demonstrated through the presentation of 16 illustrative examples as a proof of concept. These examples serve to showcase the capability of enhancing design compliance using the proposed method, which is facilitated by a logic-based computer tool known as BIMKit. Notably, the application of BIMKit in the transportation sector represents a novel approach, underscoring the effectiveness of this innovative methodology.

In conclusion, this thesis emphasizes the significance of integrating generative design into highway design and operation, offering engineers the means to create innovative and compliant solutions for highway development. By harnessing advanced algorithms, generative design substantially improves the efficiency and effectiveness of infrastructure design, ultimately contributing to the establishment of safer and more dependable transportation systems. This concept can also be applied to other types of transportation networks.

## **6.2 Research Limitations & Future Recommendations**

No study is without its constraints, and by openly recognizing these limitations, we ensure transparency and a complete understanding of the study's scope and potential implications. One limitation is the current availability of limited information, primarily comprising XYZ coordinates and manual grouping based on file organization. Although manual grouping allows for the basic separation of signs from the road, accurately labelling each road segment remains a challenge. Despite attempts to use clustering techniques to differentiate signs from the road, determining the

exact road label remains uncertain. The lack of precise labelling for individual points poses a significant obstacle in accurately determining the exact nature of the road, especially when dealing with point clouds containing missing data, leading to irregular and unpredictable shapes. The ideal scenario would involve precise labelling with essential attributes such as XYZ coordinates, directional information, and explicit indications of their belongingness to specific elements, such as road points or lines. However, the current state of available data falls short of this desirable standard. To address this challenge, one viable approach involves the investigation of semantic segmentation techniques, which have the capability to discern and categorize distinct objects within the LiDAR point cloud. Such an approach offers the potential for a finer level of data comprehension. Another avenue for resolution is the utilization of machine learning and deep learning methodologies. These algorithms can be subjected to training processes aimed at discerning patterns and characteristics within the LiDAR dataset, thereby enhancing the precision of road segment labeling.

Another limitation is the potential for improvement in the analysis using the closest point, rather than the centre, for the LeftSideOf and RightSideOf methods. This adjustment could enhance the accuracy of the analysis by considering the specific point closest to the object's centre. Although this refinement has not been implemented yet, it has minimal impact on the system's functionality.

Another significant limitation lies in the critical challenge of precise interpretation of terms and definitions utilized within relation functions, as it profoundly impacts the importance of compliance checking. The effectiveness of these relation functions is intricately linked to the clarity and precision of the language employed in the rules. Ensuring unambiguous rule sets with minimal room for misinterpretation becomes imperative during compliance checks. Thus, establishing clear and standardized definitions for the terms used in the rules becomes essential in addressing this issue. To address this challenge, it is important to acknowledge that language and terminology may undergo changes over time. Consequently, it is advisable to conduct periodic assessments and revisions of the definitions and language incorporated into relation functions, ensuring their alignment with current industry standards and emerging best practices. Additionally, a viable approach involves the integration of quality assurance checks during the rule creation process to guarantee that the language and terminology employed in relation functions adhere to predefined benchmarks for clarity and precision.

Another important aspect to consider pertains to the divergence of traffic sign placements from established guidelines. It is reasonable to assume that the engineer responsible for these decisions had specific, well-founded reasons for deviating from the prescribed guidelines. It is essential to underscore that these guidelines, while informative, are not legally mandated codes. Adhering to the guidelines does not necessarily equate to the optimal design for the given circumstances. For instance, constraints such as land ownership on either side of the road may pose challenges in ensuring that shoulder widths align precisely with the guidelines. Additionally, topographical features like cliffs, hills, and other natural landscape elements can introduce complexities that influence the design of passing lanes. Furthermore, design modifications may be driven by the objective of enhancing road resilience or sustainability, further emphasizing the multifaceted considerations that engineers must weigh when making these decisions.

Another noteworthy challenge encountered in this study pertains to the necessity of converting point clouds into meshes to facilitate compatibility with BIMKit. Given the extensive point density associated with roads, especially considering their considerable length, utilizing bounding shapes alone would result in a single, encompassing volume, which is not conducive for precise representation. Consequently, a strategic approach was adopted to segment road sections into subsegments, subsequently defining relation functions based on this segmentation. It is worth noting that, for future endeavors, an exploration of more streamlined methods and the formulation of additional relation functions may obviate the need for such extensive road segmentation, offering a more efficient and user-friendly solution.

In the context of future research endeavors, it is highly advisable to explore diverse segments of the transportation network while adhering to the pertinent guidelines specific to each respective area. This approach would yield valuable insights and serve to validate the adaptability of the generative design methodology across various contexts. Furthermore, enhancing the research by integrating more extensive and precise data sources for the precise labeling of points would bolster the robustness of findings and broaden the potential applications of the generative design approach.

Moreover, it is recommended to investigate methods for the direct importation of point cloud data into BIMKit without the necessity of intermediate conversion to mesh structures and partitioning. This streamlined approach could potentially offer significant advantages and



efficiencies in the utilization of point cloud data within the context of Building Information Modeling (BIM) processes.

## References

- [1] T. C. o. E. O. o. T. Safety, "Edmonton Road Safety Strategy 2016-2020: Vision Zero," 2014.
- [2] T. C. o. E. O. o. T. Safety, "Edmonton Motor Vehicle Collisions 2015 Report," 2015.
- [3] S. Gargoum, K. El-Basyouny, J. Sabbagh and K. Froese, "Automated highway sign extraction using lidar data," *Transportation research record*, vol. 2643, no. 1, pp. 1-8, 2017.
- [4] S. A. Gargoum and K. El Basyouny, "A literature synthesis of LiDAR applications in transportation: Feature extraction and geometric assessments of highways," *GIScience & Remote Sensing*, vol. 56, no. 6, pp. 864-893, 2019.
- [5] C. Sydora and E. Stroulia, "Rule-based compliance checking and generative design for building interiors using BIM," *Automation in Construction*, vol. 120, p. 103368, 2020.
- [6] C. Sydora and E. Stroulia, "BIM-kit: An extendible toolkit for reasoning about building information models," in *EC3 Conference 2021*, 2021.
- [7] H. Liu, C. Sydora, M. S. Altaf, S. Han and M. Al-Hussein, "Towards sustainable construction: BIM-enabled design and planning of roof sheathing installation for prefabricated buildings," *Journal of Cleaner Production*, vol. 235, pp. 1189-1201, 2019.
- [8] "Manual on Uniform Traffic Control Devices," 2009.
- [9] A. Infrastructure, "Highway geometric design guide," Alberta, Canada, 1999.
- [10] K. Chang, J. Chang and J. Liu, "Detection of pavement distresses using 3D laser scanning technology," in *Computing in civil engineering (2005)*, 2005, pp. 1-11.
- [11] J. Guo, M.-J. Tsai and J.-Y. Han, "Automatic reconstruction of road surface features by using terrestrial mobile lidar," *Automation in Construction*, vol. 58, pp. 165-175, 2015.
- [12] B.-h. Kang and S.-i. Choi, "Pothole detection system using 2D LiDAR and camera," in *2017 ninth international conference on ubiquitous and future networks (ICUFN)*, 2017.
- [13] R. Ravi, A. Habib and D. Bullock, "Pothole mapping and patching quantity estimates using LiDAR-based mobile mapping systems," *Transportation Research Record*, vol. 2674, no. 9, pp. 124-134, 2020.
- [14] R. Ravi, D. Bullock and A. Habib, "Pavement distress and debris detection using a mobile mapping system with 2d profiler lidar," *Transportation research record*, vol. 2675, no. 9, pp. 428-438, 2021.
- [15] W. Yao, S. Hinz and U. Stilla, "Extraction and motion estimation of vehicles in single-pass airborne LiDAR data towards urban traffic analysis," *ISPRS Journal of Photogrammetry and Remote Sensing*, vol. 66, no. 3, pp. 260-271, 2011.
- [16] W. Yao, M. Zhang, S. Hinz and U. Stilla, "Airborne traffic monitoring in large areas using LiDAR data--theory and experiments," *International journal of remote sensing*, vol. 33, no. 12, pp. 3930-3945, 2012.
- [17] J. Zhang, W. Xiao, B. Coifman and J. P. Mills, "Vehicle tracking and speed estimation from roadside lidar," *IEEE Journal of Selected Topics in Applied Earth Observations and Remote Sensing*, vol. 13, pp. 5597-5608, 2020.
- [18] M. Gouda, J. Mirza, J. Weiß, A. Ribeiro Castro and K. El-Basyouny, "Octree-based point cloud simulation to assess the readiness of highway infrastructure for autonomous

- vehicles," *Computer-Aided Civil and Infrastructure Engineering*, vol. 36, no. 7, pp. 922-940, 2021.
- [19] M. Gouda, I. Chowdhury, J. Weiß, A. Epp and K. El-Basyouny, "Automated assessment of infrastructure preparedness for autonomous vehicles," *Automation in construction*, vol. 129, p. 103820, 2021.
- [20] M. Gouda and K. El-Basyouny, "Safety Assessment of Lane Marking for Autonomous Vehicles Using Light Detection and Ranging (Lidar) Data," *Available at SSRN 4107155*.
- [21] C. Premebida, O. Ludwig and U. Nunes, "Exploiting LIDAR-based features on pedestrian detection in urban scenarios," in *2009 12th International IEEE Conference on Intelligent Transportation Systems*, 2009.
- [22] K. Kidono, T. Miyasaka, A. Watanabe, T. Naito and J. Miura, "Pedestrian recognition using high-definition LIDAR," in *2011 IEEE Intelligent Vehicles Symposium (IV)*, 2011.
- [23] H.-L. Tang, S.-C. Chien, W.-H. Cheng, Y.-Y. Chen and K.-L. Hua, "Multi-cue pedestrian detection from 3D point cloud data," in *2017 IEEE international conference on multimedia and expo (ICME)*, 2017.
- [24] T.-C. Lin, D. S. Tan, H.-I. Tang, S.-c. Chien, F.-c. Chang, Y.-Y. Chen, W.-H. Cheng and K.-L. Hua, "Pedestrian detection from lidar data via cooperative deep and hand-crafted features," in *2018 25th IEEE international conference on image processing (ICIP)*, 2018.
- [25] H. Guan, J. Li, Y. Yu, C. Wang, M. Chapman and B. Yang, "Using mobile laser scanning data for automated extraction of road markings," *ISPRS Journal of Photogrammetry and Remote Sensing*, vol. 87, pp. 93-107, 2014.
- [26] C. Ai and Y.-C. J. Tsai, "Critical assessment of an enhanced traffic sign detection method using mobile LiDAR and INS technologies," *Journal of Transportation Engineering*, vol. 141, no. 5, p. 04014096, 2015.
- [27] S. A. Gargoum, K. El-Basyouny, A. Shalkamy and M. Gouda, "Feasibility of extracting highway vertical profiles from LiDAR data," *Canadian Journal of Civil Engineering*, vol. 45, no. 5, pp. 418-421, 2018.
- [28] M. Gouda, B. Arantes de Achilles Mello and K. El-Basyouny, "Automated object detection, mapping, and assessment of roadside clear zones using LiDAR data," *Transportation research record*, vol. 2675, no. 12, pp. 432-448, 2021.
- [29] Y. Yue, M. Gouda and K. El-Basyouny, "Automatic detection and mapping of highway guardrails from mobile lidar point clouds," in *2021 IEEE International Geoscience and Remote Sensing Symposium IGARSS*, 2021.
- [30] M. Gouda, A. Shalkamy, X. Li and K. El-Basyouny, "Fully automated algorithm for light pole detection and mapping in rural highway environment using mobile light detection and ranging point clouds," *Transportation research record*, vol. 2676, no. 7, pp. 617-629, 2022.
- [31] M. Gouda, A. Epp, R. Tilroe and K. El-Basyouny, "Traffic sign extraction using deep hierarchical feature learning and mobile light detection and ranging (LiDAR) data on rural highways," *Journal of Intelligent Transportation Systems*, pp. 1-22, 2022.
- [32] L. Penn, R. Raunak and E. Leworthy, "Connected and Autonomous Vehicle Road Scoring Index," 2020/21.
- [33] S. Kuciemba, "CONNECTED ROADWAY CLASSIFICATION SYSTEM DEVELOPMENT," 2019.

- [34] S. A. Gargoum and K. El-Basyouny, "Exploring the association between speed and safety: A path analysis approach," *Accident Analysis & Prevention*, vol. 93, pp. 32-40, 2016.
- [35] P. C. Anastasopoulos, F. L. Mannering, V. N. Shankar and J. E. Haddock, "A study of factors affecting highway accident rates using the random-parameters tobit model," *Accident Analysis & Prevention*, vol. 45, pp. 628-633, 2012.
- [36] S. E.-B. Ibrahim and T. Sayed, "Developing safety performance functions incorporating reliability-based risk measures," *Accident Analysis & Prevention*, vol. 43, no. 6, pp. 2153-2159, 2011.
- [37] B. Dhahir and Y. Hassan, "Probabilistic, safety-explicit design of horizontal curves on two-lane rural highways based on reliability analysis of naturalistic driving data," *Accident Analysis & Prevention*, vol. 123, pp. 200-210, 2019.
- [38] N. Jesna and M. Anjaneyulu, "Reliability analysis of horizontal curves on two lane highways," *Transportation research procedia*, vol. 17, pp. 107-115, 2016.
- [39] M. Fellendorf and P. Vortisch, "Microscopic traffic flow simulator VISSIM," *Fundamentals of traffic simulation*, pp. 63-93, 2010.
- [40] M. J. Olsen, Guidelines for the use of mobile LIDAR in transportation applications, vol. 748, Transportation Research Board, 2013.
- [41] S. Krish, "A practical generative design method," *Computer-Aided Design*, vol. 43, no. 1, pp. 88-100, 2011.
- [42] J.-C. Jong, M. K. Jha and P. Schonfeld, "Preliminary highway design with genetic algorithms and geographic information systems," *Computer-Aided Civil and Infrastructure Engineering*, vol. 15, no. 4, pp. 261-271, 2000.
- [43] Y. Guoyan, W. Xiaozhen and L. Peng, "A constraint based evolutionary decision support system for product design," in *2009 Chinese Control and Decision Conference*, 2009.
- [44] D. Rodriguez-Roman, "A surrogate-assisted genetic algorithm for the selection and design of highway safety and travel time improvement projects," *Safety science*, vol. 103, pp. 305-315, 2018.
- [45] J.-C. Jong, Optimizing highway alignments with genetic algorithms, University of Maryland, College Park, 1998.
- [46] M. K. Jha and P. Schonfeld, "Integrating genetic algorithms and geographic information system to optimize highway alignments," *Transportation Research Record*, vol. 1719, no. 1, pp. 233-240, 2000.
- [47] K. Shea, R. Aish and M. Gourtovaia, "Towards integrated performance-driven generative design tools," *Automation in Construction*, vol. 14, no. 2, pp. 253-264, 2005.
- [48] S. Agina, A. Shalkamy, M. Gouda and K. El-Basyouny, "Automated assessment of passing sight distance on rural highways using mobile LiDAR data," *Transportation research record*, vol. 2675, no. 12, pp. 676-688, 2021.
- [49] S. Gargoum and K. El-Basyouny, "Effects of LiDAR point density on extraction of traffic signs: A sensitivity study," *Transportation research record*, vol. 2673, no. 1, pp. 41-51, 2019.
- [50] K. Williams, M. J. Olsen, G. V. Roe and C. Glennie, "Synthesis of transportation applications of mobile LiDAR," *Remote Sensing*, vol. 5, no. 9, pp. 4652-4692, 2013.

- [51] C. Sydora, "Rule Language Based Automated Compliance Checking for Interior Generative Design Using BIM," 2019.
- [52] C. Sydora and E. Stroulia, "Comparative analysis of room generation methods using rule language-based evaluation in BIM," in *EC3 Conference 2023*, 2023.